Serial No. N7692 NAFO SCR Doc. 25/046

SCIENTIFIC COUNCIL MEETING –NOVEMBER 2025

High Resolution Climate Projections to 2100 for Use in Species Distribution Modelling of Vulnerable Marine Ecosystem Indicators in the NAFO Regulatory Area

by

N. Paulin, E. Kenchington, F.J. Murillo, R. Danielson, and Z. Wang

Department of Fisheries and Oceans, Bedford Institute of Oceanography, Dartmouth, NS, Canada.

PAULIN, N., KENCHINGTON, E., MURILLO, F. J., DANIELSON, R., & WANG, Z. 2025. High Resolution Climate Projections to 2100 for Use in Species Distribution Modelling of Vulnerable Marine Ecosystem Indicators in the NAFO Regulatory Area. *NAFO Scientific Council Research Document*, SCR Doc. 25/046: 1-91.

Abstract

Statistical downscaling and bias correction of a 22-member global climate model ensemble, generated at approximately 100 km horizontal native resolution in Phase 6 of the Coupled Model Intercomparison Project (CMIP6), enhanced the resolution of ocean projections for species distribution modelling, and provides insights for marine conservation under climate change. By adjusting downscaled projections across four CMIP6 scenarios, known as Shared Socio-economic Pathways (SSPs), which represent a spectrum of low to high emissions reduction paths: SSP1-2.6, SSP2-4.5, SSP3-7.0 and SSP5-8.5, finer resolution is imposed in the ocean temperature, salinity, mixed layer depth (MLD) and bottom current changes that could threaten ecosystem structure and marine species. A neural network mapping technique was applied to each grid cell in the NAFO study area at a resolution of ~9 km (1/12°). Bi-decadal means, minimums, maximums, ranges and climatologies for Period 1 (P1: 2020-2039), Period 2 (P2: 2040-2059), Period 3 (P3: 2060-2079), and Period 4 (P4: 2080-2099) were calculated for each of the investigated variables under each of the SSPs. These geospatial data products are intended to be used in future species distribution models (SDMs) to assess the impacts of climate change on vulnerable marine ecosystems and area closures in the NAFO Regulatory Area (NRA).

Table of Contents

Introduction

Oceans are affected by seasonal and year-to-year climate variability as well as long-term climate change. Increasing levels of greenhouse gases in the atmosphere cause global temperatures to increase. As the oceans absorb this heat and carbon dioxide, they become warmer and more acidic, oxygen levels drop, summer sea ice in the Arctic decreases, and marine heatwaves become more frequent. Ocean currents and mixing redistribute the heat and carbon dioxide absorbed at the sea surface to deeper waters causing further changes to marine ecosystems that can be expected to last for decades. Species distribution models (SDMs) predict future species habitats under climate change by correlating known species locations with environmental factors like temperature and salinity (e.g., Beazley et al., 2020; Wang et al., 2022; Busch et al., 2024). These models use current and projected future climate data, alongside chosen climate models and emission scenarios, to map potential species ranges. The outcome is a prediction of habitat suitability, showing areas where a species might persist, shift, or decline, offering crucial data for conservation and management strategies. Further, areas of analogous and novel environments in future can be identified (Wang et al., 2022).

The Coupled Model Intercomparison Project Phase 6 (CMIP6 represents the latest efforts by a global scientific community to generate climate model projections for high resolution impact studies (Eyring et al., 2016). The CMIP6 models are designed to simulate various components of Earth's climate system, including the atmosphere, oceans, land surface, cryosphere, and carbon system. There are over 100 CMIP6 models from more than 50 modelling groups contributing to the project, though the specific number can vary depending on the specific dataset or model intercomparison being considered. The previous CMIP5 exercise used Representative Concentration Pathways (RCPs) to represent greenhouse gas concentration trajectories, whereas CMIP6 introduces a greater diversity of socio-economic scenarios or Shared Socio-economic Pathways (SSPs) from SSP1-2.6 to SSP5-8.5 (IPCC, 2021a). Following previous efforts to drive marine ecosystem models (Tittensor et al., 2019) using a high resolution representation of the CMIP6 models (Lange, 2019), we seek to improve the precision in an ensemble of physical ocean variables, each of which are adjusted using a single-step statistical downscaling and bias correction.

The CMIP6 models provide SSP-forced climate simulations that are global and free-running (i.e., without data assimilation), but they are performed at relatively large spatial scales (~100 km) and each model has

systematic biases compared to observations (e.g., Wang et al., 2023). Biases are often associated with processes that a climate model does not resolve, and when finer scales are required to assess the impact on ocean species, systematic adjustments using downscaling approaches can be useful (e.g., Drenkard et al., 2021). Dynamical downscaling involves a nested regional climate model that uses CMIP6 model output as its boundary conditions, but like global climate models, this method incurs a large computational cost (Drenkard et al., 2021). Although climate models do not assimilate observations, an ocean data assimilation system like the GLobal Ocean ReanalYsis and Simulation (GLORYS12) (Lellouche et al., 2021) performs systematic adjustments that can be applied to climate model output as a parameterization. Thus, an alternative to dynamic downscaling is to train a neural network by taking GLORYS12 as a reference and training a relationship, or mapping, from CMIP6 predictors to corresponding GLORYS12 predictands.

A method of statistical downscaling and bias correction was developed by Lange (2019) to obtain high resolution representations of CMIP5 and CMIP6 models, which provided forcing for SDMs and other marine ecosystem models (Tittensor et al., 2019). A relatively direct downscaling and bias correction is also possible using neural networks that offer greater precision by design (Danielson et al., 2025; McKee et al., 2025). Parameterizations obtained using historical data can then be applied to projections to 2100. With the caveat that these parameterizations are fixed in time, local climate change impacts can be assessed at higher resolution and with greater precision across CMIP6 models.

Here, projections from a suite of 22 CMIP6 models (Table 1) were analysed and downscaled using neural networks trained with GLORYS12 predictands for a suite of environmental variables (sea surface temperature (SST), bottom temperature (BT), sea surface salinity (SSS), bottom salinity (BS), mixed layer depth (MLD), bottom current speed (BCS) and the derived variable bottom stress (τ_b)) deemed of interest for species distribution modelling (SDM). Simulations from each of four Shared Socio-economic Pathway (SSP) scenarios SSP1-2.6, SSP2-4.5, SSP3-7.0, and SSP5-8.5, and four time periods (P1 (near term): 2020-2039, P2 (mid term): 2040-2059, P3 (mid term): 2060-2079, and P4 (end of century): 2080-2099) were variously summarized to provide environmental data layers for SDMs.

Methods

The 22 CMIP6 Earth System Models (ESMs) used in this study (Table 1) were selected from those available in 2021 (IPCC, 2021b) that included a biogeochemical component in their formulation. Further details of these 22 ESMs are given by Wang et al. (2023). An ESM provides numerical simulations of coupled global biogeochemical and physical systems. They are an advance over global climate models that focus on processes of the cryosphere, ocean and atmosphere. ESM tuning involves adjustments toward both process-level knowledge and emergent (i.e., observed) behaviour (Schmidt et al., 2017; Danielson et al., 2025).

Downscaling and bias correction can be considered as the complementary forms of tuning that are employed after numerical simulations are provided. The former is endorsed as part of the CMIP6 effort (CORDEX; Eyring et al., 2016) because model resolution is always limited, but regarding bias correction and emergent behaviour, it is also well known that CMIP6 models are not yet sufficiently constrained by observations to perform high resolution impact studies (e.g., Drenkard et al., 2022). Thus, an offline calibration of CMIP6 simulations to a high-resolution reanalysis is a relatively low-cost effort, a) to parameterize observational constraints during the historical period, and b) to apply these fixed constraints to CMIP6 projections to 2100. Although data files may be large, low-cost refers to a CPU-based statistical downscaling and bias correction that can be performed on a conventional workstation. Neural networks are employed for their flexibility, and we refer to this single-step adjustment or calibration as “AI mapping” (McKee et al., 2025).

CMIP6 Historical Simulations and Projections

For each climate scenario, we followed Wang et al. (2023) and employed an ensemble member provided by each of 22 modelling groups (Table 1) from the Earth System Grid Federation (ESGF; https://esgf-node.llnl.gov/search/cmip6). We examined simulations from each of four Shared Socio-economic Pathway

(SSP) scenarios[1], SSP1-2.6, SSP2-4.5, SSP3-7.0, and SSP5-8.5 (Figure 1), whose forcing is characterized as (see Riahi et al., 2017):

Classification	SSP	Description
Low (Sustainability – Taking the Green Road; Low challenges to mitigation and adaptation)	SSP1-2.6	Radiative forcing reaches a level of 2.6 W/m^2 by 2100. Policy focused on sustainable development.
Intermediate (Middle of the Road – Medium challenges to mitigation and adaptation)	SSP2-4.5	Radiative forcing reaches a level of 4.5 W/m^2 by 2100, representing the medium range of plausible future pathways.
High (Regional Rivalry – A Rocky Road; High challenges to mitigation and adaptation)	SSP3-7.0	Radiative forcing reaches a level of 7.0 W/m^2 by 2100, representing the medium-to-high end of plausible future pathways.
Very High (Fossil-fueled Development –High challenges to mitigation, low challenges to adaptation)	SSP5-8.5	Radiative forcing reaches a level of 8.5 W/m^2 by 2100, representing the upper boundary of the range of scenarios.

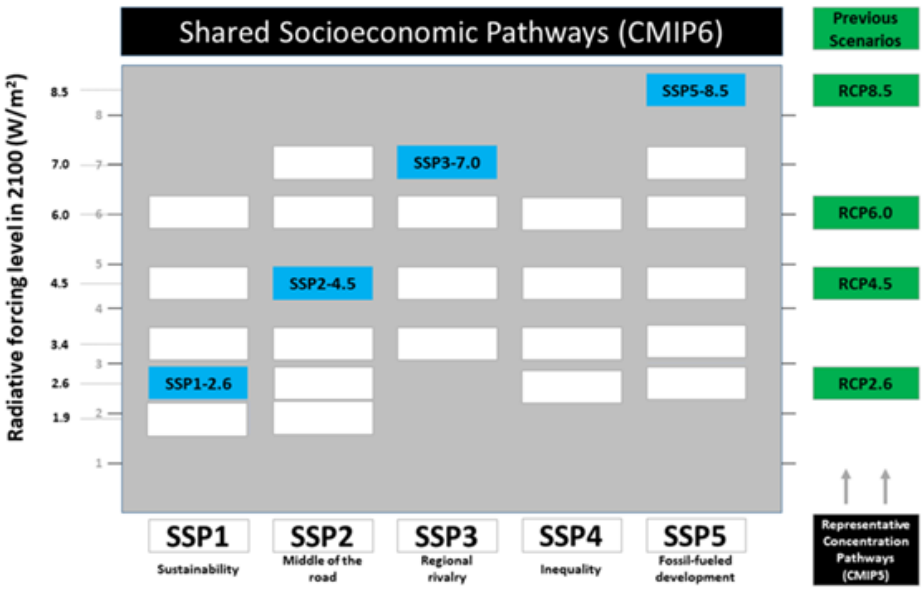

Figure 1. Selected Shared Socio-economic Pathways (SSPs) used in this study in comparison with previous Representative Concentration Pathways (RCPs). Figure modified from O'Neill et al. (2016).

[1]Understanding Shared Socio-economic Pathways (SSPs) https://climatedata.ca/resource/understanding-shared-socio-economic-pathways-ssps/#:~:text=Shared%20Socioeconomic%20Pathways%20(SSPs)%20are%20a%20set,than%20RCP8.5%2C%20which%20has%20higher%20methane%20emissions. Accessed 30 September 2025.

Table 1. Source and resolution of the 22 CMIP6 Earth system models of Wang et al. (2023), where each Digital Object Identifier (DOI) is preceded by 'https://doi.org/10.22033/ESGF/CMIP6.' for the historical, SSP1-2.6, SSP2-4.5, SSP3-7.0, and SSP5-8.5 data, respectively.

Earth system model name (DOI numbers: historical, SSP1-2.6; SSP2-4.5; SSP3-7.0; SSP5-8.5)	Institution	Atmosphere: approximate resolution (km)	Ocean: approximate resolution (km)
ACCESS-CM2 (4271,4319,4321,4323,4332)	Commonwealth Scientific and Industrial Research Organisation / Australian Research Council – Centre of Excellence for Climate System Science	250	100
ACCESS-ESM1.5 (4272,4320,4322,4324,4333)	Commonwealth Scientific and Industrial Research Organisation	250	100
AWI-CM 1.1 MR (2686,2796,2800,2803,2817)	Alfred Wegener Institute	100	25
CAMS-CSM 1.0 (9754,11046,11047,11048,11052)	Chinese Academy of Meteorological Sciences	100	100
CanESM5 (3610,3683,3685,3690,3696)	Canadian Centre for Climate Modelling and Analysis	500	100
CESM2 (7627,7746,7748,7753,7768)	National Center for Atmospheric Research	100	100
CESM2-WACCM (10071,10100,10101,10102,10115)	National Center for Atmospheric Research	100	100
CMCC-CM2-SR5 (3825,3887,3889,3890,3896)	Centro Euro-Mediterraneo sui Cambiamenti Climatici	100	100
CNRM-CM6-1 (4066,4184,4189,4197,4224)	Centre National de Recherches Météorologiques / Centre Européen de Recherche et de Formation Avancée en Calcul Scientifique	250	100
CNRM-CM6-1-HR (4067,4185,4190,4198,4225)	Centre National de Recherches Météorologiques / Centre Européen de Recherche et de Formation Avancée en Calcul Scientifique	100	25
CNRM-ESM2-1 (4068,4186,4191,4199,4226)	Centre National de Recherches Météorologiques / Centre Européen de Recherche et de Formation Avancée en Calcul Scientifique	250	100
EC-Earth3 (4700,4874,4880,4884,4912)	European Community Earth Consortium	100	100
GISS-E2.1G (7127,7410,7415,7426,7460)	NASA Goddard Institute for Space Studies	250	100
IPSL-CM6A-LR (5195,5262,5264,5265,5271)	Institut Pierre-Simon LaPlace	250	100
MIROC-ES2L (5602,5742,5745,5751,5770)	Japan Agency for Marine-Earth Science and Technology / Atmosphere and Ocean Research Institute (The University of Tokyo) / National Institute for Environmental Studies	500	100
MIROC6 (5603,5743,5746,5752,5771)	Japan Agency for Marine-Earth Science and Technology / Atmosphere and Ocean Research Institute (The University of Tokyo) / National Institute for Environmental Studies	250	100
MPI-ESM1.2-HR (6594,4397,4398,4399,4403)	Max-Planck-Institut für Meterologie	100	50
MPI-ESM1.2-LR	Max-Planck-Institut für Meterologie	250	250

(6595,6690,6693,6695,6705)			
MRI-ESM2.0 (6842,6909,6910,6915,6929)	Meteorological Research Institute (Japan Meteorological Agency)	100	100
NorESM2-LM (8036,8248,8253,8268,8319)	Norsk Klimasenter	250	100
TaiESM 1.0 (9755,9806,9808,9809,9823)	Academia Sinica – Research Centre for Environmental Changes	100	100
UKESM1.0-LL (6113,6333,6339,6347,6405)	Meteorological Office Hadley Centre	250	100

GLORYS12 Reanalysis

GLORYS12 (version 1) is a global, eddy-resolving, physical ocean and sea ice reanalysis at 1/12-degree resolution covering the 1993-present altimetry period. A reduced-order Kalman filter is used to assimilate ocean observations, including altimeter sea level anomalies, satellite sea surface temperature, and sea ice concentration, as well as *in situ* temperature and salinity profiles (Lellouche et al., 2021; Mercator Océan International, 2022). Numerous studies highlight the spatiotemporal coverage and resolution that is provided. McKee et al. (2023) found that GLORYS12 bottom temperature is comparable to *in situ* observations and a monthly gridded analysis on the Scotian Shelf. To the north of this region, previous versions of GLORYS were consistent with observed flows along the Labrador Shelf (Wang and Greenan, 2013), and Andres et al. (2024) employed GLORYS12 in lieu of sparse observations to document the downstream movement of the cold intermediate layer. Along the US east coast, eight reanalyses found that GLORYS12 captures the Gulf Stream position and variance well, and was consistent with altimetric observations (Castillo-Trujillo et al., 2023). As in McKee et al. (2023), they also confirmed that GLORYS12 is consistent with observations at depth.

Observational consistency is aided by adjustments that are applied to the forcing and predictive components of GLORYS12 (Lellouche et al., 2021). Specifically, precipitation and radiative fluxes are adjusted toward satellite observations and model prognostic tendencies are nudged to reduce large scale model-observation differences in temperature and salinity, as given by a variational (3DVar) analysis. In principle, emergent (observed) behaviour may be used to constrain the input (forcing), predictions, and output of any model (e.g., Danielson et al., 2025). The impetus for using GLORYS12 as a calibration reference here is thus partly owing to constraints that can be said to apply equally to GLORYS12 and CMIP6 models, even if it is only adjustments to CMIP6 ocean model output that were considered here.

Spatial Domain

A bounding box for data extraction was drawn (Figure 2) using an EPSG 4326 (World Geodetic System 1984) co-ordinate system. The bounds for the box were:

bottom right: x = -43.16955, y = 42.34121
bottom left: x = -52.66456, y = 42.34121
top right: x = -43.16955, y = 49.23432
top left: x = -52.66456, y = 49.23432

This domain contains 9660 grid cells (84 by 115 grid at 1/12-degree resolution), with each cell being approximately 9.25 km in each dimension. This bounding box was used for downscaling and bias correction of the CMIP6 ESMs. Within that larger bounding box a study area, referred to as the 'NAFO study area', was selected for extracting and mapping the suite of environmental variables for use in SDMs. This area is shown by the polygon outlined in Figure 2. The NAFO study area includes the NAFO Regulatory Area but extends into deeper water to match the spatial domain of previous SDMs (Murillo et al., 2024; Murillo et al., 2025).

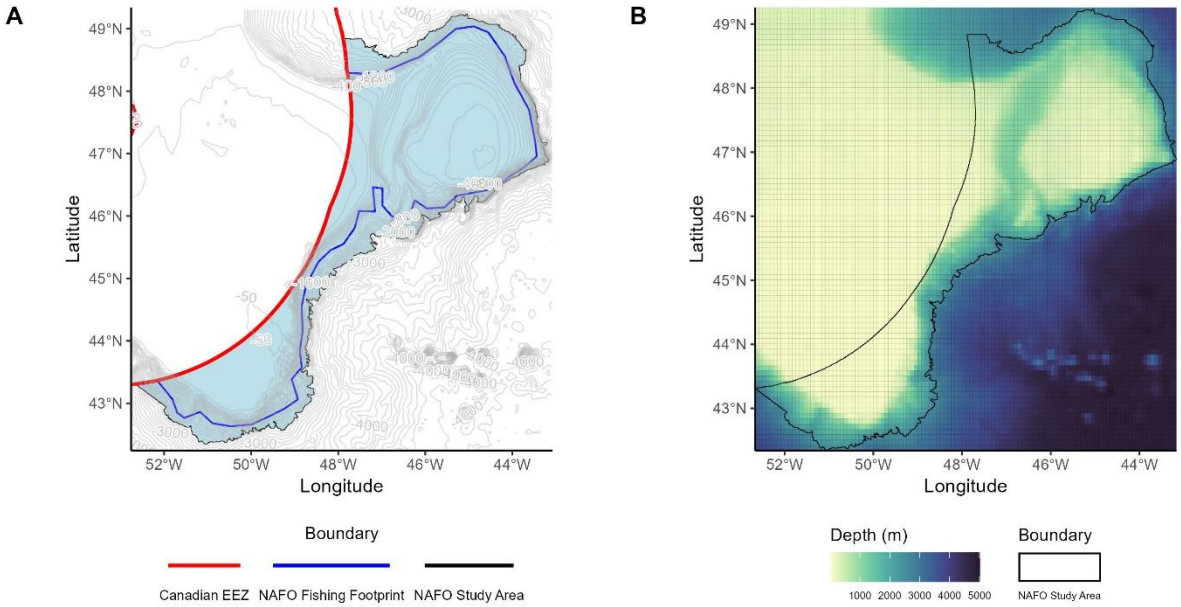

Figure 2. **A.** The NAFO study area(blue shade) where the data layers for the species distribution modelling are given in relation to the Canadian EEZ (red outline) and the NAFO fishing footprint (blue outline). **B.** The spatial extent of the bounding box used for the CMIP6 adjustments (84 by 115 grid at 1/12-degree resolution) and the NAFO study area (black outline). Depth is shown in (m).

Calibration and Processing

Each neural network was treated as a spatially local parameterization that maps CMIP6 to GLORYS12. With 39 free parameters, each network is flexible and easy to train, but its fixed structure is *ad hoc*, so trained weights at individual nodes are not easy to associate with specific physical processes. The same neural network calibration is performed for each of six variables: sea surface temperature (SST), bottom temperature (BT), sea surface salinity (SSS), bottom salinity (BS), mixed layer depth (MLD), and bottom current speed (BCS). A total of 22 CMIP6 models (Table 1) were employed under four SSP climate scenarios: SSP1-2.6, SSP2-4.5, SSP3-7.0, and SSP5-8.5. Ensembled averages of all the CMIP6 models were used to provide a consensus of future projections, in part to reduce uncertainties and improve predictive skill (Loder et al., 2015; Wang et al., 2023). The model resolutions of CMIP6 are coarse (mostly ~100 km), whereas the GLORYS12 has a resolution of ~9 km. The processing (Steps 1 and 2) and mapping (Step 3, Figure 3) steps were:

Step 1: Interpolate monthly data for the 22 CMIP6 models onto the GLORYS12 grid using the Climate Data Operators (Schulzweida, 2023) nearest neighbour interpolation function.

Step 2: Apply a neural network to adjust the monthly CMIP6 model data. One neural network is trained for every model (22), variable (6), and grid cell in the full spatial extent. Each neural network is defined by 39 parameters (i.e., 3 nodes for input and output, with a four-node hidden layer). Parameters were trained (Innes et al., 2024) using historical data (1993-2014) with CMIP6 model data as input and GLORYS12 data as output (the three variables are monthly, centered one-year, and multiyear one-month averages). In turn, the trained neural networks are applied to raw CMIP6 model data for each year and grid cell for the period 2015-2099. Spatial structure that is present in GLORYS12 is thus introduced, but climate trends in the original CMIP6 data are preserved. Following Maraun (2016), trends are determined by the CMIP6 models, even at high resolution.

Step 3: Calculate bi-decadal means, minimums, maximums and ranges for Period 1 (P1: 2020-2039), Period2 (P2: 2040-2059), Period 3 (P3: 2060-2079), and Period 4 (P4: 2080-2099) for the investigated variables under each SSP for the grid cells within the spatial extent of the NAFO study area. These time periods were chosen as greater reliability in projections is placed when values are averaged over a number of years. Values were calculated by calculating the means, minimums, maximums and ranges for each of the 12 months within each

of the 20 years within each time period for each grid cell (Table 2, Figure 3). For mixed layer depth, values were calculated averaged across the full time period and for seasonal time periods (Winter: January – March; Spring: April - June; Summer: July - September; Fall: October – December). Bottom stress (τ_b) was calculated as $\tau b = 3.5 \times 10^{-3} \times \rho \times U_b^2$ where ρ is the density of seawater (kg m^{-3}) and U_b is the bottom current speed (BCS). Density was calculated as in Busch et al. (2024) using the gsw-package in R. Results were mapped across the spatial extent of the NAFO study area (Figure 2).

	**A data product is produced for each grid cell from the monthly average of the 22 statistically downsized and bias corrected ensembled CMIP6 models.**
	**For each bi-decadal time period and SSP (scenarios) there will be 12 (months) x 20 (years) values (240 values) per grid cell.**
	**Trend line figures showing trends across time by SSP: the annual mean values for each year (2015 to 2100) across the full spatial domain of the NAFO study area were plotted.**
	**Bar chart figures showing the mean, minimum, maximum and range values calculated across the full spatial domain of the NAFO study area for each scenario were plotted.**
	**Spatial mapping and production of environmental data layers for SDMs: the mean, minimum, maximum and range of the 240 values per grid cell are mapped for the NAFO study area for each scenario (only results for SSP1-2.6/Period 1 and SSP5-8.5/Period 4 are illustrated).**

Figure 3. Workflow for producing the environmental data layers for use in species distribution modelling (SDM) and the figures shown in this report.

Table 2. Water column variables (Max: Maximum; Min: Minimum).

Variable	Abbreviation	Metric	Unit	Native Resolution
Bottom Salinity	BS	Mean, Max, Min, Range	N/A*	1/12º lat/long
Bottom Temperature	BT	Mean, Max, Min, Range	°C	1/12º lat/long
Bottom Current Speed	BCS	Mean, Max, Min, Range	m s^{-1}	1/12º lat/long
Bottom Stress	BStr (τ_b)	Mean, Max, Min, Range	Pa = kg/m s^{-1}	1/12º lat/long
Surface Salinity	SS	Mean, Max, Min, Range	N/A*	1/12º lat/long
Surface Temperature	SST	Mean, Max, Min, Range	°C	1/12º lat/long
Mixed Layer Depth	MLD	Mean, Max, Min, Range	m	1/12º lat/long
Summer MLD	MLD_{Su}	Mean, Max, Min, Range	m	1/12º lat/long
Fall MLD	MLD_{F}	Mean, Max, Min, Range	m	1/12º lat/long
Winter MLD	MLD_{W}	Mean, Max, Min, Range	m	1/12º lat/long
Spring MLD	MLD_{Sp}	Mean, Max, Min, Range	m	1/12º lat/long

*Salinity is considered unitless because it's defined as a ratio of conductivity, rather than a direct mass measurement.

Comparison with BNAM Products

Recent species distribution modelling in NAFO (Murillo et al., 2024; Murillo et al., 2025) used a single ocean model, the Bedford Institute of Oceanography North Atlantic Model (BNAM; Wang et al., 2018), to obtain monthly temperature, salinity, current speed, bottom stress and mixed layer depth for the period 1990-2023. Mean, maximum, minimum and range values derived from BNAM were calculated for all months within a year and averaged across all years. Using ArcGIS Pro's Geostatistical Wizard, BNAM (and BNAM-derived) point data were interpolated using ordinary kriging, and the resulting geostatistical layers were exported to the final raster surfaces.

Here we used the same suite of variables as those derived from BNAM, except for Surface Current Speed, which we did not calculate (Table 2). For minimum and maximum values, we took the lowest and highest value in each grid cell for the SSP/Period as this would reflect the lowest/highest modeled temperature experienced in each cell and the values are already the average from the 22 CMIP6 models. We also have not applied kriging, with each grid cell having the same value throughout.

We compared the BNAM surfaces from the period 1990-2023 to the values for Period 1 (2020-2039) recognizing that they are not identical but overlap partially. We used SSP2-4.5 as a lower emission scenario to compensate for the later time frame. It should be noted that values for the period beginning in 2015 are projections from the CMIP6 simulations. In contrast, the data from BNAM for the period 1990–2023 represents a model hindcast forced by atmospheric reanalysis products.

Methods for BNAM-CMIP layer comparisons

BNAM layers were loaded into R (R Core Team, 2025) as rasters using the `terra` package's (Hijmans, 2025) `rast` function. These layers were reprojected from NAD83 UTM zone 23N (EPSG 26923) to WGS84 (EPSG 4326) using the terra `project` function to match the coordinate reference system of the CMIP layers.

CMIP data needed to be transformed into rasters of the same extent and resolution to compare with the BNAM layers. To do so, a separate dataset for each variable and statistic for period 1 (2020-2039) and SSP 2.4-5 was created by filtering the starting dataset. Each dataframe was converted to an `sf` spatial dataframe using the `sf` package (Pebesma, 2018) `st_as_sf` function, with the coords argument set to the longitude and latitude fields and the crs argument set to 4326 to match the desired projection. Each spatial dataframe was then converted to a vector of point coordinates using terra's `vect` function. A raster template was created using the terra `rast` function with the NAFO boundary limits used as the extent for the xmin, xmax, ymin, and ymax arguments, the resolution argument set to match the distance between points, and the crs argument set to 4326. The vector of points was then matched to the raster template using the terra `rasterize` function with the field argument set to the variable and statistic of interest. Finally, the terra `resample` function was used to

transform each CMIP raster to match the BNAM rasters' resolution and extent using a bilinear interpolation method.

Following these raster transformations, the CMIP and BNAM layers could be directly compared. The difference between the two sets of layers was calculated by subtracting the CMIP raster from the BNAM raster for each variable and statistic combination that both models had in common (mean/min/max bottom stress, temperature, salinity, and velocity; mean/min/max surface temperature and salinity; max annual and seasonal mixed layer depth). Pearson correlations were made between each variable.

Results

The statistical downscaling for the CMIP6 data showing model performance compared with GLORYS12 products is illustrated in Figure 4 for SSP2-4.5, before and after bias corrections respectively. SSP2-4.5 is often considered a likely or middle-of-the-road scenario (Riahi et al., 2017), possibly reflecting the world's current trajectory of policies and development, but it is not necessarily the most likely scenario for the future, as this depends on future government actions and choices.

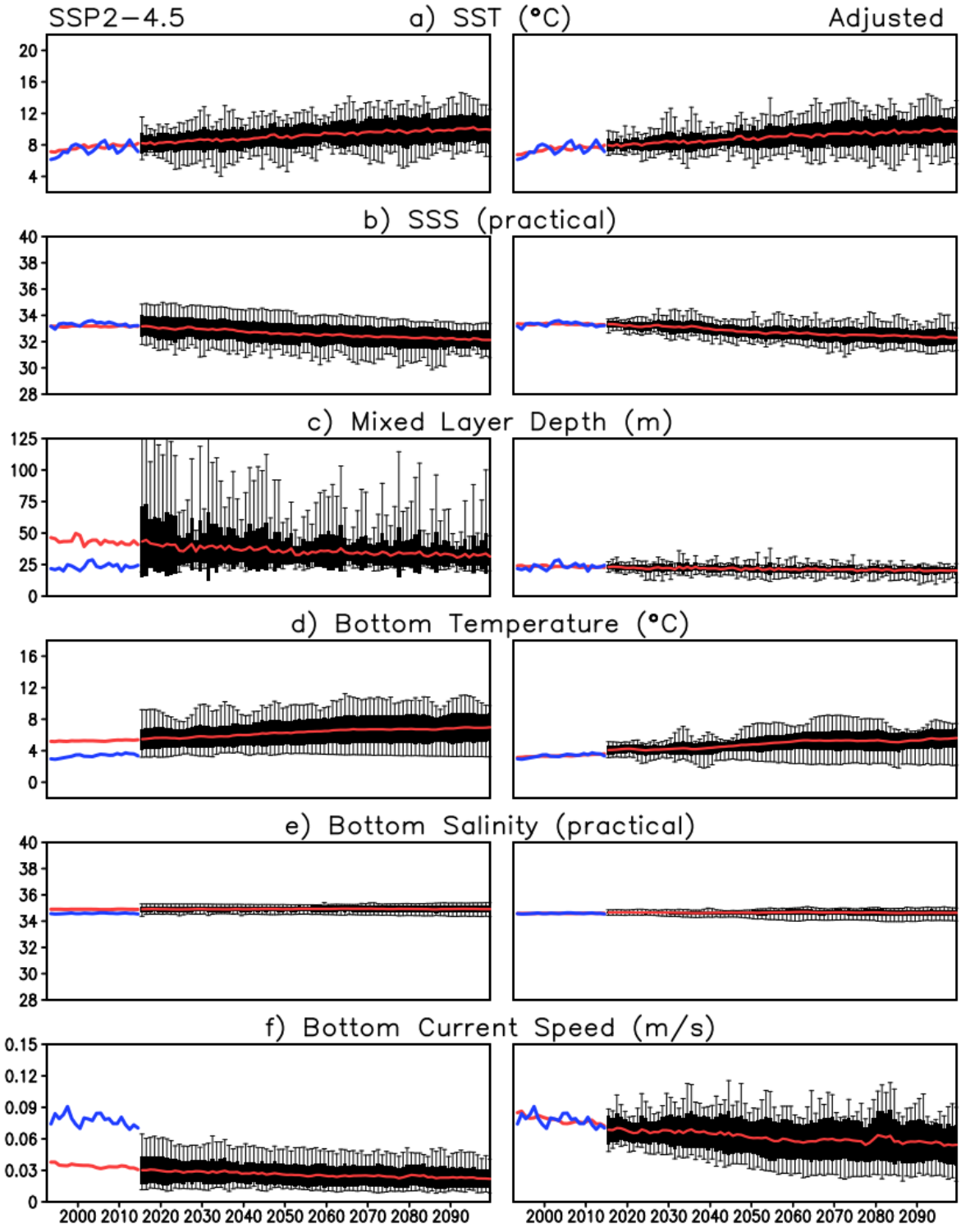

Figure 4. Annual averages and standard deviations among SSP2-4.5 model projections of six variables before (left column) and after (right column) AI mapping for the NAFO study area. Blue lines are the GLORYS12 reference. Red lines are the 22 CMIP6 model ensemble average (Table 1). The black shading indicates one standard deviation above and below the 22-model average and the bars are the two outer model values.

Sea Surface Temperature (SST)

The trends in modeled mean annual SST from 2015 to 2100 show positive slopes for each SSP, with the slope steepening with increasing W/m^2 scenarios (Figure 5). From 2015 to about 2035, mean annual SST for SSP1-2.6 > SSP2-4.5 > SSP3-7.0 > SSP5-8.5, but assumes the expected relationship thereafter (Figure 5), that is SSP1-2.6 < SSP2-4.5 < SSP3-7.0 < SSP5-8.5. The mean annual SST to 2035 is between 7.5 and 8.5°C for all SSP but by 2100 SSP1-2.5 projects mean temperatures of about 9°C while SSP5-8.5 projects temperatures of 12.5°C. Similar results are shown in Table 3 where the mean SST and standard deviations for each SSP and bi-decadal time frame for the full spatial extent are provided. Figure 6 shows that there is very little difference among the mean, minimum, maximum and range values of SST over time under the low emission SSP1-2.6 scenario. As radiative forcing increases the mean, minimum and maximum values averaged over the spatial extent show increases with highest values under SSP5-8.5, while the range in SST values remains more similar (Table 3, Figure 6). The effect of SSP becomes more pronounced after P2 (2040-2059) in P3 (2060-2079), and P4 (2080-2099).

The spatial distribution of the variables is shown in Figures 7, 8, 9 and 10 for each variable for SSP1-2.6 and SSP5-8.5. There is a clear increase in modeled mean SST across all parts of the NAFO study area but on Flemish Cap and Grand Bank in particular (Figure 8). Similar patterns are seen with the minimum (Figure 8) and maximum (Figure 9) SST, which show SST of 28°C on the Tail of Grand Bank in P4 (2080-2099). The greatest range in SST was seen on the Tail of Grand Bank (Figure 9).

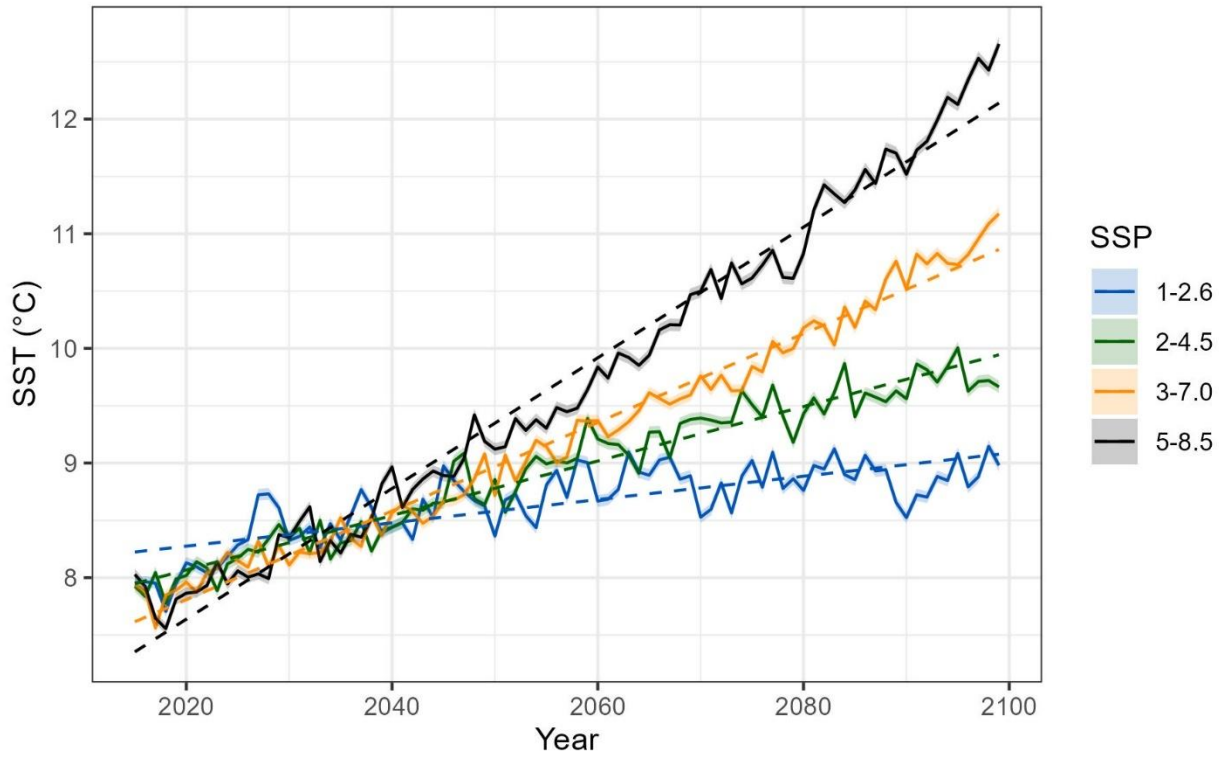

Figure 5. Annual mean Sea Surface Temperature (SST) in °C trends from the 22 ensembled CMIP6 models for the NAFO study area are shown for each of four Shared Socio-economic Pathways (SSPs) and each year from 2015 to 2100. Dashed lines indicate linear fit to the data. Shaded areas are the 95% confidence intervals for the ensembled means.

Table 3. The mean ± standard deviation from the 22 ensembled CMIP6 models of Sea Surface Temperature (SST) in °C for the NAFO study area for each of four Shared Socio-economic Pathways (SSPs) and time periods.

SSP	2020-2039	2040-2059	2060-2079	2080-2099
1-2.6	8.39 ± 1.77	8.68 ± 1.88	8.84 ± 1.92	8.89 ± 1.89
2-4.5	8.26 ± 1.76	8.82 ± 1.89	9.31 ± 1.88	9.66 ± 1.88
3-7.0	8.21 ± 1.83	8.88 ± 1.83	9.62 ± 1.89	10.59 ± 1.90
5-8.5	8.22 ± 1.79	9.16 ± 1.90	10.33 ± 1.91	11.76 ± 1.86

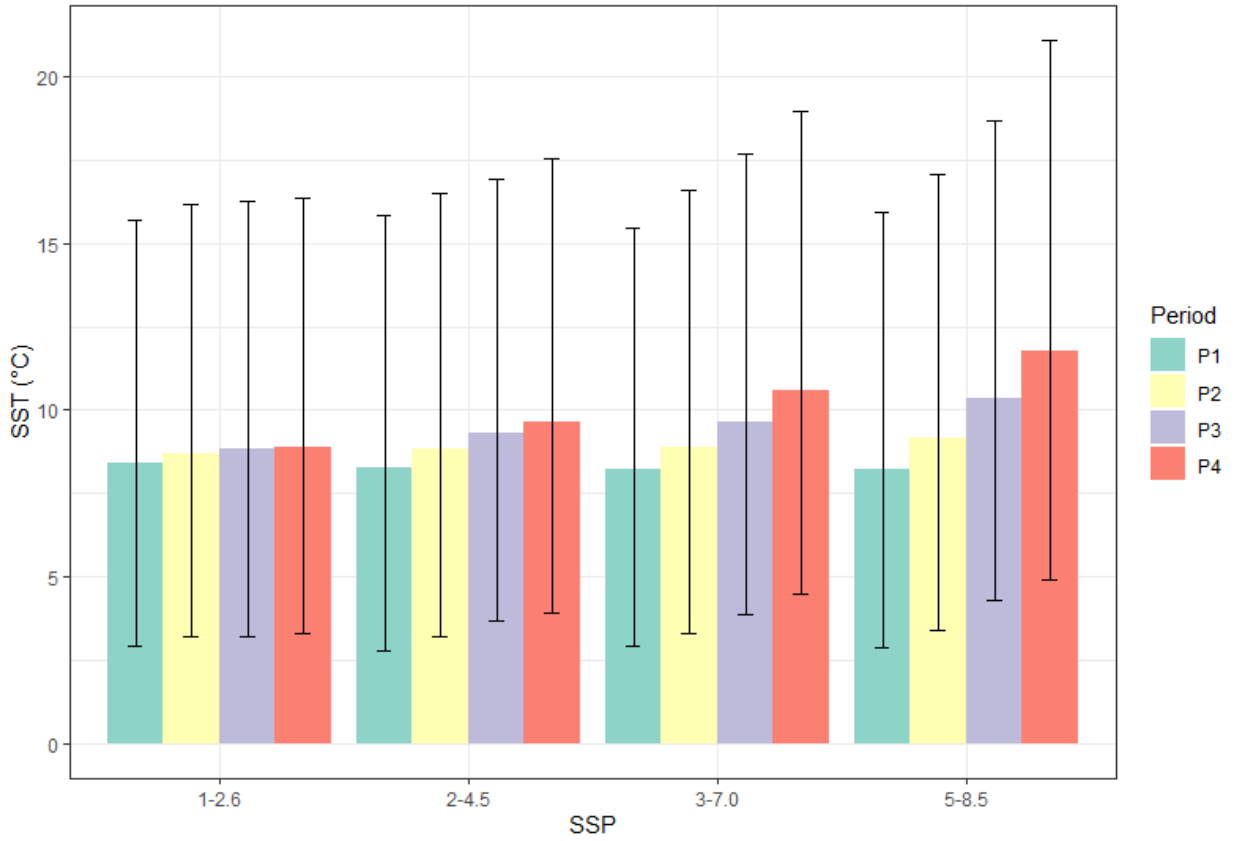

Figure 6. The mean Sea Surface Temperature (SST) in °C from the 22 ensembled CMIP6 models for the NAFO study area is shown for each of four Shared Socio-economic Pathways (SSPs) and time periods (P1: 2020-2039, P2: 2040-2059, P3: 2060-2079, P4: 2080-2099). Bars represent minimum, maximum values and range of the data products averaged over the spatial extent.

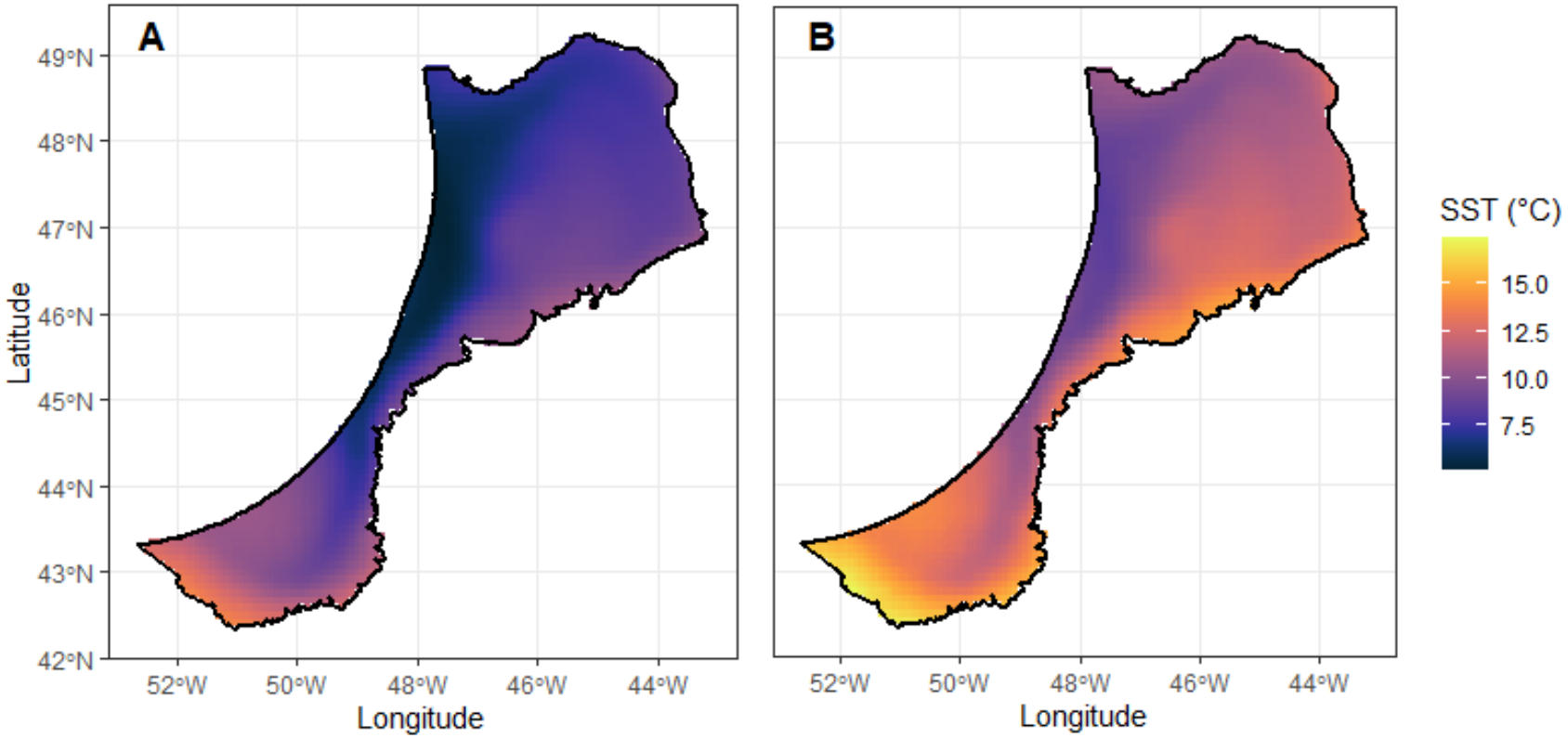

Figure 7. The spatial distribution of Mean Sea Surface Temperature (SST) (°C) from the 22 ensembled CMIP6 models for the NAFO study area. **A)** Time period 2020-2039 for Shared Socio-economic Pathway (SSP) 1-2.6. **B)** Time period 2080-2099 for Shared Socio-economic Pathway (SSP) 5-8.5.

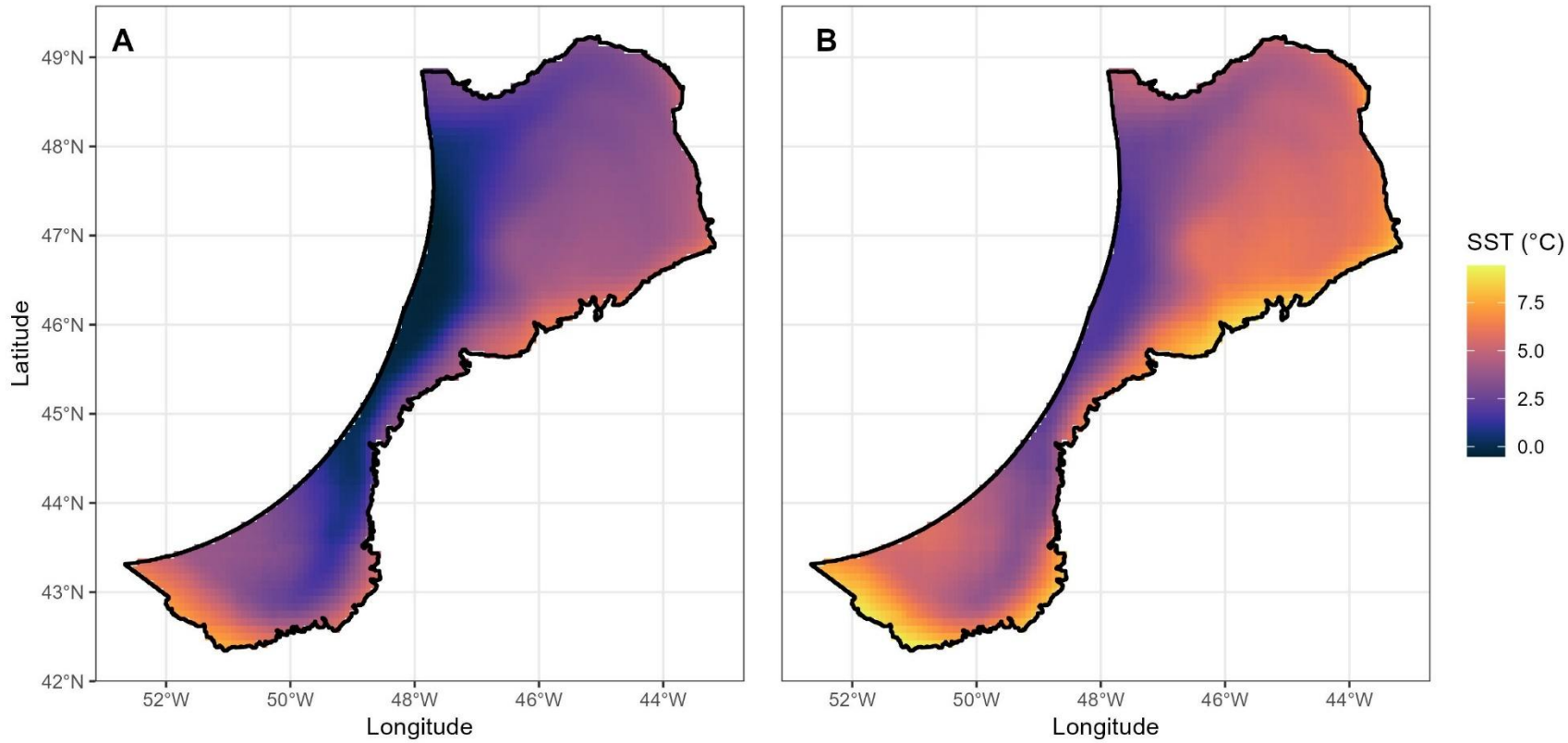

Figure 8. The spatial distribution of Minimum Mean Sea Surface Temperature (SST) (°C) from the 22 ensembled CMIP6 models for the NAFO study area. **Left panel.** Averaged for the time period 2020-2039 for Shared Socio-economic Pathway (SSP) 1-2.6. **Right panel.** Averaged for the time period 2080-2099 for Shared Socio-economic Pathway (SSP) 5-8.5.

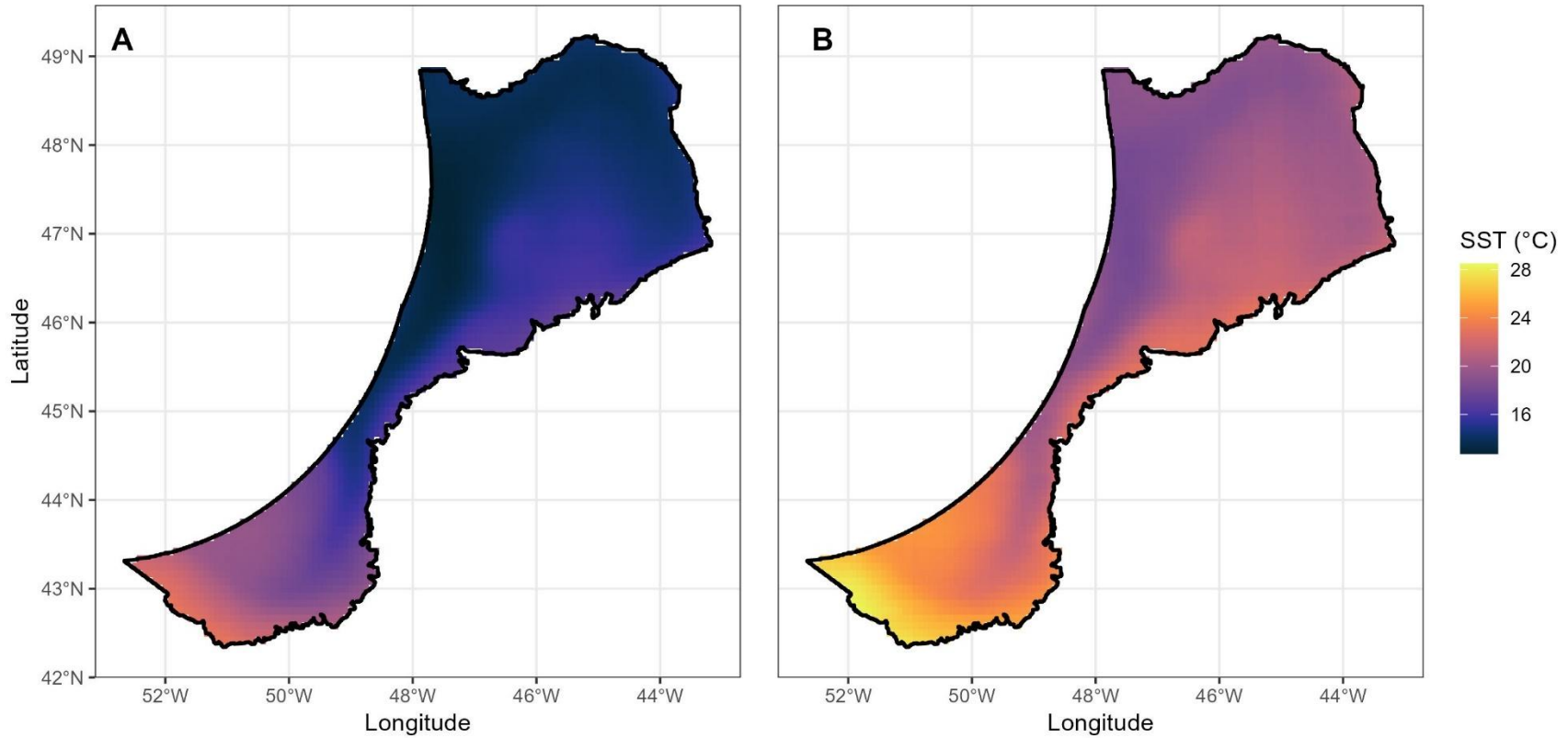

Figure 9. The spatial distribution of Maximum Mean Sea Surface Temperature (SST) (°C) from the 22 ensembled CMIP6 models for the NAFO study area. **Left panel.** Averaged for the time period 2020-2039 for Shared Socio-economic Pathway (SSP) 1-2.6. **Right panel.** Averaged for the time period 2080-2099 for Shared Socio-economic Pathway (SSP) 5-8.5.

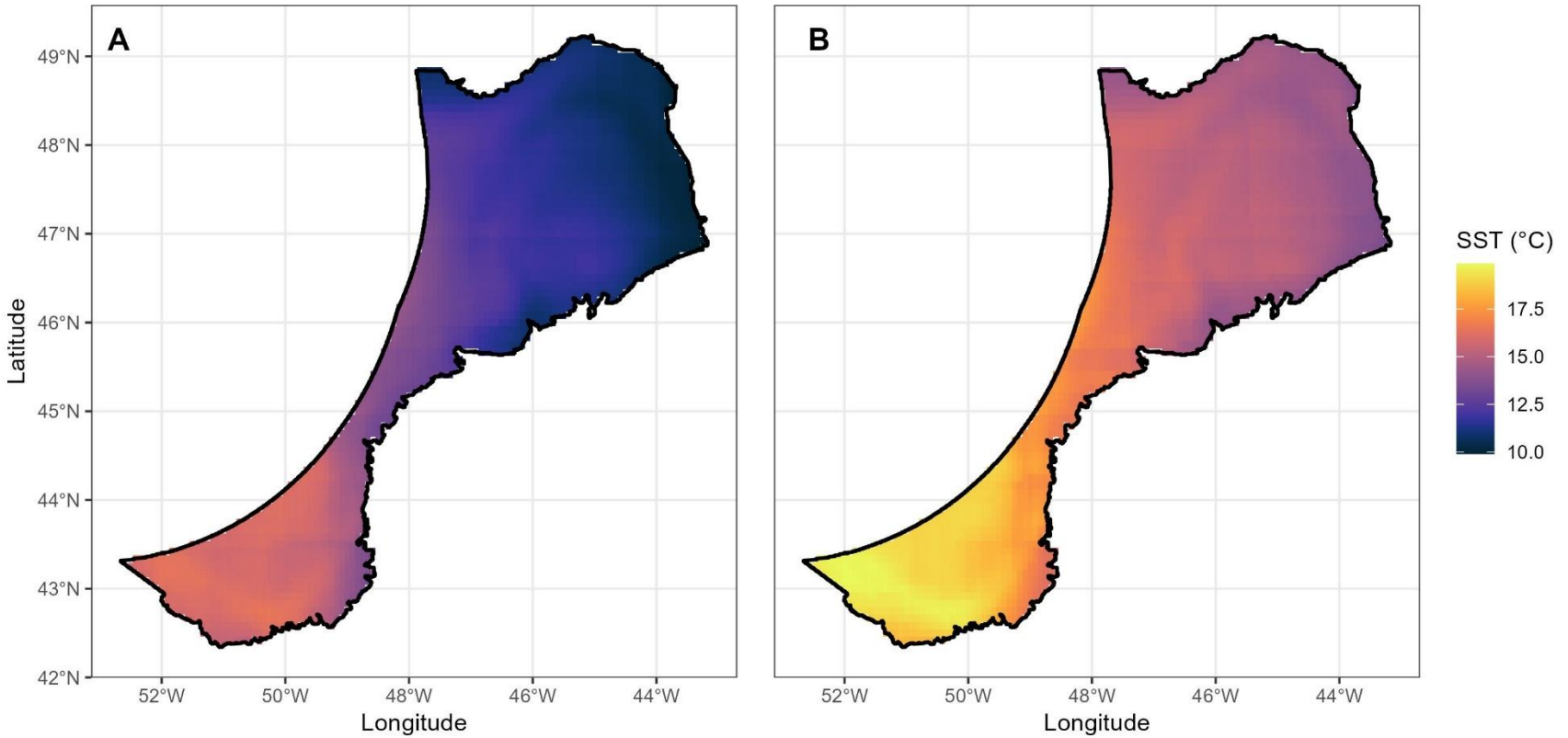

Figure 10. The spatial distribution of Range of Mean Sea Surface Temperature (SST) (°C) from the 22 ensembled CMIP6 models for the NAFO study area. **Left panel.** Averaged for the time period 2020-2039 for Shared Socio-economic Pathway (SSP) 1-2.6. **Right panel.** Averaged for the time period 2080-2099 for Shared Socio-economic Pathway (SSP) 5-8.5.

Sea Surface Salinity (SSS)

The trends in modeled mean annual SSS from 2015 to 2100 show negative slopes for each SSP, with the slope steepening with SSP and time period (Figure 11) as expected due to increased precipitation and melting ice (Greenan et al., 2018). The mean annual SSS ranges from 33.12 to 31.98 (Table 4) reflecting the predicted slight long-term freshening of upper-ocean waters in this region (Greenan et al., 2018). Figure 12 shows that there is very little effect of SSP within a time period, except for Period 4, but that within each SSP there lower SSS over time.

The spatial distribution of the variables is shown in Figures 13, 14, 15 and 16 for each variable for SSP1-2.6 and SSP5-8.5. There is a clear decrease in modeled mean SSS across all parts of the NAFO study area with mean SSS lowest on the Tail of Grand Bank in each SSP (Figure 13). Similar patterns are seen with the minimum (Figure 14) and maximum (Figure 15) SSS. The greatest range in SSS was seen on the Tail of Grand Bank under SSP5-8.5 in Period 4 (Figure 16).

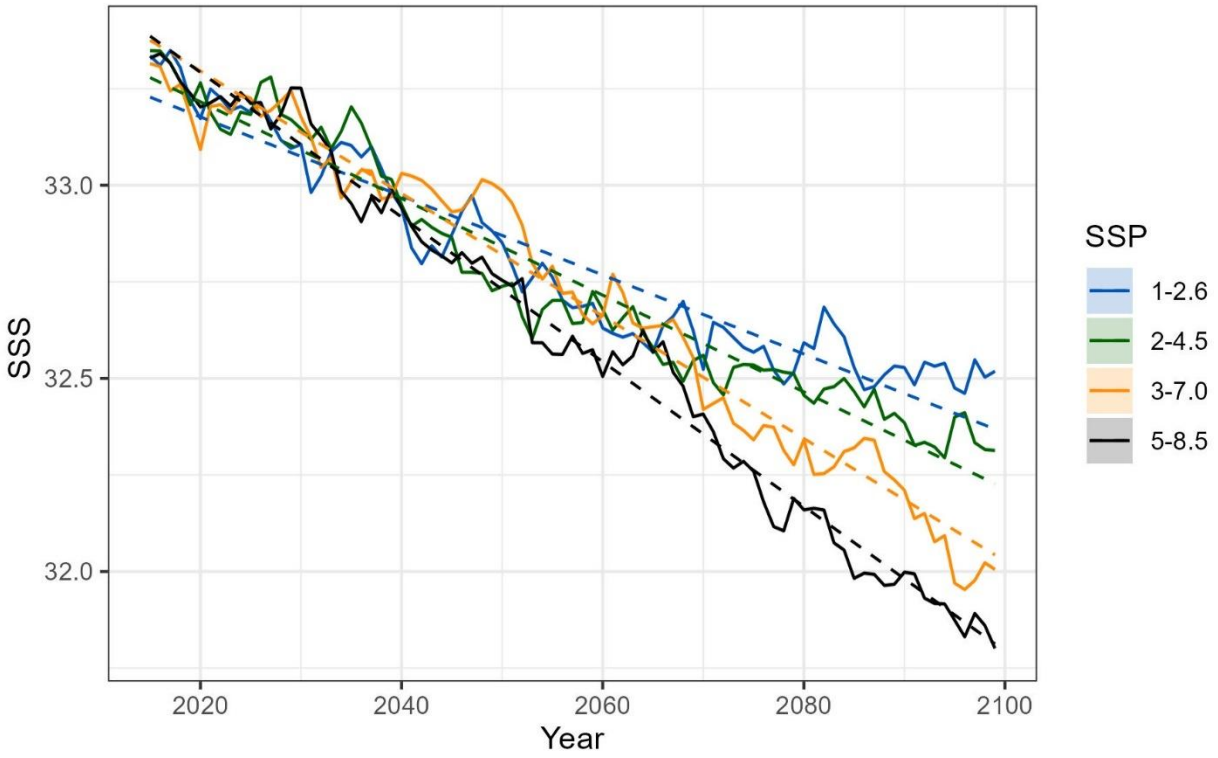

Figure 11. Annual mean Sea Surface Salinity (SSS) trends from the 22 ensembled CMIP6 models for the NAFO study area are shown for each of four Shared Socio-economic Pathways (SSPs) and each year from 2015 to 2100. Dashed lines indicate linear fit to the data. Shaded areas are the 95% confidence intervals for the ensembled means.

Table 4. The mean ± standard deviation from the 22 ensembled CMIP6 models of Sea Surface Salinity (SSS) for the NAFO study area for each of four Shared Socio-economic Pathways (SSPs) and time periods.

SSP	2020-2039	2040-2059	2060-2079	2080-2099
1-2.6	33.12 ± 0.53	32.81 ± 0.53	32.60 ± 0.54	32.54 ± 0.53
2-4.5	33.16 ± 0.56	32.76 ± 0.55	32.56 ± 0.56	32.40 ± 0.55
3-7.0	33.12 ± 0.56	32.89 ± 0.62	32.51 ± 0.59	32.18 ± 0.59
5-8.5	33.12 ± 0.57	32.73 ± 0.55	32.39 ± 0.58	31.98 ± 0.58

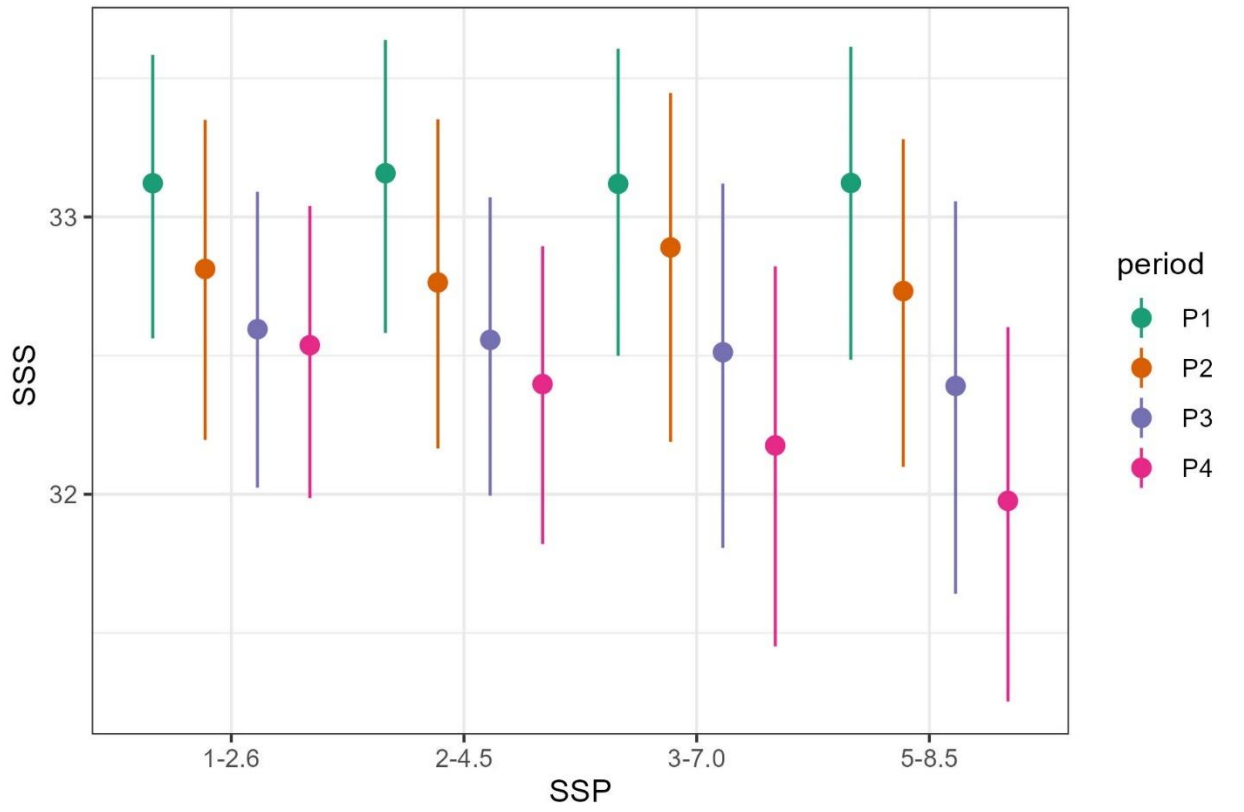

Figure 12. The mean Sea Surface Salinity (SSS) from the 22 ensembled CMIP6 models for the NAFO study area is shown for each of four Shared Socio-economic Pathways (SSPs) and time periods (P1: 2020-2039, P2: 2040-2059, P3: 2060-2079, P4: 2080-2099). Bars represent minimum, maximum values and range of the data products averaged over the spatial extent.

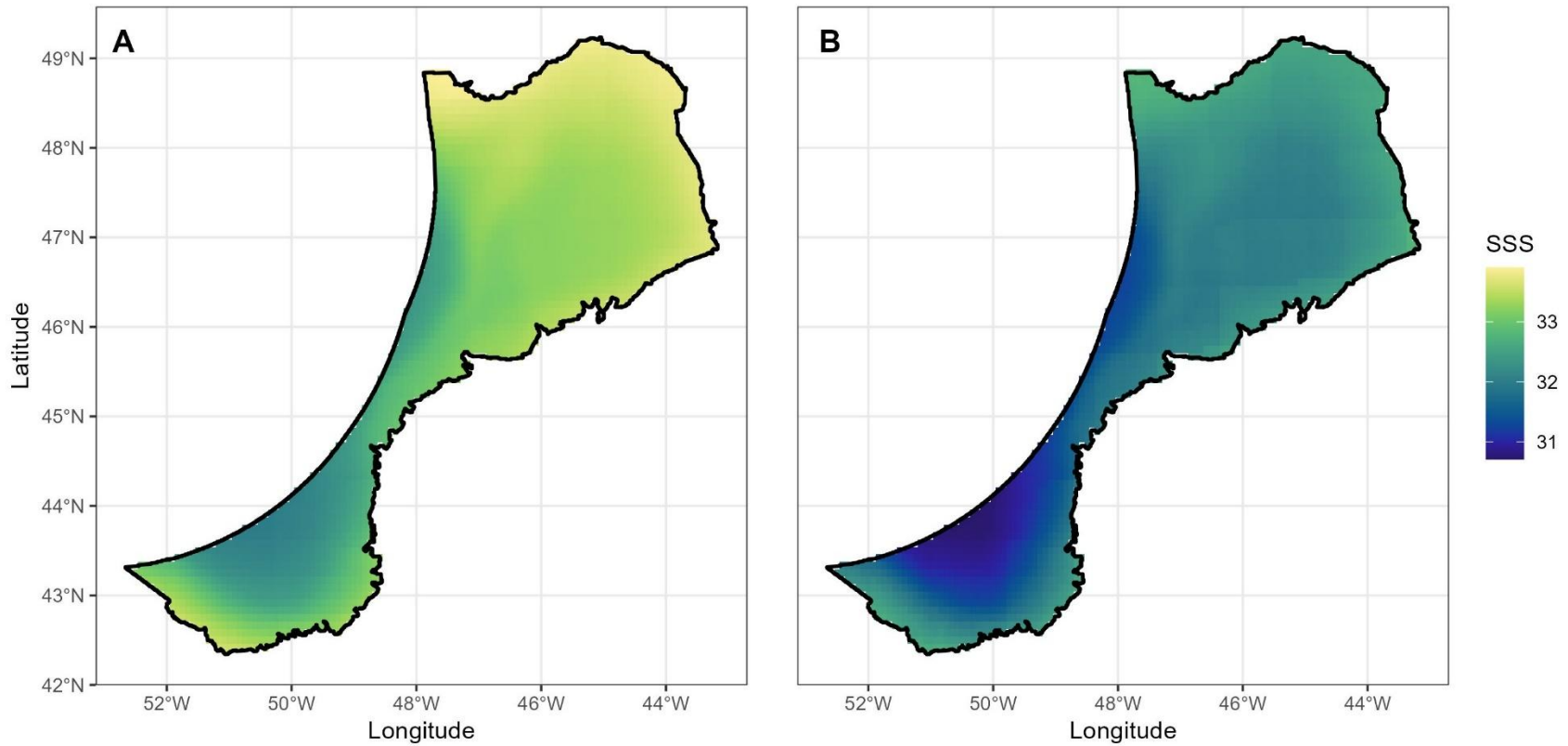

Figure 13. The spatial distribution of Mean Sea Surface Salinity (SSS) from the 22 ensembled CMIP6 models for the NAFO study area. **A)** Time period 2020-2039 for Shared Socio-economic Pathway (SSP) 1-2.6. **B)** Time period 2080-2099 for Shared Socio-economic Pathway (SSP) 5-8.5.

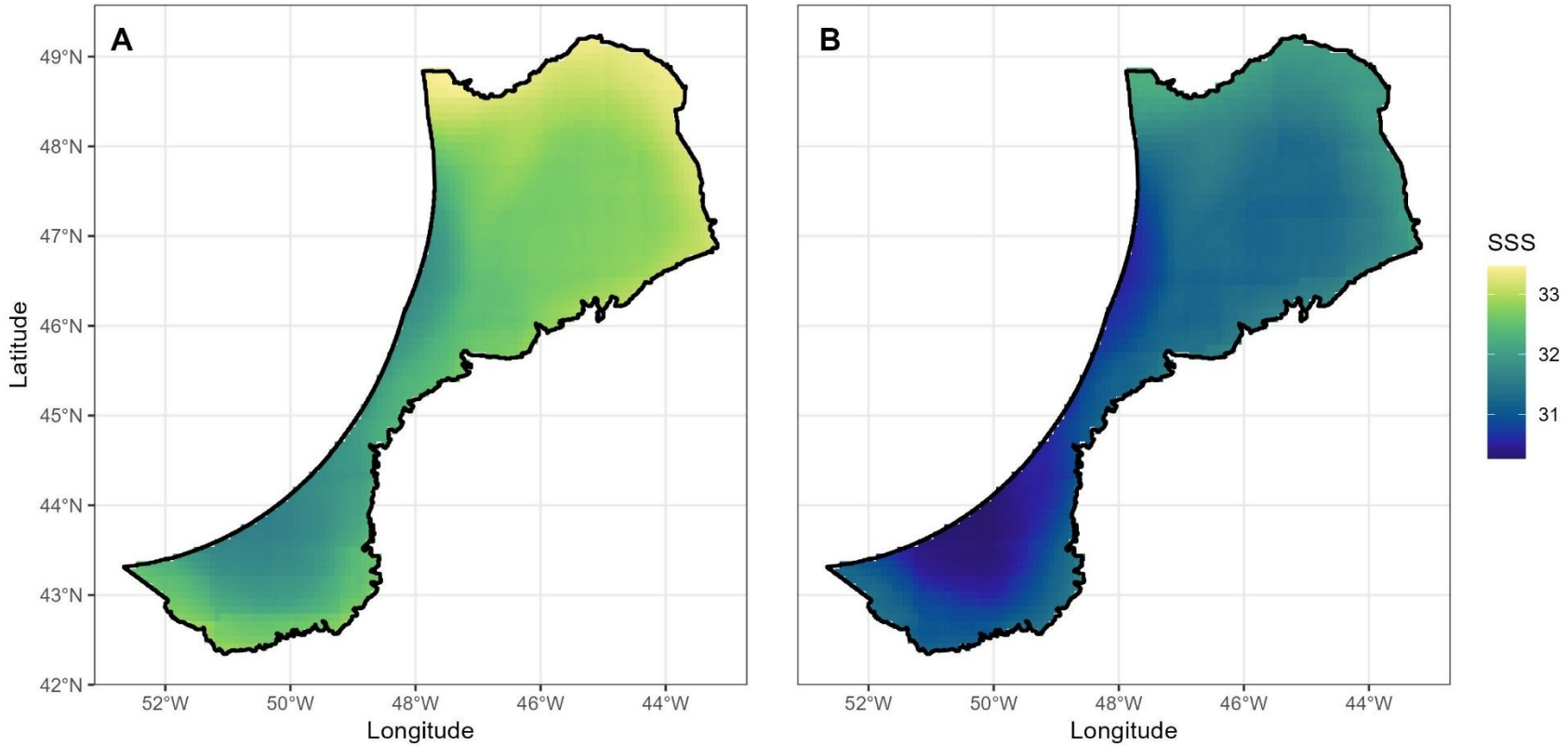

Figure 14. The spatial distribution of Minimum Mean Sea Surface Salinity (SSS) from the 22 ensembled CMIP6 models for the NAFO study area. **Left panel.** Averaged for the time period 2020-2039 for Shared Socio-economic Pathway (SSP) 1-2.6. **Right panel.** Averaged for the time period 2080-2099 for Shared Socio-economic Pathway (SSP) 5-8.5.

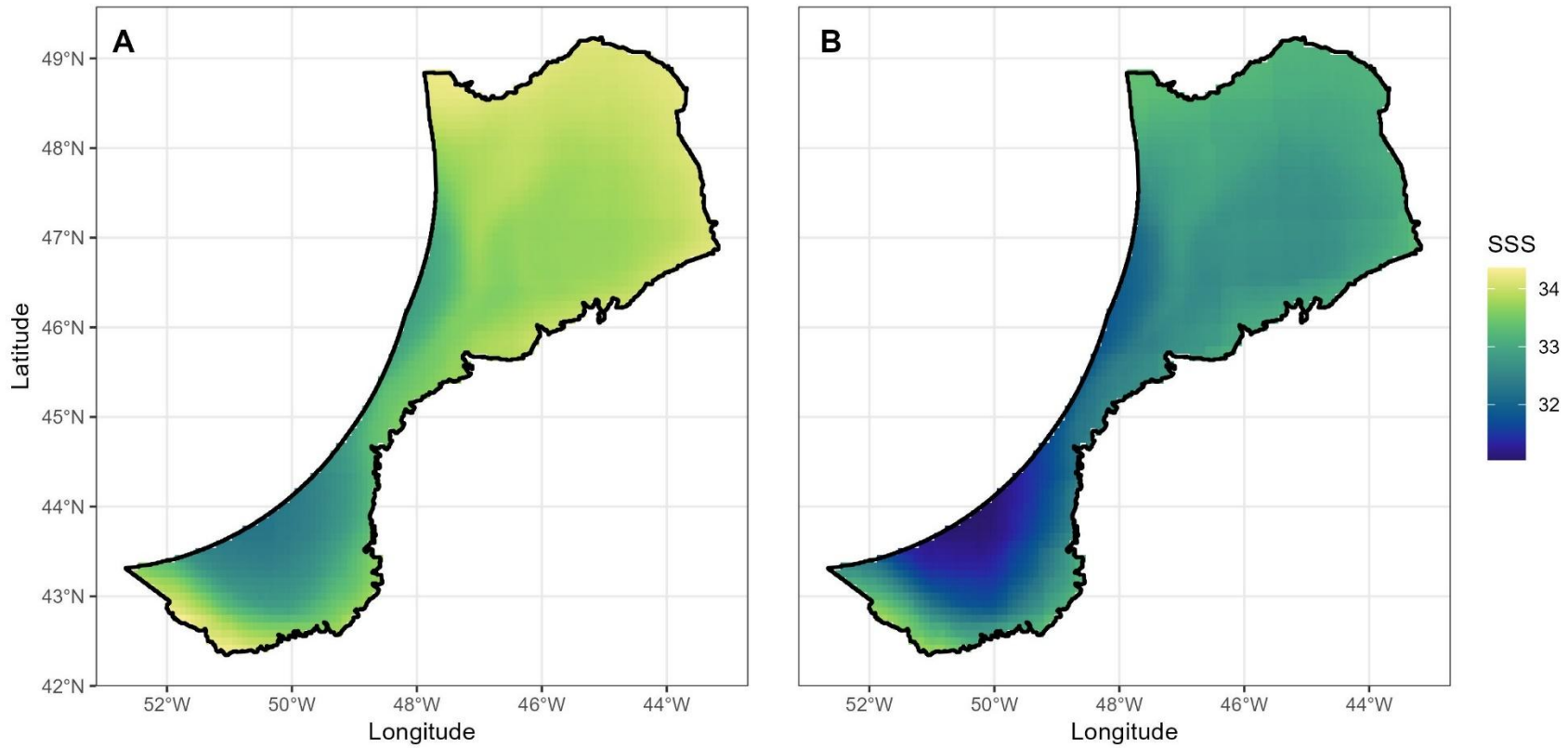

Figure 15. The spatial distribution of Maximum Mean Sea Surface Salinity (SSS) from the 22 ensembled CMIP6 models for the NAFO study area. **Left panel.** Averaged for the time period 2020-2039 for Shared Socio-economic Pathway (SSP) 1-2.6. **Right panel.** Averaged for the time period 2080-2099 for Shared Socio-economic Pathway (SSP) 5-8.5.

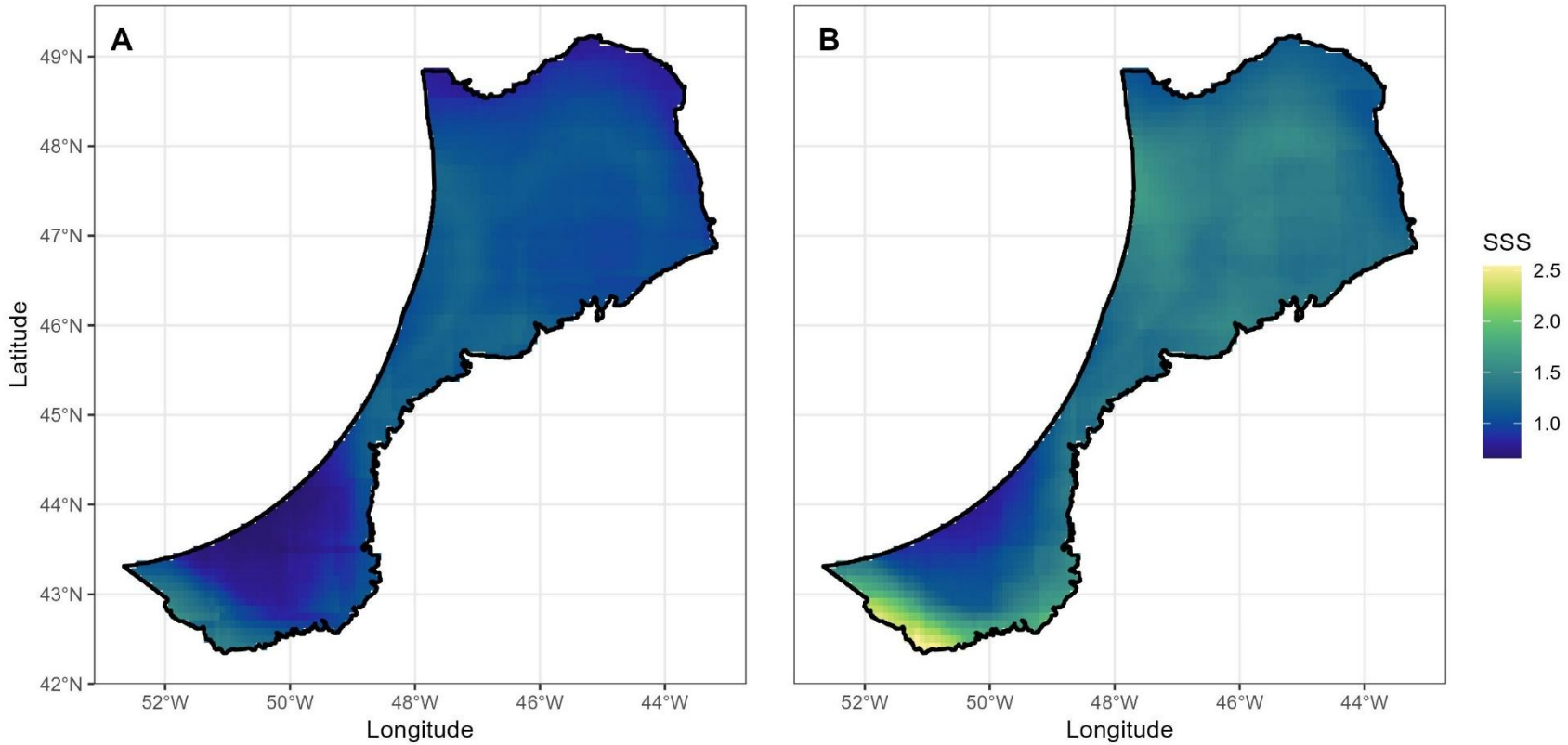

Figure 16. The spatial distribution of Range of Mean Sea Surface Salinity (SSS) from the 22 ensembled CMIP6 models for the NAFO study area. **Left panel.** Averaged for the time period 2020-2039 for Shared Socio-economic Pathway (SSP) 1-2.6. **Right panel.** Averaged for the time period 2080-2099 for Shared Socio-economic Pathway (SSP) 5-8.5.

Mixed Layer Depth (MLD)

The trends in modeled mean mixed layer depth (MLD) from 2015 to 2100 show negative slopes for each SSP, with the slope steepening with SSP and time period (Figure 17). This is consistent with the expectation that Mixed Layer Depth (MLD) in the northwest Atlantic is decreasing due to increasing upper-ocean stratification caused by surface warming (SST) and freshening (SSS) (Greenan et al., 2018). The mean annual MLD ranges from 19.13 to 22.24 m (Table 5). Figure 18 shows the effect of SSP is more pronounced in P3 and P4.

The spatial distribution of the variables is shown in Figures 19, 20, 21 and 22 for each variable for SSP1-2.6 and SSP5-8.5. There is a clear decrease in modeled mean MLD (m) across all parts of the NAFO study area with shallower depths on the Tail of Grand Bank and the deepest MLD at the top of Flemish Pass (Figure 139). Minimum mean MLD was variable over the spatial extent (Figure 20) while maximum MLD (Figure 21) and range (Figure 22) were more similar to the mean in spatial distribution.

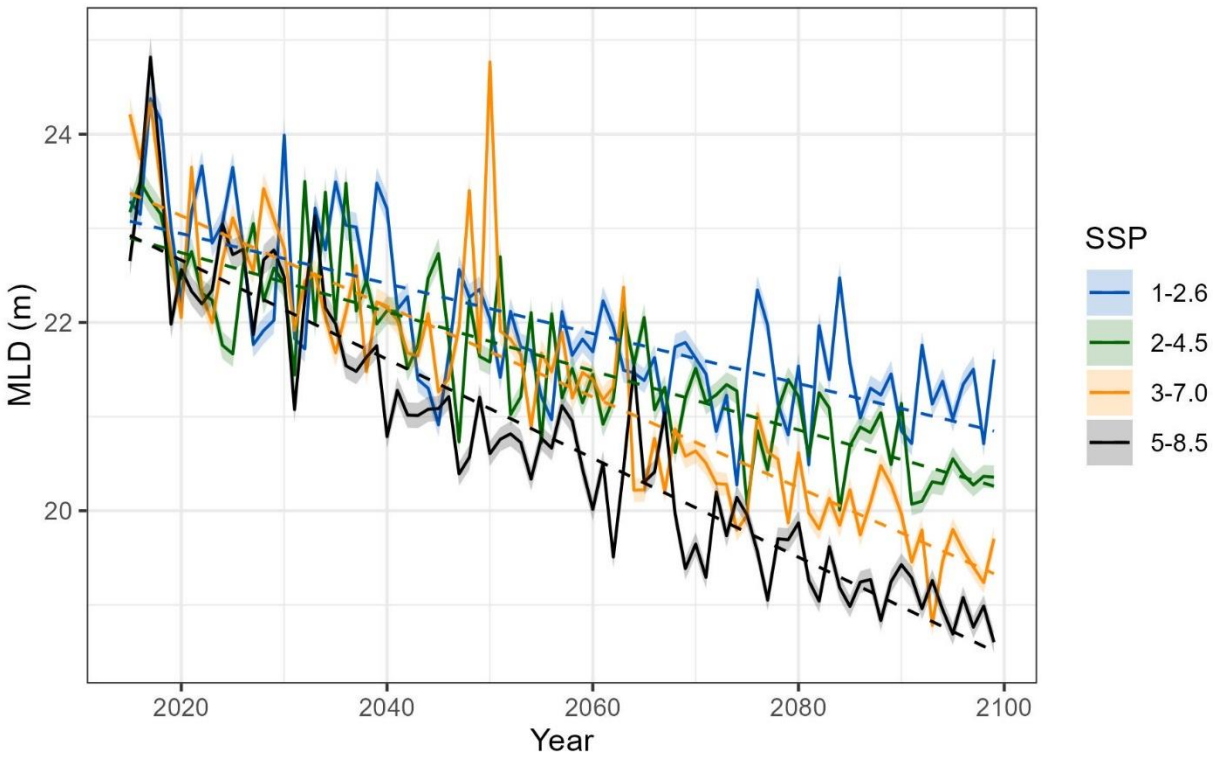

Figure 17. Annual mean Mixed Layer Depth (MLD) (m) trends from the 22 ensembled CMIP6 models for the NAFO study area are shown for each of four Shared Socio-economic Pathways (SSPs) and each year from 2015 to 2100. Dashed lines indicate linear fit to the data. Shaded areas are the 95% confidence intervals for the ensembled means.

Table 5. The mean ± standard deviation from the 22 ensembled CMIP6 models of Mixed Layer Depth (MLD (m) for the NAFO study area for each of four Shared Socio-economic Pathways (SSPs) and time periods.

SSP	2020-2039	2040-2059	2060-2079	2080-2099
1-2.6	22.80 ± 13.86	21.84 ± 12.84	21.47 ± 12.29	21.32 ± 12.20
2-4.5	22.42 ± 13.69	21.72 ± 12.76	21.19 ± 12.11	20.60 ± 11.37
3-7.0	22.47 ± 13.54	21.90 ± 13.38	20.63 ± 11.86	19.82 ± 11.16
5-8.5	22.24 ± 13.61	20.84 ± 11.92	20.01 ± 11.37	19.13 ± 10.63

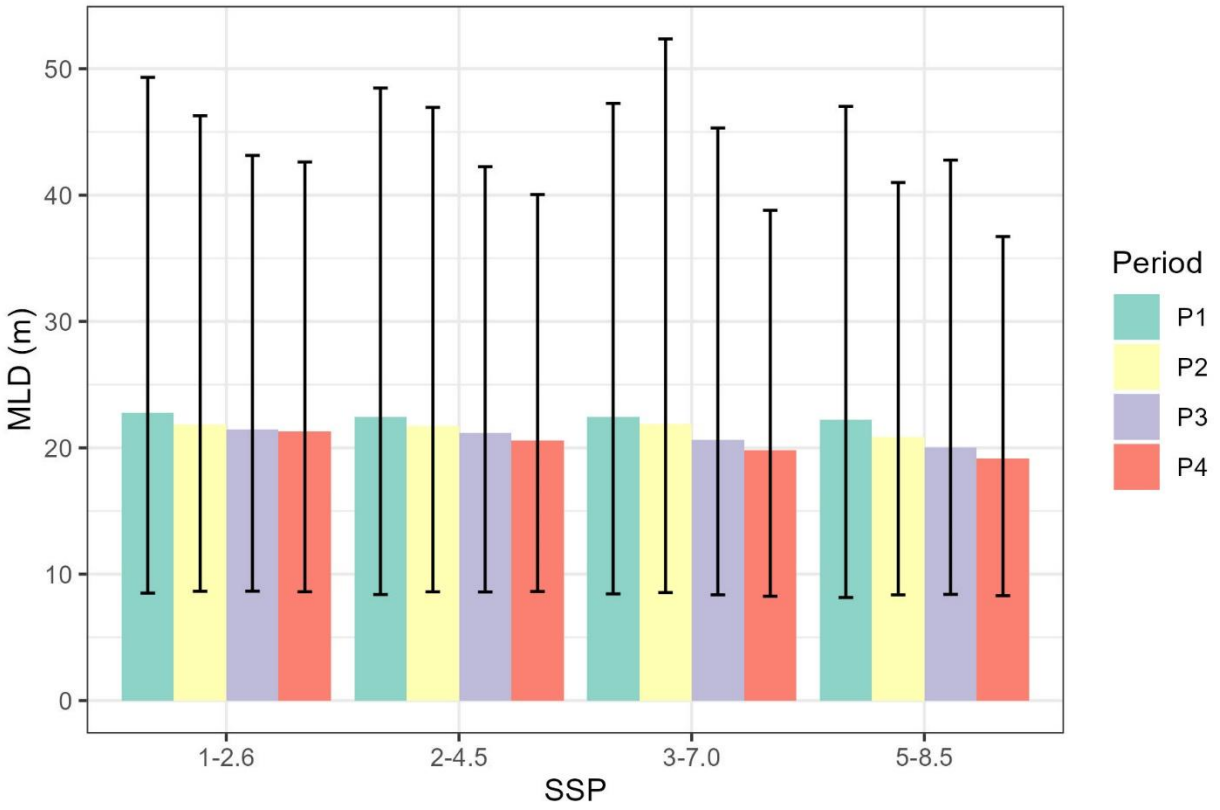

Figure 18. The mean Mixed Layer Depth (MLD) (m) from the 22 ensembled CMIP6 models for the NAFO study area is shown for each of four Shared Socio-economic Pathways (SSPs) and time periods (P1: 2020-2039, P2: 2040-2059, P3: 2060-2079, P4: 2080-2099). Bars represent minimum, maximum values and range of the data products averaged over the spatial extent.

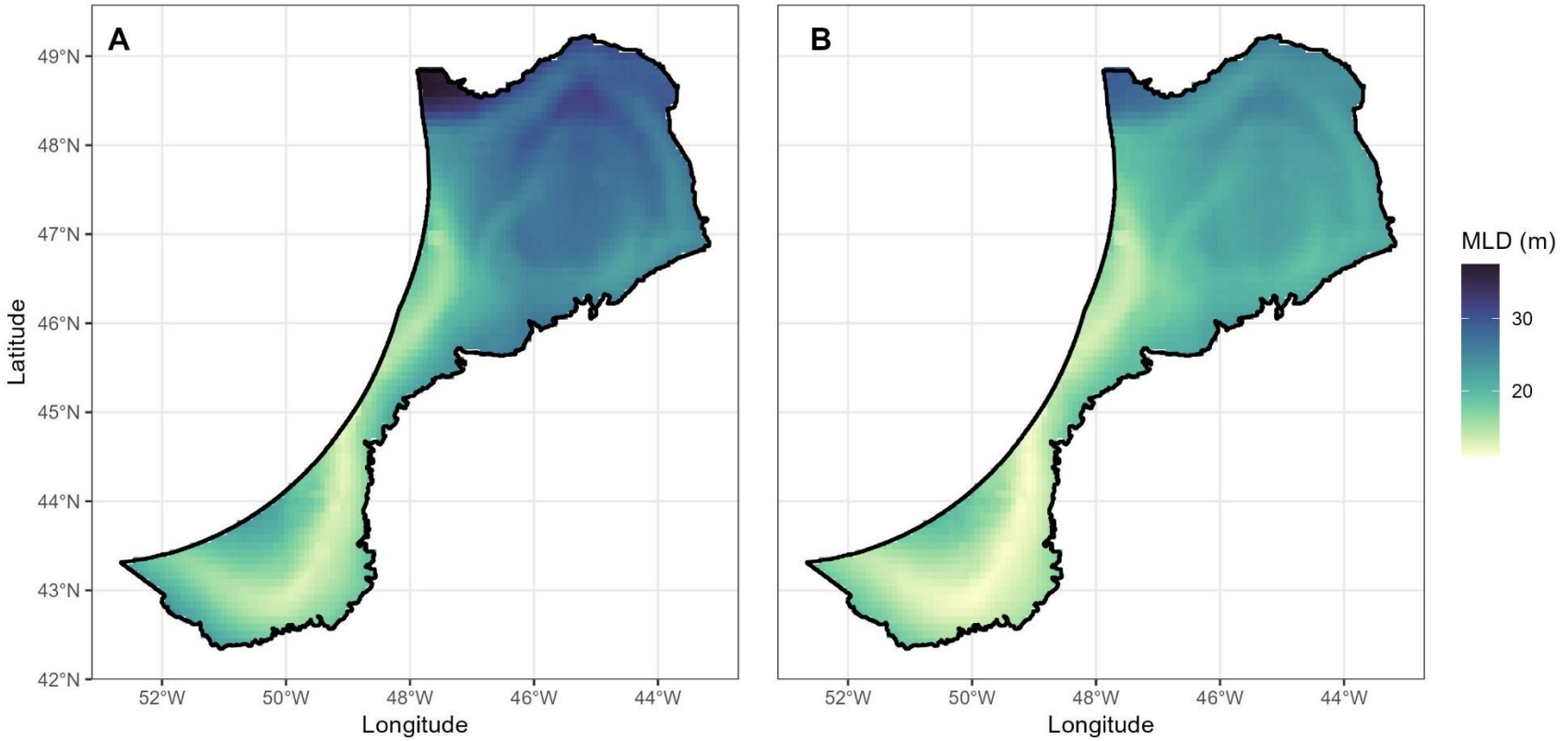

Figure 19. The spatial distribution of Mean Mixed Layer Depth (MLD) from the 22 ensembled CMIP6 models for the NAFO study area. **A)** Time period 2020-2039 for Shared Socio-economic Pathway (SSP) 1-2.6. **B)** Time period 2080-2099 for Shared Socio-economic Pathway (SSP) 5-8.5.

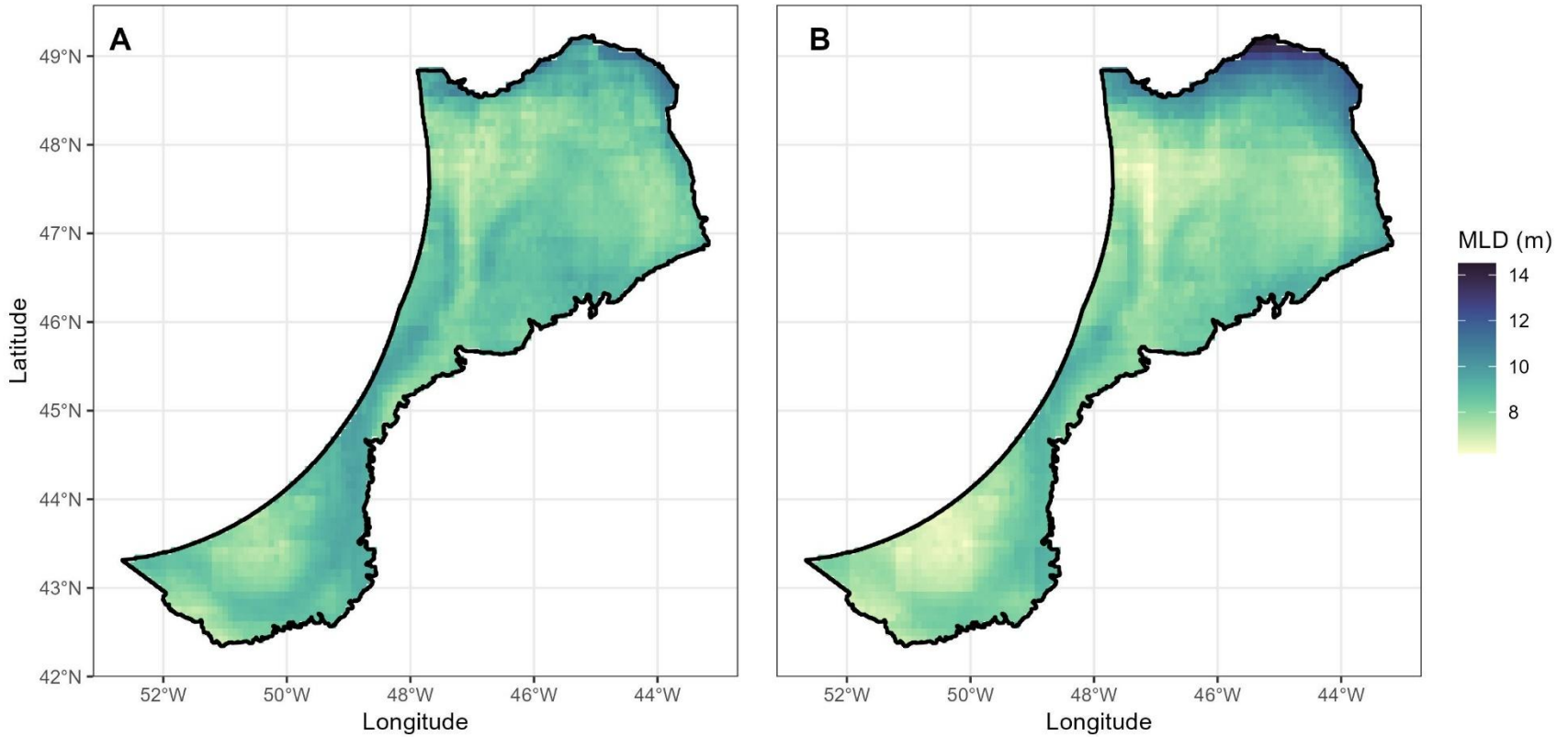

Figure 20. The spatial distribution of Minimum Mean Mixed Layer Depth (MLD) from the 22 ensembled CMIP6 models for the NAFO study area. **Left panel.** Averaged for the time period 2020-2039 for Shared Socio-economic Pathway (SSP) 1-2.6. **Right panel.** Averaged for the time period 2080-2099 for Shared Socio-economic Pathway (SSP) 5-8.5.

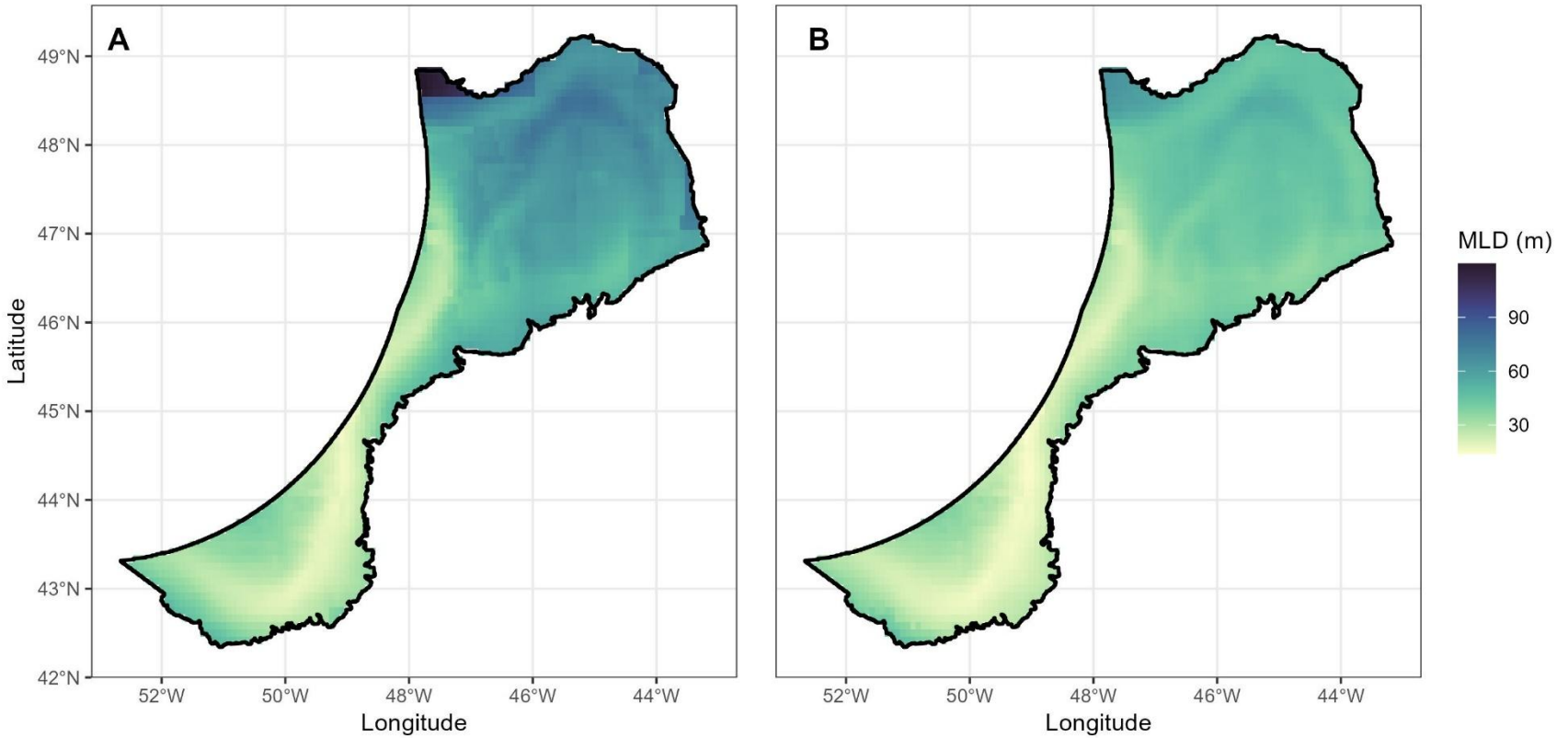

Figure 21. The spatial distribution of Maximum Mean Mixed Layer Depth (MLD) from the 22 ensembled CMIP6 models for the NAFO study area. **Left panel.** Averaged for the time period 2020-2039 for Shared Socio-economic Pathway (SSP) 1-2.6. **Right panel.** Averaged for the time period 2080-2099 for Shared Socio-economic Pathway (SSP) 5-8.5.

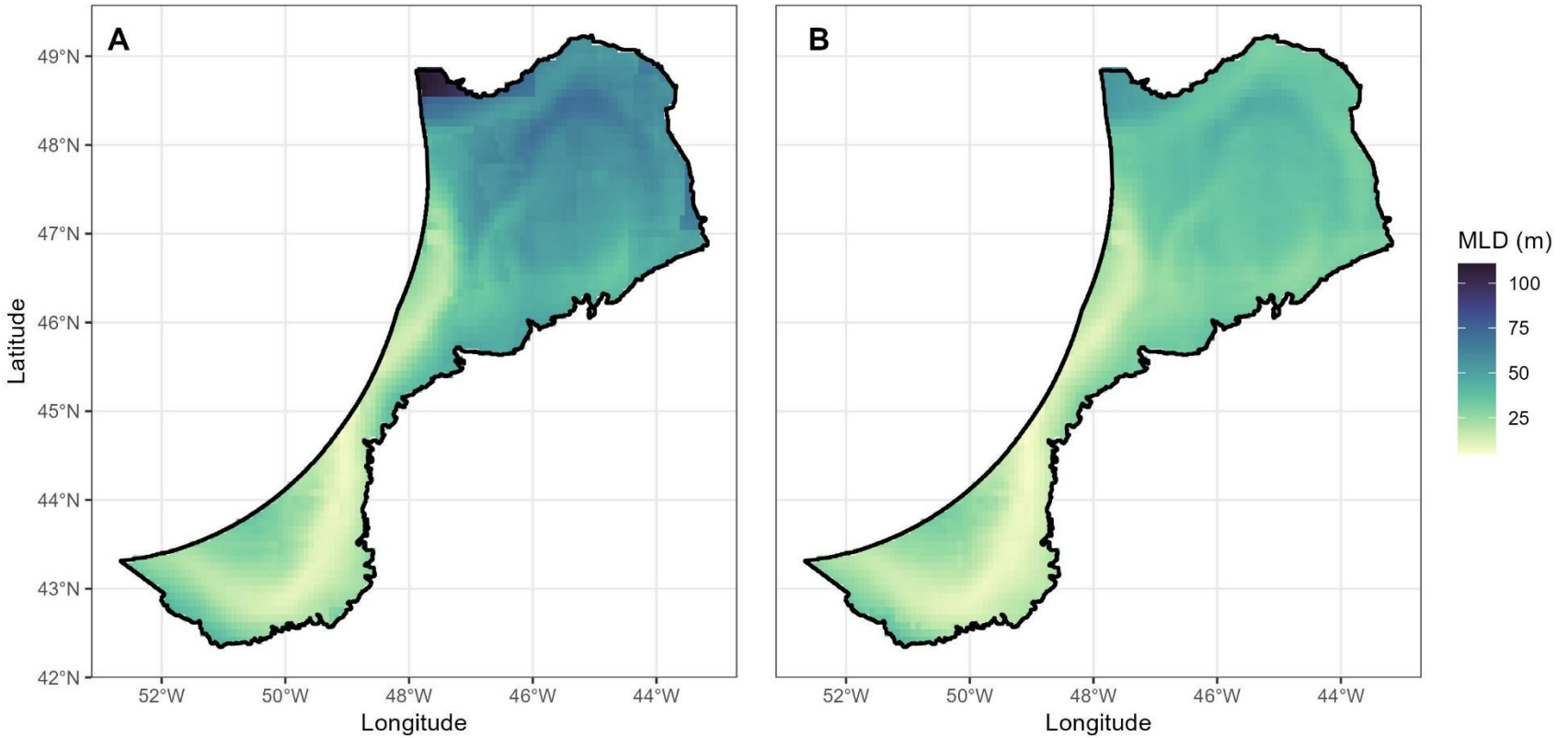

Figure 22. The spatial distribution of Range of Mean Mixed Layer Depth (MLD) from the 22 ensembled CMIP6 models for the NAFO study area. **Left panel.** Averaged for the time period 2020-2039 for Shared Socio-economic Pathway (SSP) 1-2.6. **Right panel.** Averaged for the time period 2080-2099 for Shared Socio-economic Pathway (SSP) 5-8.5.

Summer MLD (MLD_{Su})

Mixed layer depths in the summer months (Table 6) were much shallower than the yearly average (Table 5) and shallowest of the seasonal values. The trends in modeled mean mixed layer depth in the summer months (MLD_{Su}) from 2015 to 2100 show decreasing trends among successive time periods (Figure 23) with steeper declines under SSP3-7.0 and 5-8.5 than the lower emission scenarios (Figure 23). Mean MLD_{Su} ranged from 9.22 in P4 to 10.09 m in P1 (Table 6) with maximum values varying more than minimum values (Figure 24).

The spatial distribution of the variables is shown in Figures 25, 26, 27 and 28 for each variable for SSP1-2.6 and SSP5-8.5.

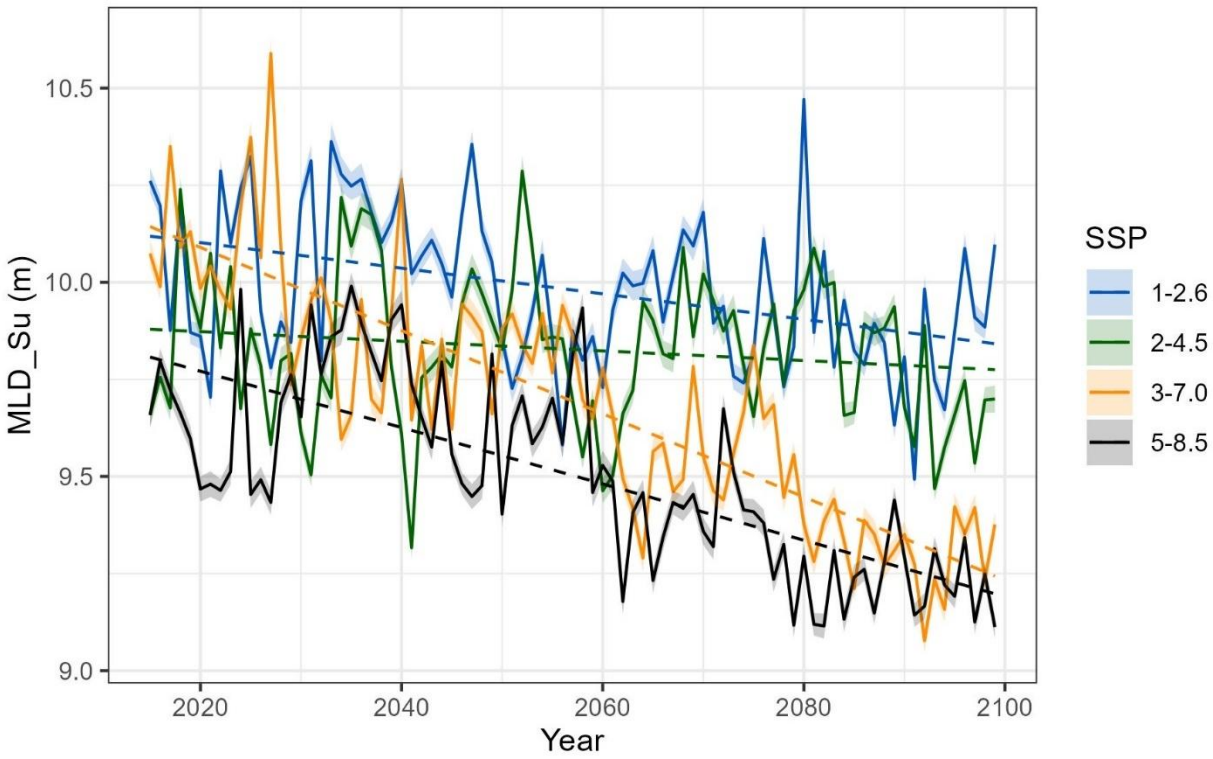

Figure 23. Annual mean Summer Mixed Layer Depth (MLD_{Su}) (m) trends from the 22 ensembled CMIP6 models for the NAFO study area are shown for each of four Shared Socio-economic Pathways (SSPs) and each year from 2015 to 2100. Dashed lines indicate linear fit to the data. Shaded areas are the 95% confidence intervals for the ensembled means.

Table 6. The mean ± standard deviation from the 22 ensembled CMIP6 models of Summer Mixed Layer Depth (MLD_{Su}) (m) for the NAFO study area for each of four Shared Socio-economic Pathways (SSPs) and time periods.

SSP	2020-2039	2040-2059	2060-2079	2080-2099
1-2.6	10.09 ± 1.63	9.98 ± 1.68	9.94 ± 1.65	9.88 ± 1.51
2-4.5	9.87 ± 1.61	9.83 ± 1.55	9.82 ± 1.65	9.77 ± 1.49
3-7.0	9.96 ± 1.66	9.83 ± 1.63	9.57 ± 1.53	9.31 ± 1.47
5-8.5	9.71 ± 1.59	9.65 ± 1.57	9.38 ± 1.50	9.22 ± 1.40

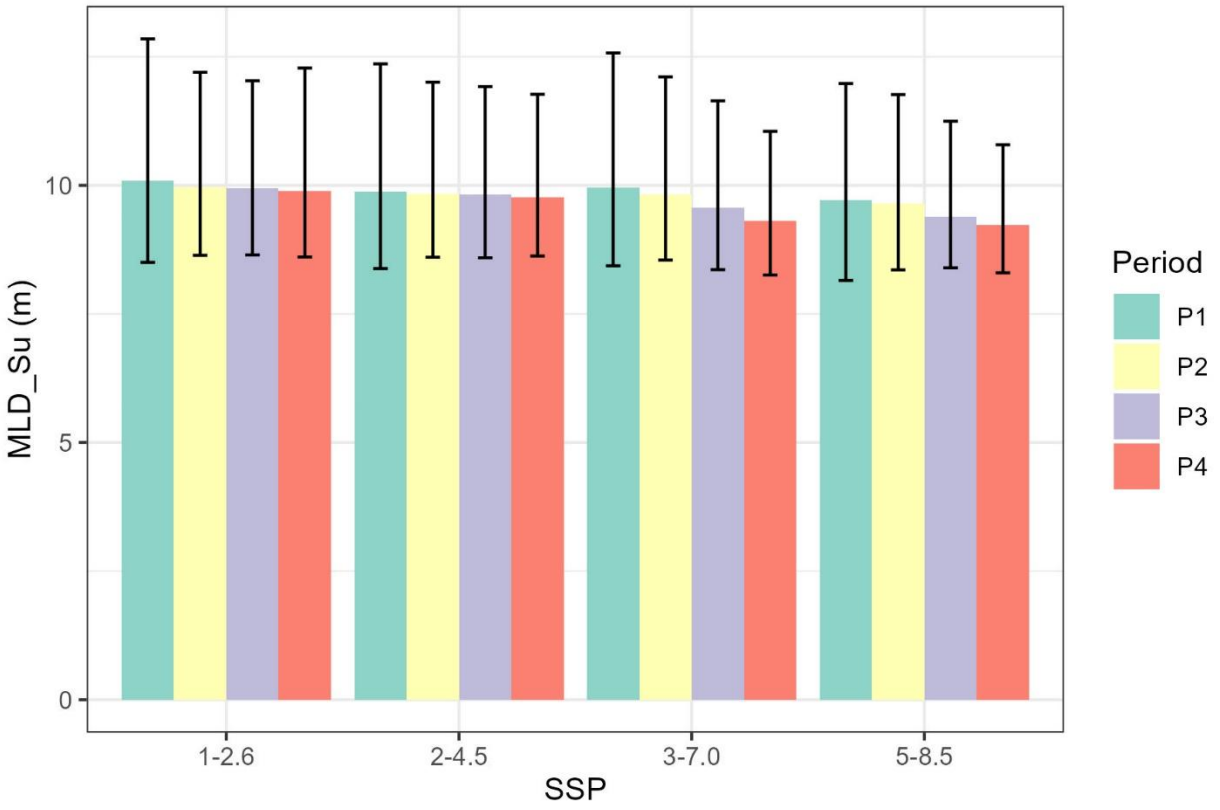

Figure 24. The mean Summer Mixed Layer Depth (MLD_{Su}) (m) from the 22 ensembled CMIP6 models for the NAFO study area is shown for each of four Shared Socio-economic Pathways (SSPs) and periods (P1: 2020-2039, P2: 2040-2059, P3: 2060-2079, P4: 2080-2099). Bars represent minimum, maximum and range of the data products averaged over the spatial extent.

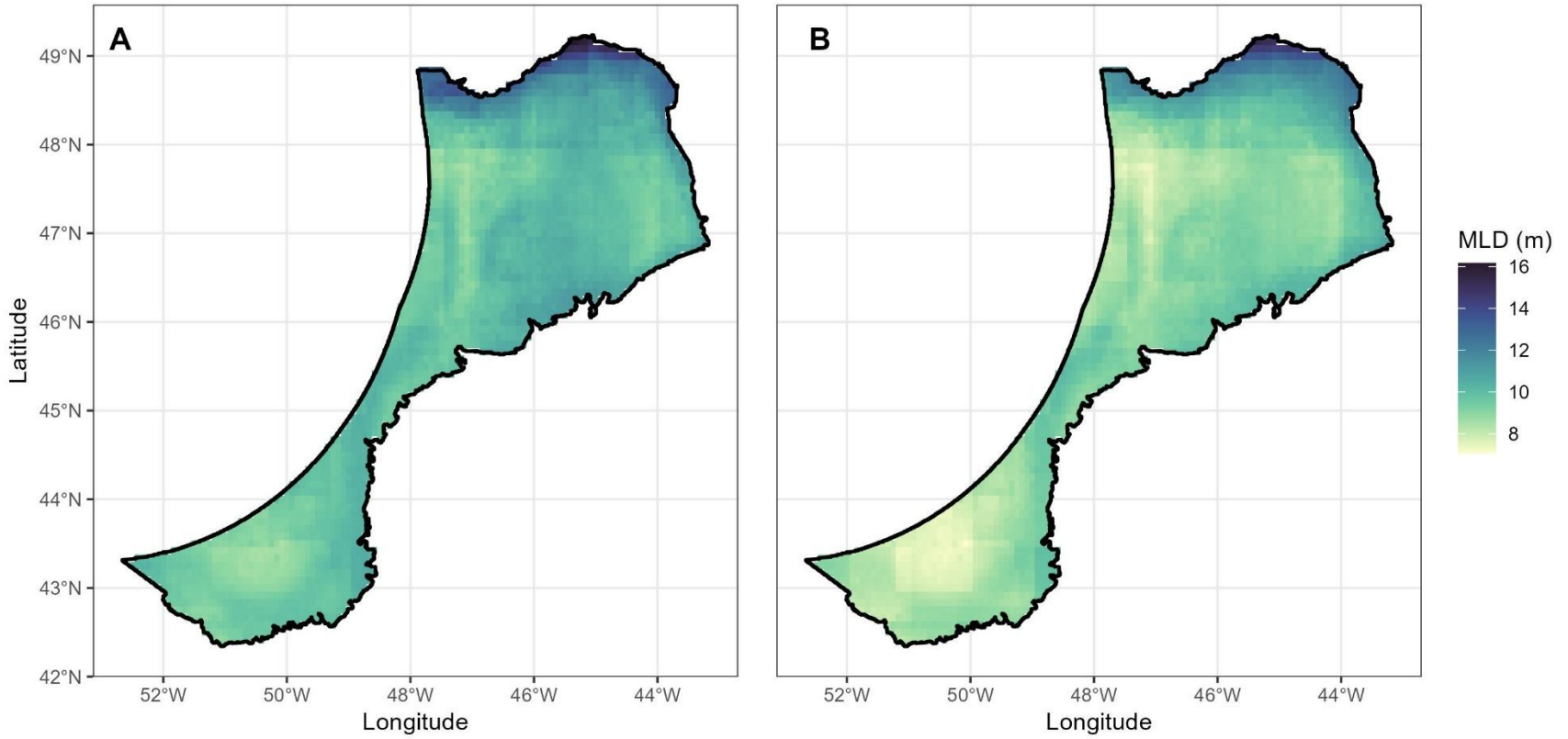

Figure 25. The spatial distribution of Mean Summer Mixed Layer Depth (MLD_{Su}) from the 22 ensembled CMIP6 models for the NAFO study area. **A)** Time period 2020-2039 for Shared Socio-economic Pathway (SSP) 1-2.6. **B)** Time period 2080-2099 for Shared Socio-economic Pathway (SSP) 5-8.5.

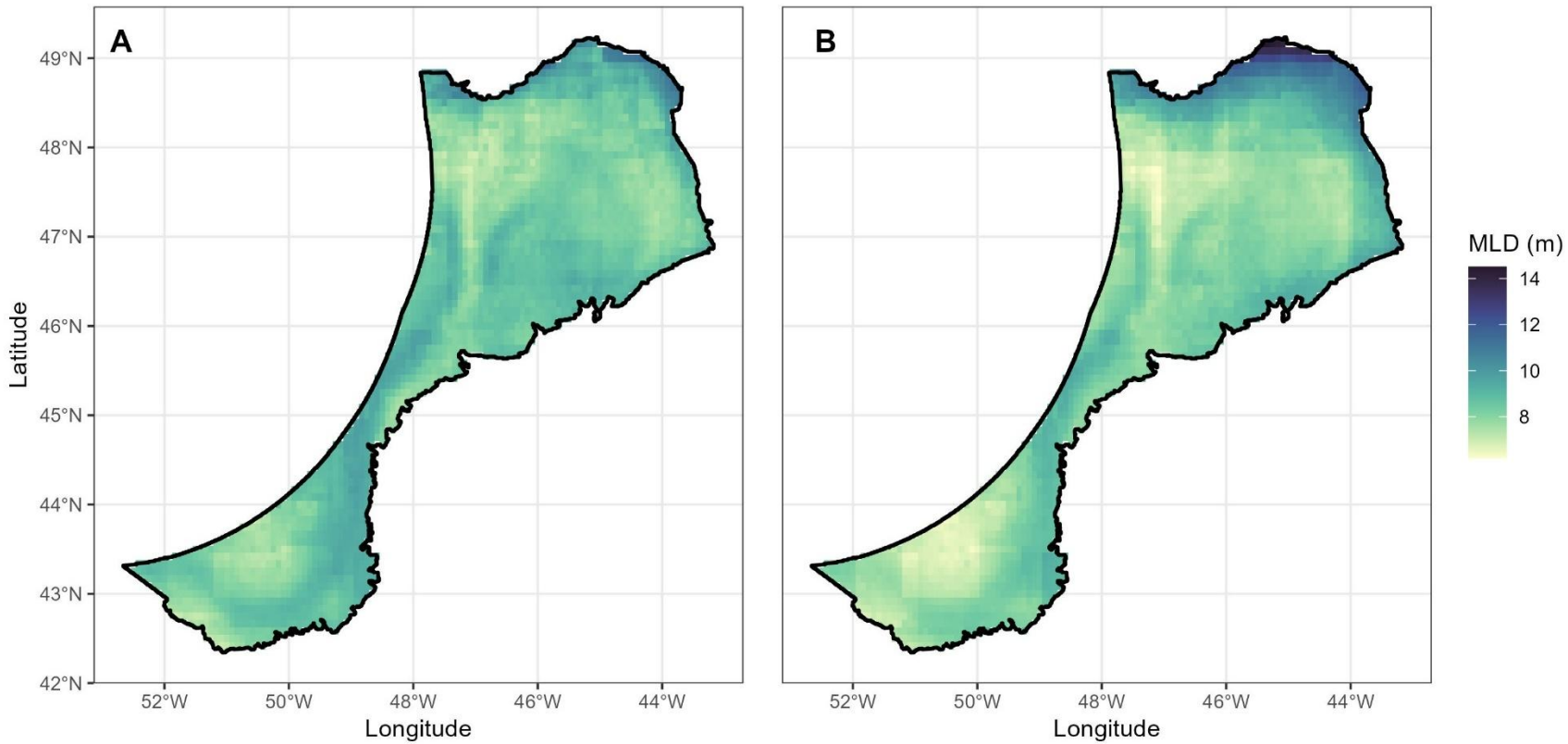

Figure 26. The spatial distribution of Minimum Mean Summer Mixed Layer Depth (MLD_{Su}) from the 22 ensembled CMIP6 models for the NAFO study area. **Left panel.** Averaged for the time period 2020-2039 for Shared Socio-economic Pathway (SSP) 1-2.6. **Right panel.** Averaged for the time period 2080-2099 for Shared Socio-economic Pathway (SSP) 5-8.5.

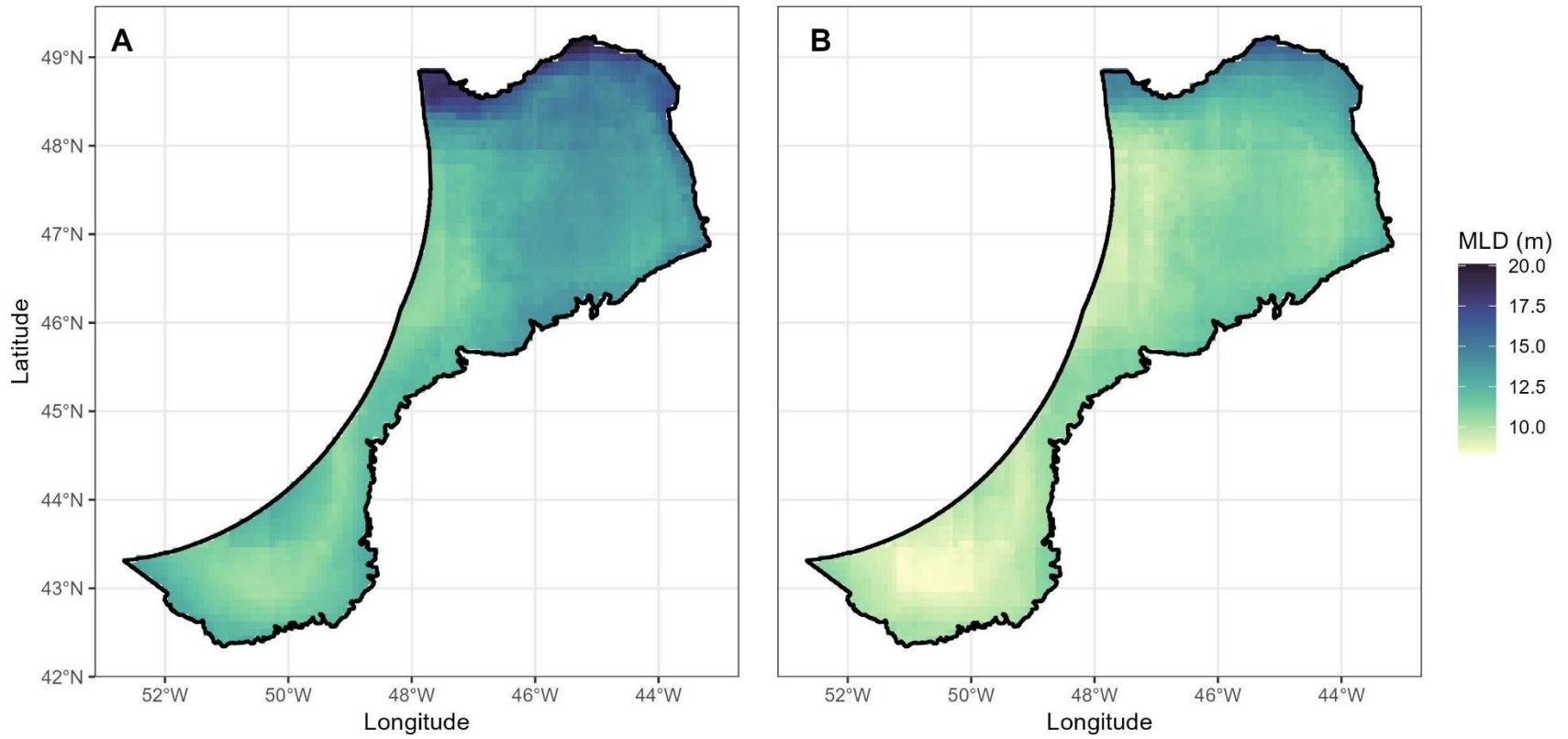

Figure 27. The spatial distribution of Maximum Mean Summer Mixed Layer Depth (MLD_{Su}) from the 22 ensembled CMIP6 models for the NAFO study area. **Left panel.** Averaged for the time period 2020-2039 for Shared Socio-economic Pathway (SSP) 1-2.6. **Right panel.** Averaged for the time period 2080-2099 for Shared Socio-economic Pathway (SSP) 5-8.5.

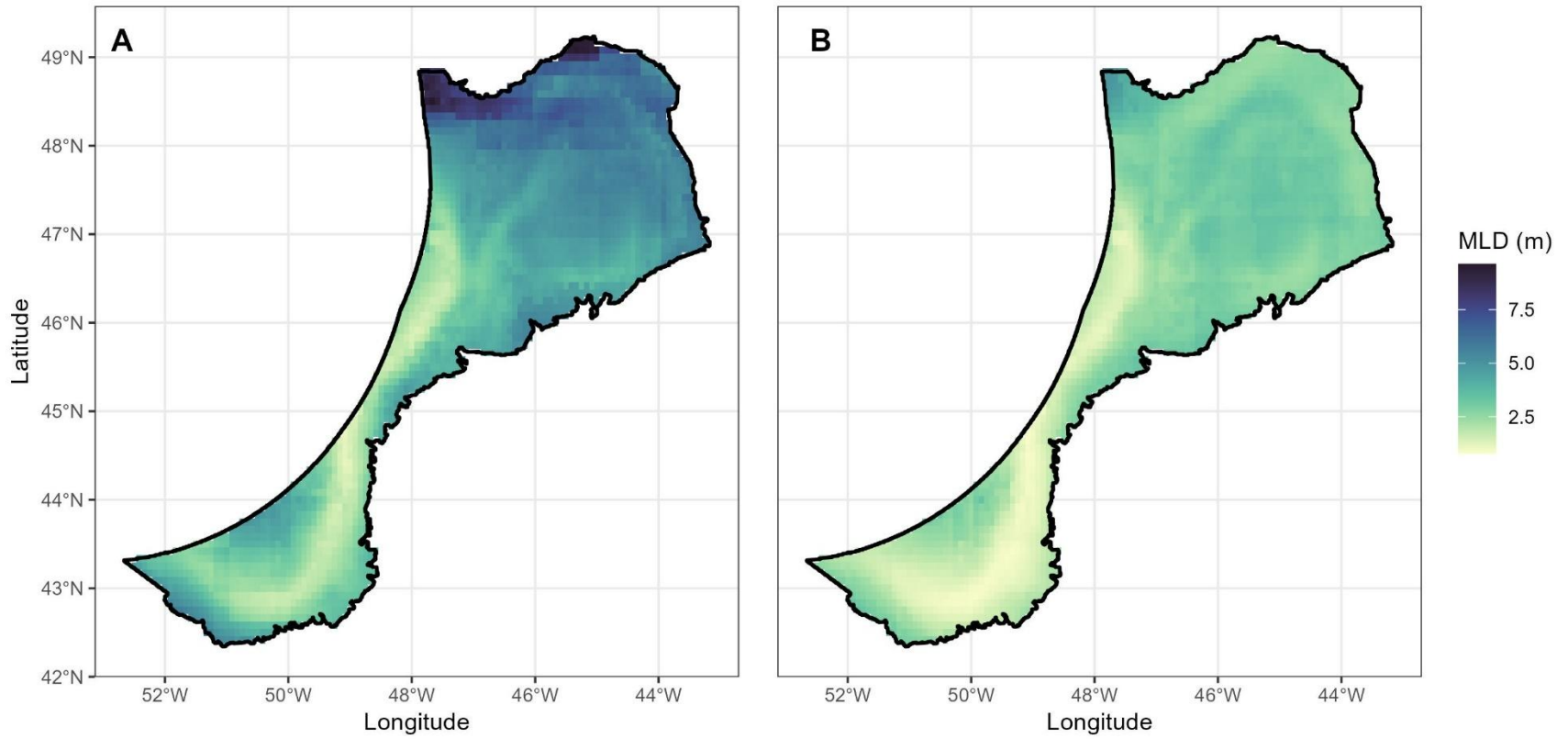

Figure 28. The spatial distribution of Range of Mean Summer Mixed Layer Depth (MLD_{Su}) from the 22 ensembled CMIP6 models for the NAFO study area. **Left panel.** Averaged for the time period 2020-2039 for Shared Socio-economic Pathway (SSP) 1-2.6. **Right panel.** Averaged for the time period 2080-2099 for Shared Socio-economic Pathway (SSP) 5-8.5.

Fall MLD (MLD_F)

Mixed layer depths in the fall months (Table 7) were deeper than the yearly average (Table 5). The trends in modeled mean mixed layer depth in the fall (MLD_F) from 2015 to 2100 show decreasing trends among successive time periods and SSPs (Figure 29) with steeper declines under SSP3-7.0 and 5-8.5 than the lower emission scenarios (Figure 29) but with the distinction less marked than in the summer months (Figure 23). Mean MLD_F ranged from 21.25 in P4 to 24.70 m in P1 (Table 7) with maximum values varying more than minimum values (Figure 30).

The spatial distribution of the variables is shown in Figures 31, 32, 33 and 34 for each variable for SSP1-2.6 and SSP5-8.5. The largest range in values was seen on the northern extent of the study area (Figure 34).

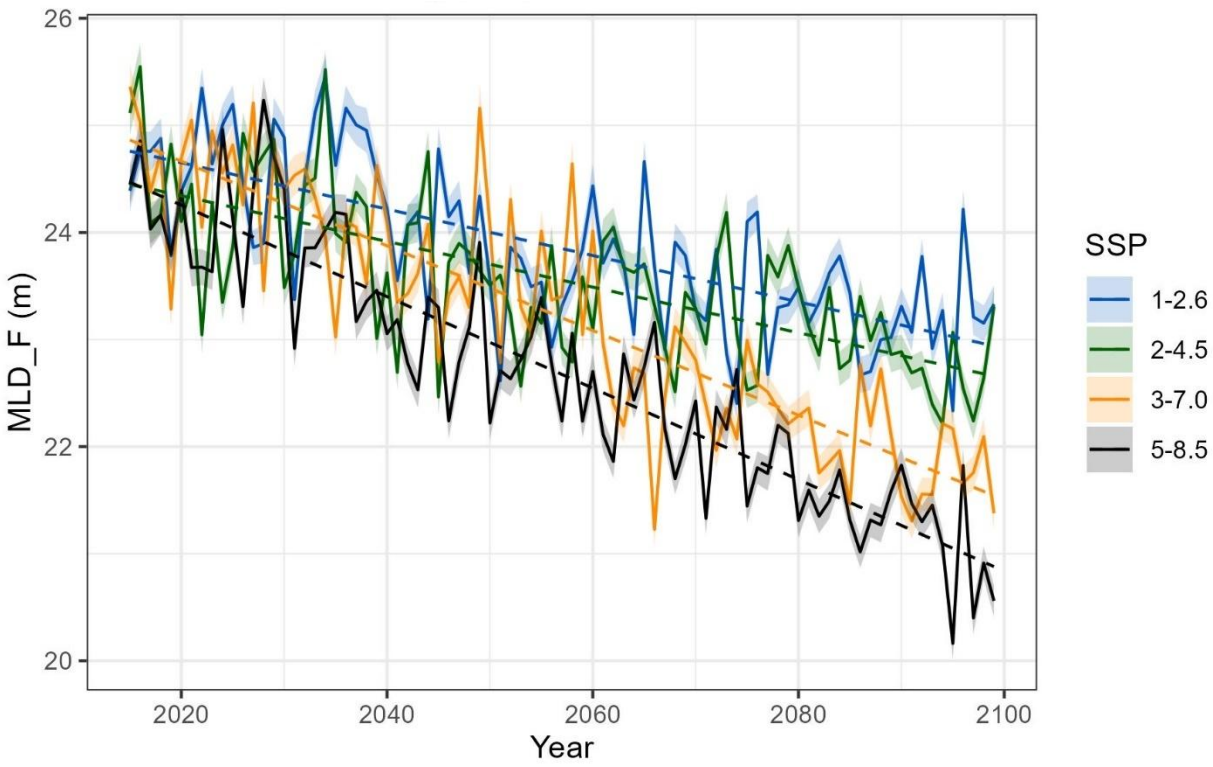

Figure 29. Annual mean Fall Mixed Layer Depth (MLD_F) trends from the 22 ensembled CMIP6 models for the NAFO study area are shown for each of four Shared Socio-economic Pathways (SSPs) and each year from 2015 to 2100. Dashed lines indicate linear fit to the data. Shaded areas are the 95% confidence intervals for the ensembled means.

Table 7. The mean ± standard deviation from the 22 ensembled CMIP6 models of Fall Mixed Layer Depth (MLD_F) (m) for the NAFO study area for each of four Shared Socio-economic Pathways (SSPs) time periods.

SSP	2020-2039	2040-2059	2060-2079	2080-2099
1-2.6	24.70 ± 8.47	23.74 ± 7.98	23.55 ± 7.80	23.24 ± 7.64
2-4.5	24.17 ± 8.22	23.47 ± 7.78	23.39 ± 7.85	22.89 ± 7.45
3-7.0	24.35 ± 8.24	23.64 ± 7.99	22.55 ± 7.47	21.94 ± 7.29
5-8.5	23.98 ± 8.11	22.87 ± 7.56	22.21 ± 7.44	21.25 ± 7.08

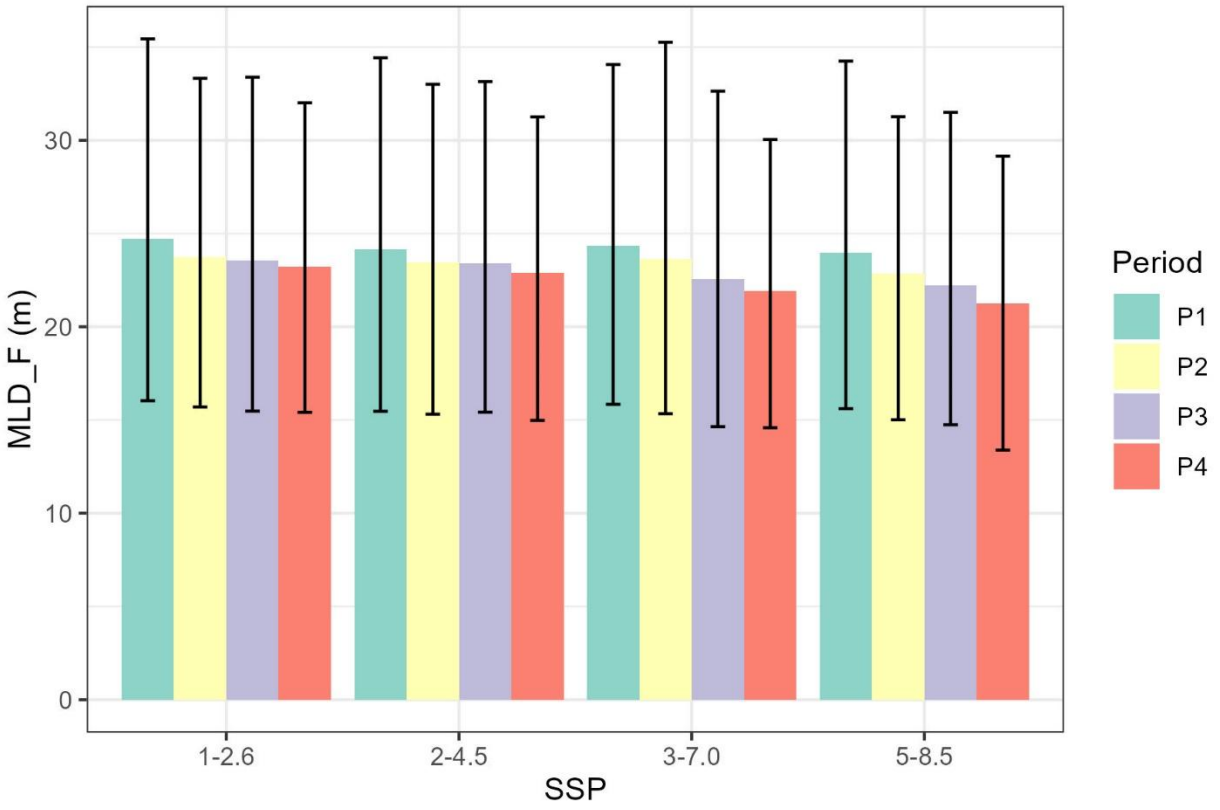

Figure 30. The mean Fall Mixed Layer Depth (MLD_F) (m) from the 22 ensembled CMIP6 models for the NAFO study area is shown for each of four Shared Socio-economic Pathways (SSPs) and time periods (P1: 2020-2039, P2: 2040-2059, P3: 2060-2079, P4: 2080-2099). Bars represent minimum, maximum values and range of the data products averaged over the spatial extent.

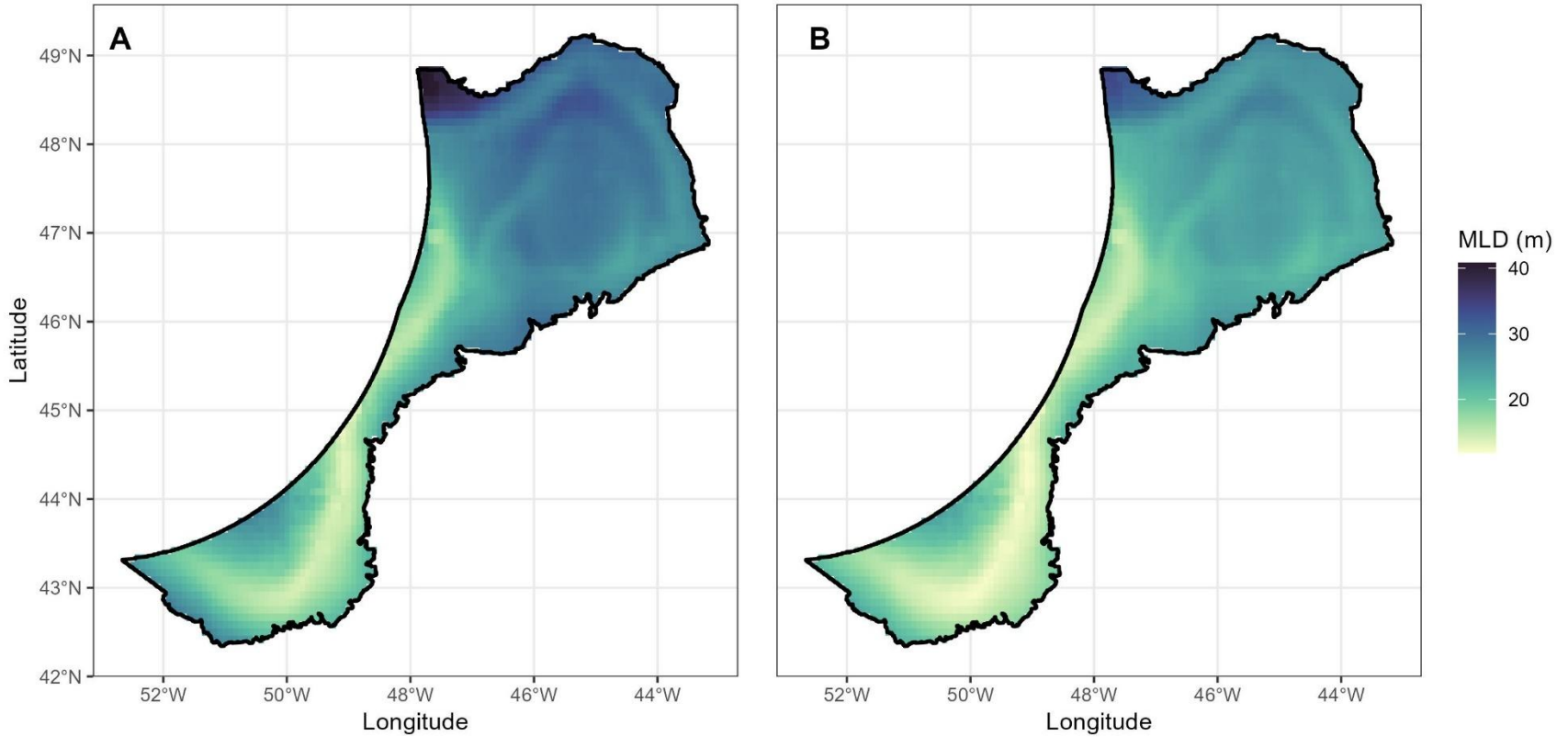

Figure 31. The spatial distribution of Mean Fall Mixed Layer Depth (MLD_F) from the 22 ensembled CMIP6 models for the NAFO study area. **A)** Time period 2020-2039 for Shared Socio-economic Pathway (SSP) 1-2.6. **B)** Time period 2080-2099 for Shared Socio-economic Pathway (SSP) 5 8.5.

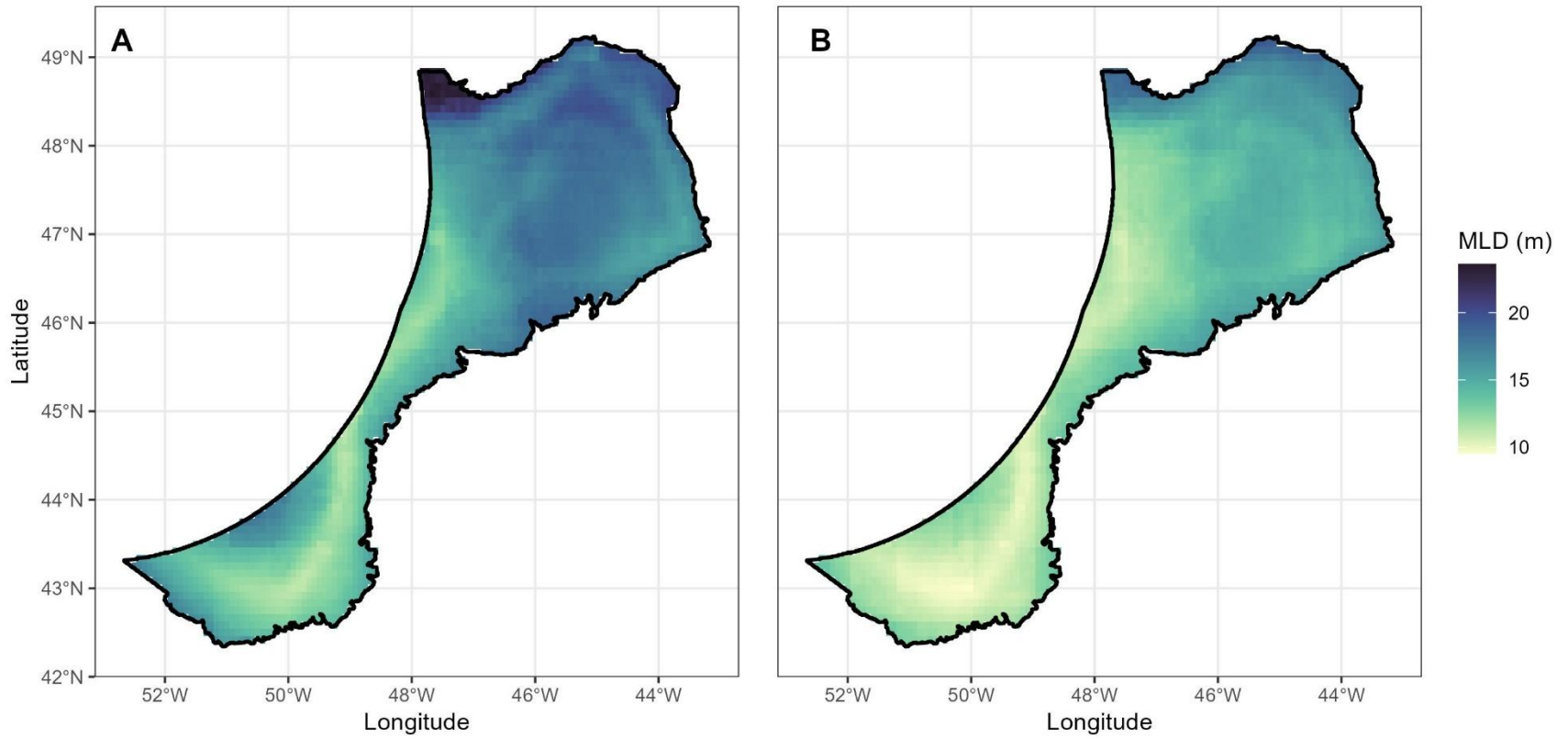

Figure 32. The spatial distribution of Minimum Mean Fall Mixed Layer Depth (MLD_F) from the 22 ensembled CMIP6 models for the NAFO study area. **Left panel.** Averaged for the time period 2020-2039 for Shared Socio-economic Pathway (SSP) 1-2.6. **Right panel.** Averaged for the time period 2080-2099 for Shared Socio-economic Pathway (SSP) 5-8.5.

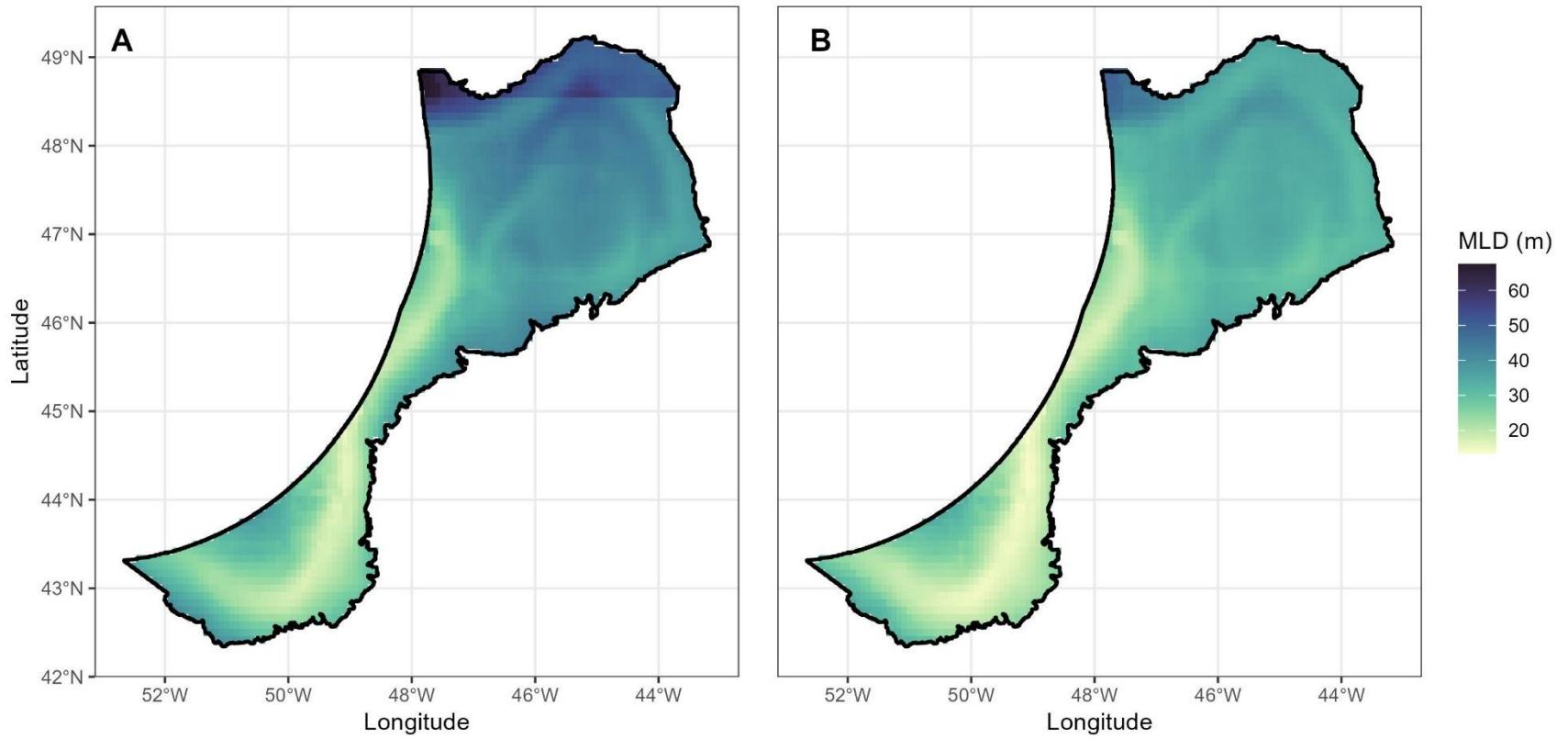

Figure 33. The spatial distribution of Maximum Mean Fall Mixed Layer Depth (MLD_F) from the 22 ensembled CMIP6 models for the NAFO study area. **Left panel.** Averaged for the time period 2020-2039 for Shared Socio-economic Pathway (SSP) 1-2.6. **Right panel.** Averaged for the time period 2080-2099 for Shared Socio-economic Pathway (SSP) 5-8.5.

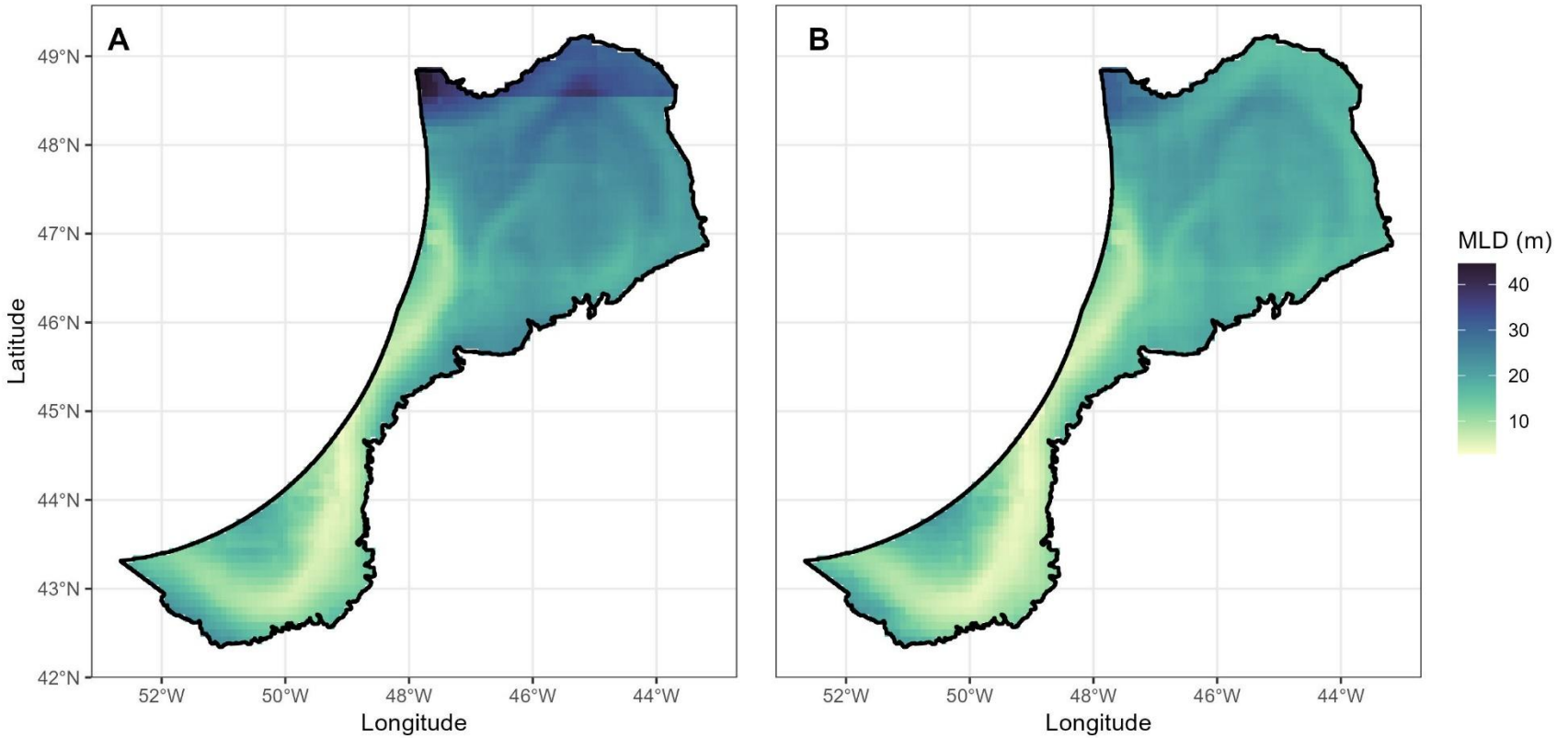

Figure 34. The spatial distribution of Range of Mean Fall Mixed Layer Depth (MLD_F) from the 22 ensembled CMIP6 models for the NAFO study area. **Left panel.** Averaged for the time period 2020-2039 for Shared Socio-economic Pathway (SSP) 1-2.6. **Right panel.** Averaged for the time period 2080-2099 for Shared Socio-economic Pathway (SSP) 5-8.5.

Winter MLD (MLD_W)

Mixed layer depths in the winter months (Table 8) were deeper than the yearly average (Table 5) and than in other seasons (Tables 6, 7 and 9). The trends in modeled mean mixed layer depth in the winter (MLD_W) from 2015 to 2100 show decreasing trends among successive time periods and SSPs (Figure 35). Mean MLD_W ranged from 31.75 in P4 to 39.15 m in P1 (Table 8) with both minimum and maximum values showing decreases with SSP and time period, with the exception of the maximum value for SSP3-7.0 in P2 which was greater than that of P1 (Figure 36).

The spatial distribution of the variables is shown in Figures 37, 38, 39 and 40 for each variable for SSP1-2.6 and SSP5-8.5.

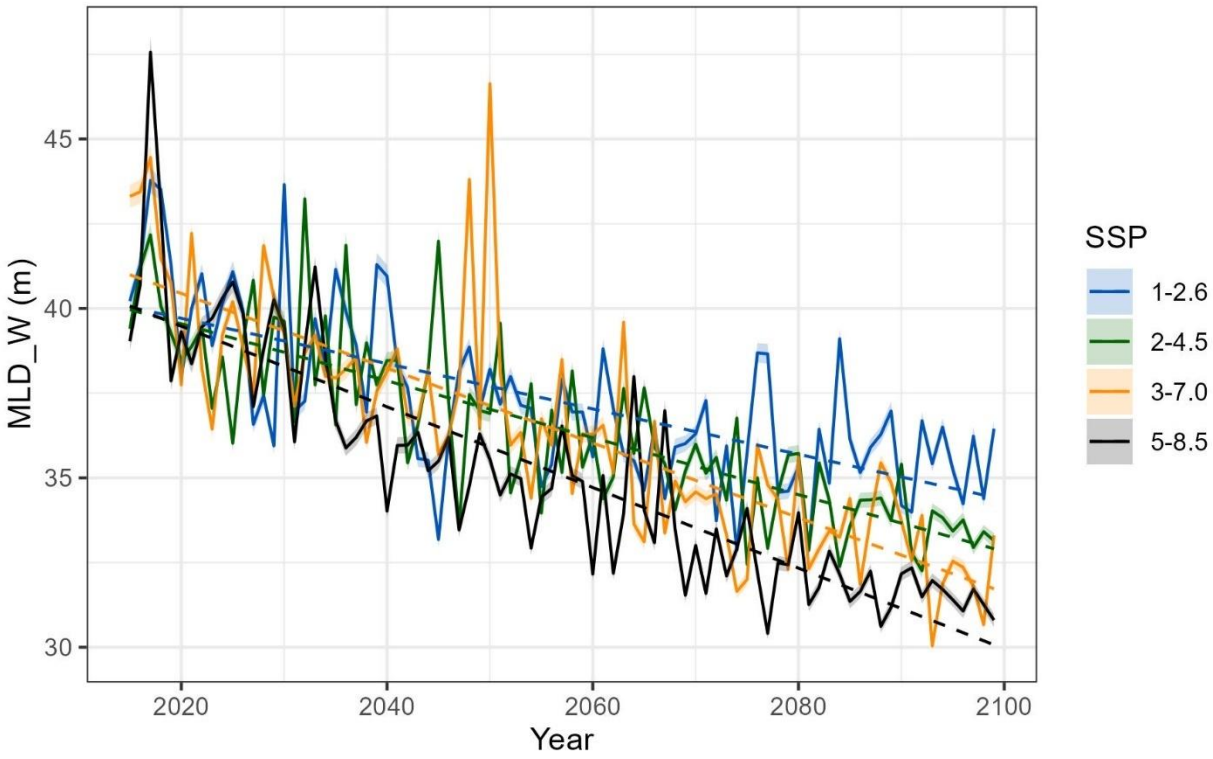

Figure 35. Annual mean Winter Mixed Layer Depth (MLD_W) (m) trends from the 22 ensembled CMIP6 models for the NAFO study area are shown for each of four Shared Socio-economic Pathways (SSPs) and each year from 2015 to 2100. Dashed lines indicate linear fit to the data. Shaded areas are the 95% confidence intervals for the ensembled means.

Table 8. The mean ± standard deviation from the 22 ensembled CMIP6 models of Winter Mixed Layer Depth (MLD_W) (m) for the NAFO study area for each of four Shared Socio-economic Pathways (SSPs) and time periods.

SSP	2020-2039	2040-2059	2060-2079	2080-2099
1-2.6	39.15 ± 13.13	37.05 ± 11.93	35.92 ± 11.10	35.62 ± 11.20
2-4.5	38.74 ± 12.85	36.92 ± 11.63	35.28 ± 10.99	33.81 ± 10.05
3-7.0	38.66 ± 12.44	37.60 ± 13.13	34.57 ± 10.75	33.03 ± 9.75
5-8.5	38.52 ± 12.64	35.12 ± 10.53	33.26 ± 10.28	31.75 ± 9.26

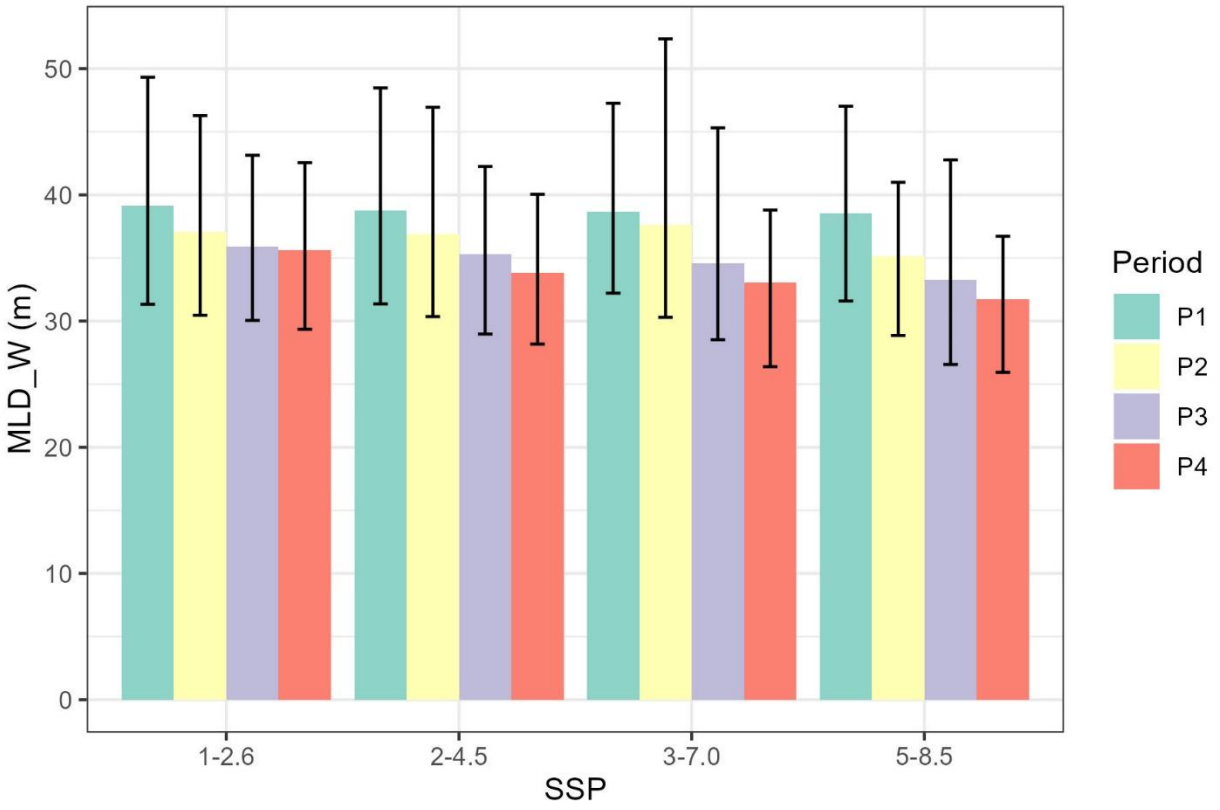

Figure 36. The mean Winter Mixed Layer Depth (MLD_W) (m) from the 22 ensembled CMIP6 models for the NAFO study area is shown for each of four Shared Socio-economic Pathways (SSPs) and time periods (P1: 2020-2039, P2: 2040-2059, P3: 2060-2079, P4: 2080-2099). Bars represent minimum, maximum values and range of the data products averaged over the spatial extent.

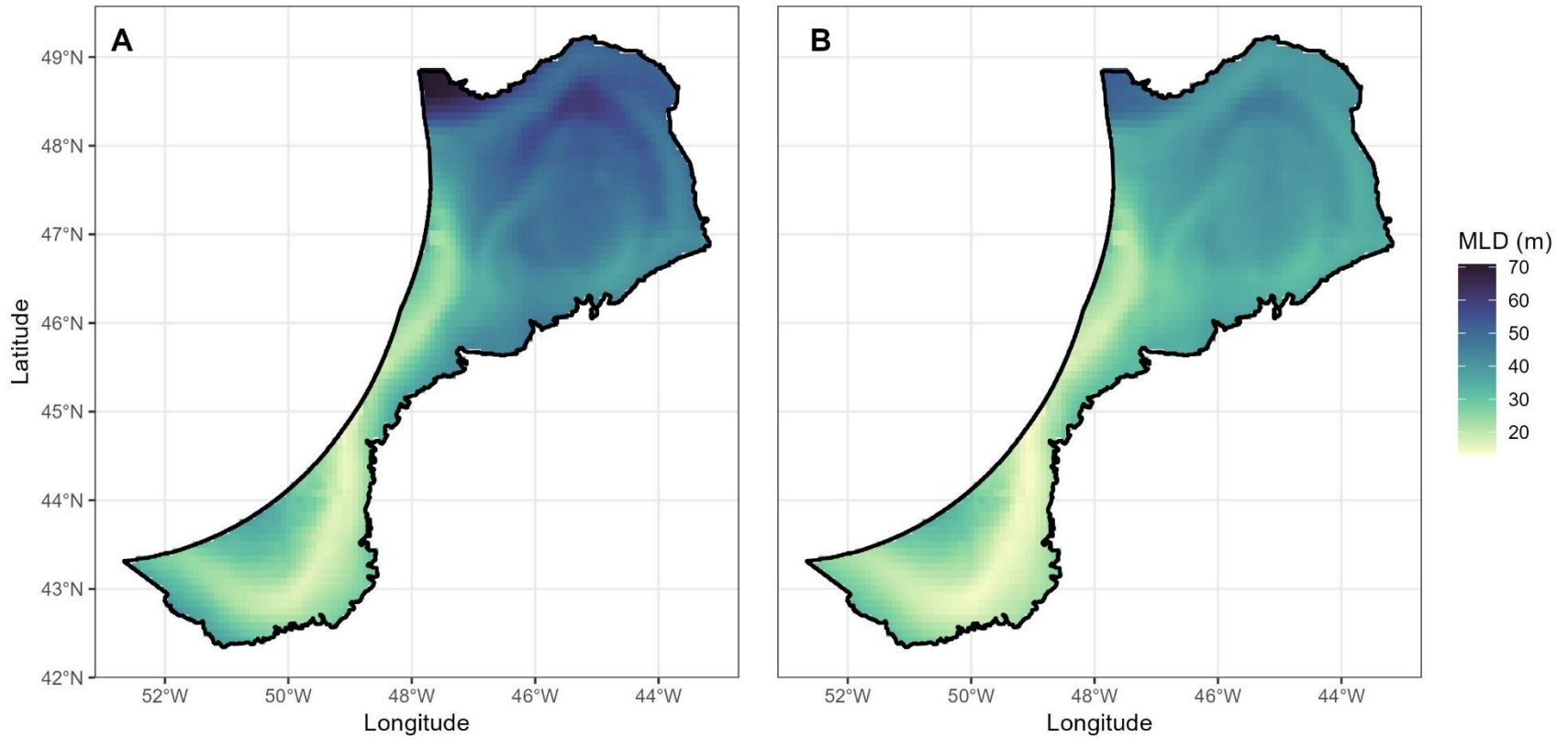

Figure 37. The spatial distribution of Mean Winter Mixed Layer Depth (MLD_W) from the 22 ensembled CMIP6 models for the NAFO study area. **A)** Time period 2020-2039 for Shared Socio-economic Pathway (SSP) 1-2.6. **B)** Time period 2080-2099 for Shared Socio-economic Pathway (SSP) 5-8.5.

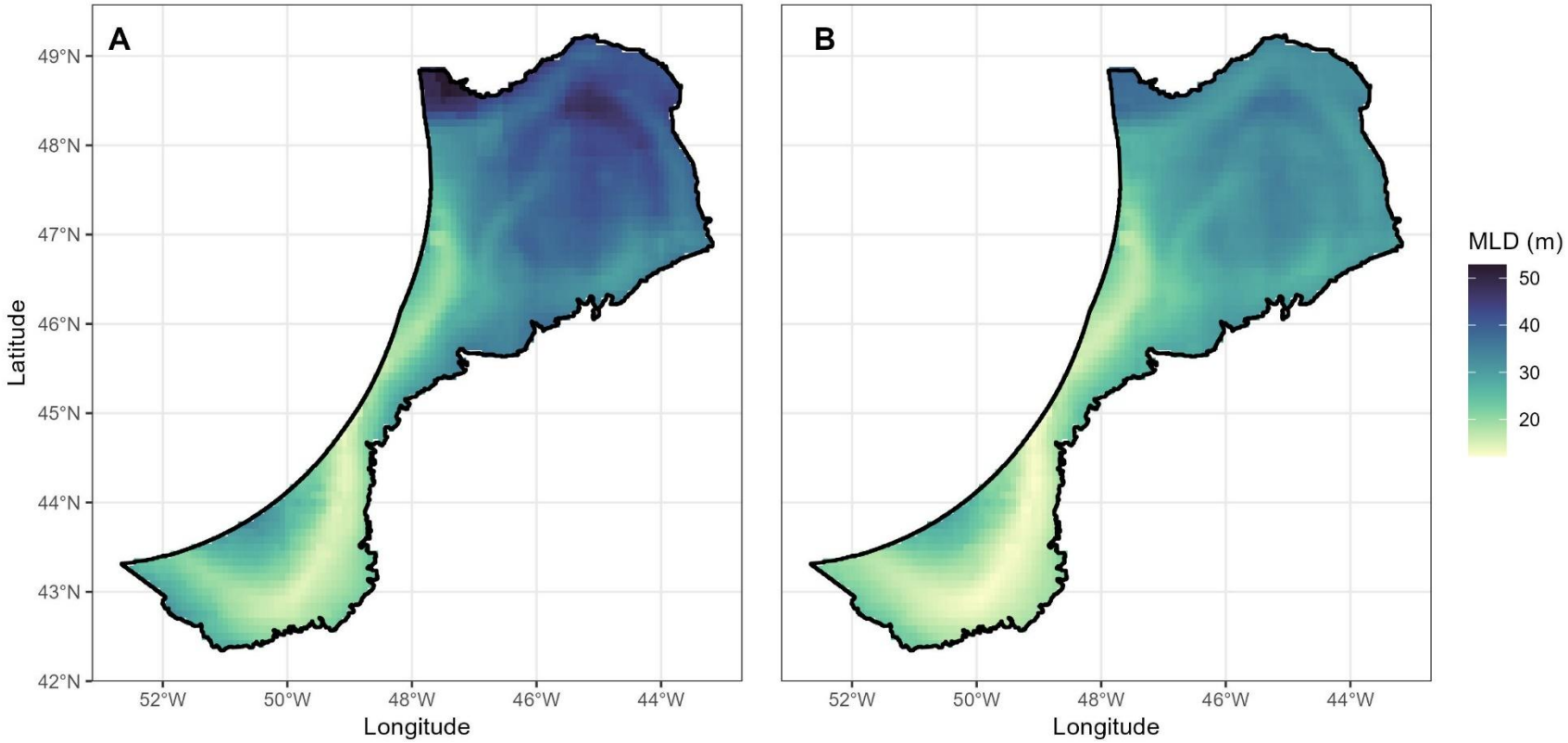

Figure 38. The spatial distribution of Minimum Mean Winter Mixed Layer Depth (MLD_W) from the 22 ensembled CMIP6 models for the NAFO study area. **Left panel.** Averaged for the time period 2020-2039 for Shared Socio-economic Pathway (SSP) 1-2.6. **Right panel.** Averaged for the time period 2080-2099 for Shared Socio-economic Pathway (SSP) 5-8.5.

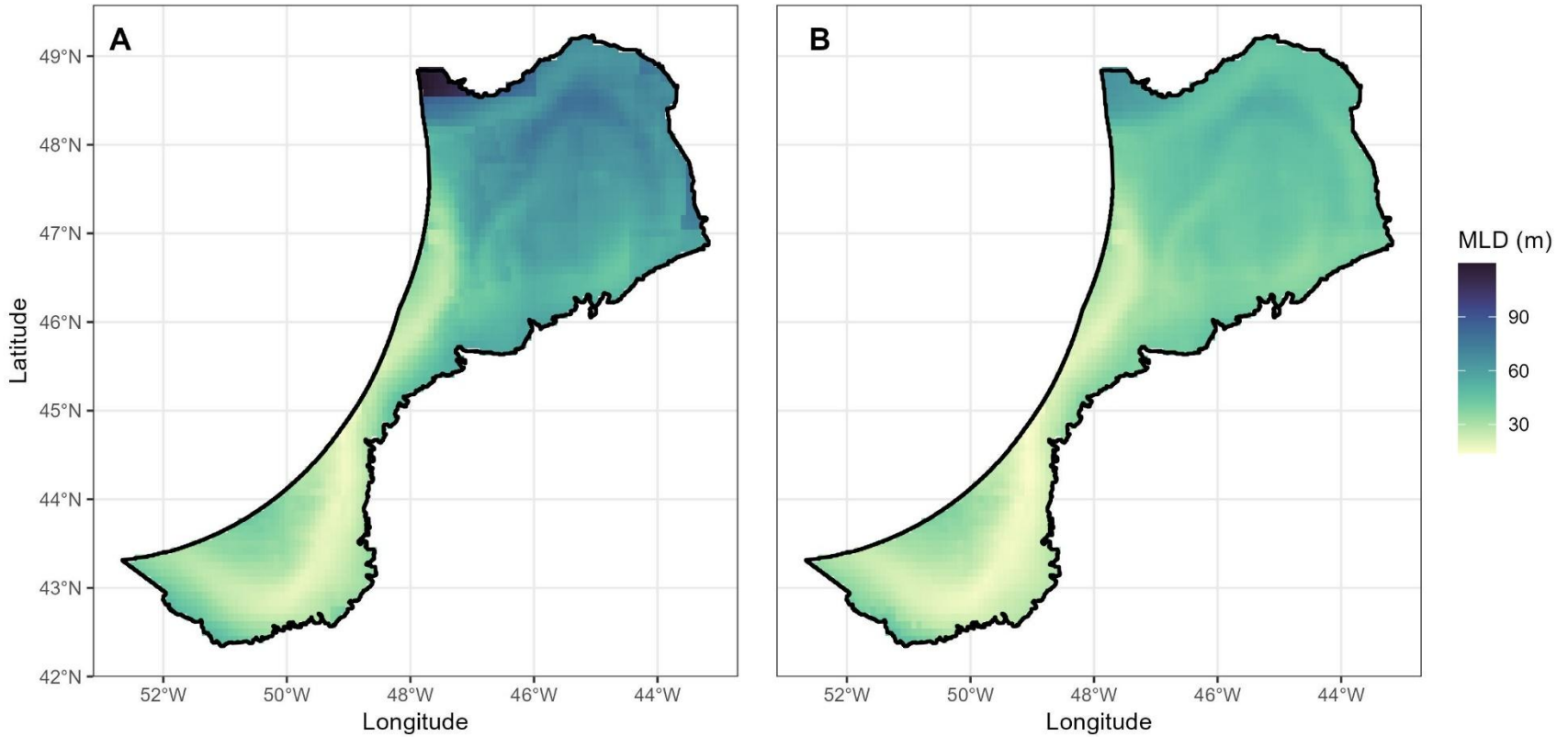

Figure 39. The spatial distribution of Maximum Mean Winter Mixed Layer Depth (MLD_W) from the 22 ensembled CMIP6 models for the NAFO study area. **Left panel.** Averaged for the time period 2020-2039 for Shared Socio-economic Pathway (SSP) 1-2.6. **Right panel.** Averaged for the time period 2080-2099 for Shared Socio-economic Pathway (SSP) 5-8.5.

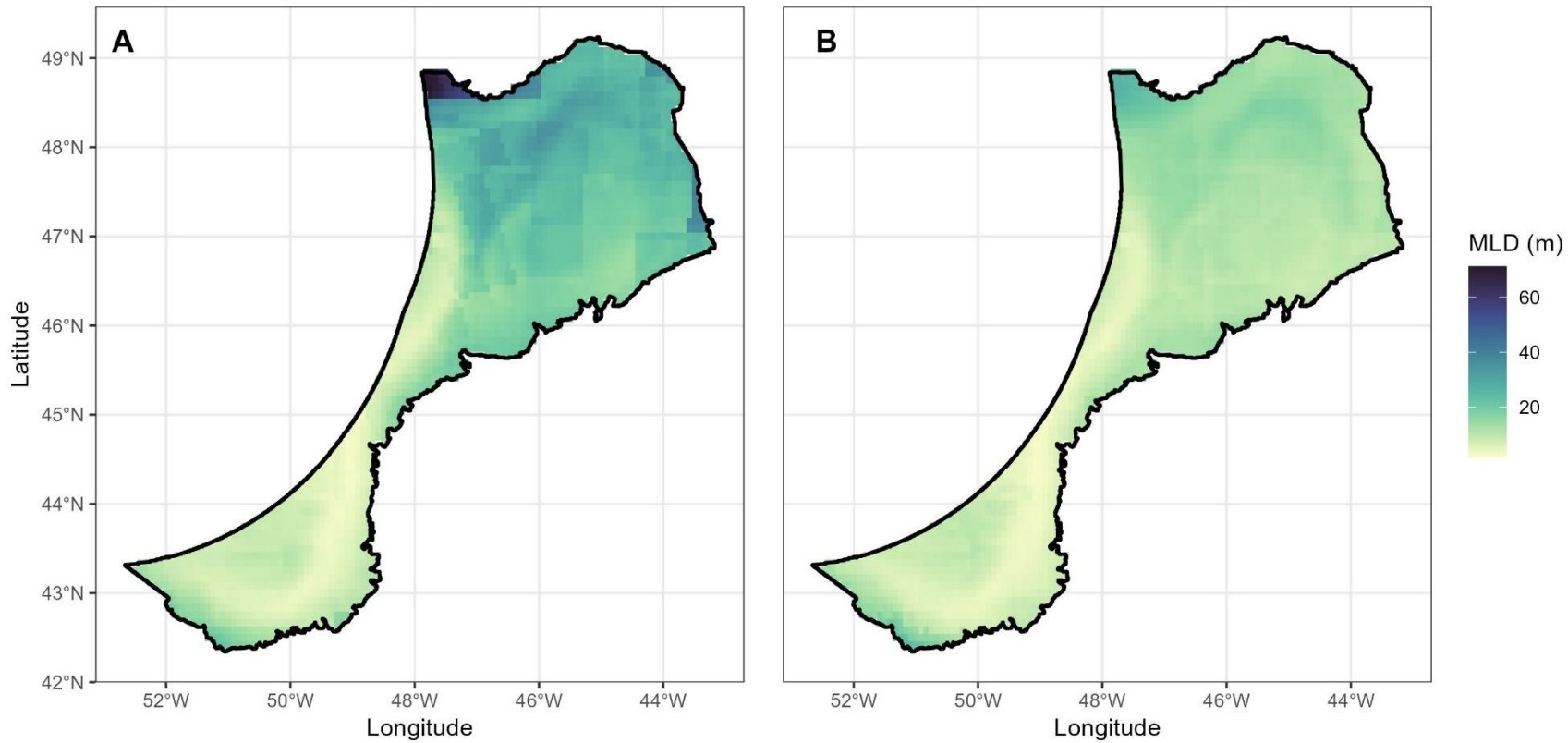

Figure 40. The spatial distribution of Range of Mean Winter Mixed Layer Depth (MLD_W) from the 22 ensembled CMIP6 models for the NAFO study area. **Left panel.** Averaged for the time period 2020-2039 for Shared Socio-economic Pathway (SSP) 1-2.6. **Right panel.** Averaged for the time period 2080-2099 for Shared Socio-economic Pathway (SSP) 5-8.5.

Spring MLD (MLD_{Sp})

Mixed layer depths in the spring months (Table 9) were shallower than the yearly average (Table 5) but not as shallow as in summer when stratification was strongest (Tables 6). The trends in modeled mean mixed layer depth in the winter (MLD_{Sp}) from 2015 to 2100 show decreasing trends among successive time periods and SSPs (Figure 41). Mean MLD_{Sp} ranged from 14.29 in P4 to 17.27 m in P1 (Table 9) with maximum values showing greater variation than the minimum (Figure 42).

The spatial distribution of the variables is shown in Figures 43, 44, 45 and 46 for each variable for SSP1-2.6 and SSP5-8.5.

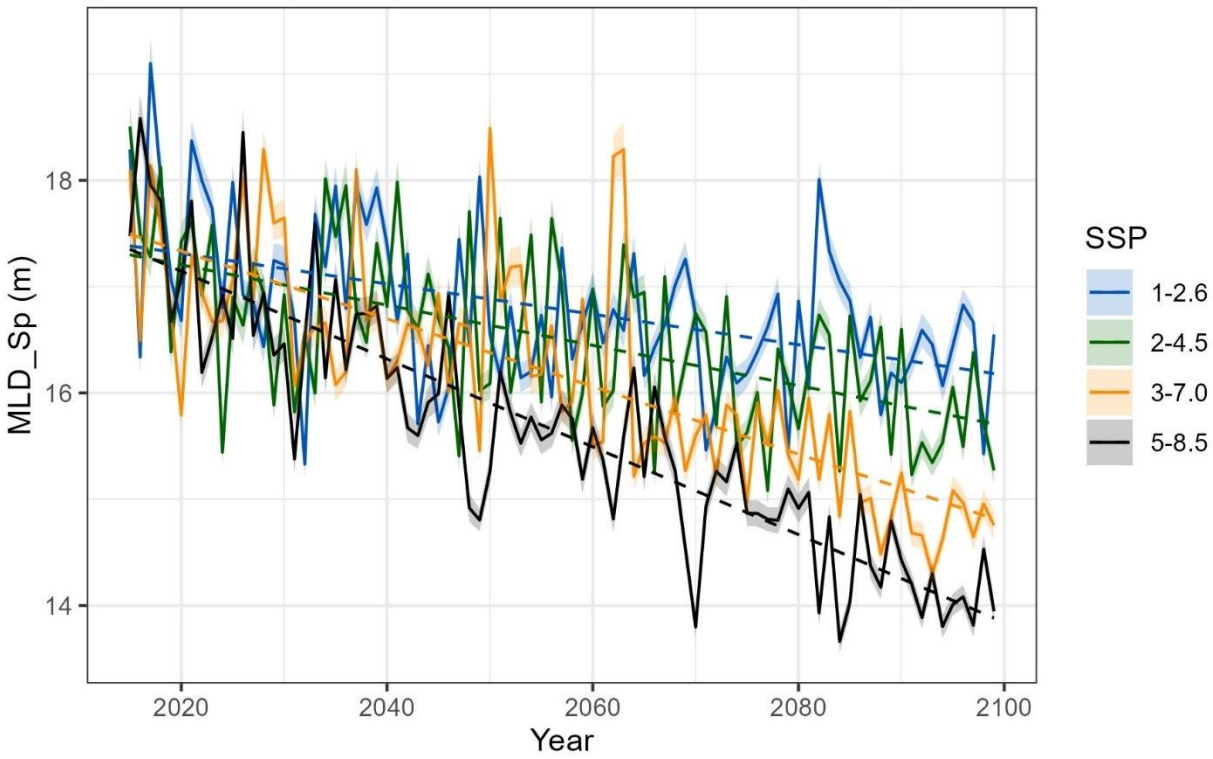

Figure 41. Annual mean Spring Mixed Layer Depth (MLD_{Sp}) (m) trends from the 22 ensembled CMIP6 models for the NAFO study area are shown for each of four Shared Socio-economic Pathways (SSPs) and each year from 2015 to 2100. Dashed lines indicate linear fit to the data. Shaded areas are the 95 confidence intervals for the ensembled means.

Table 9. The mean ± standard deviation from the 22 ensembled CMIP6 models of Spring Mixed Layer Depth (MLD_{Sp}) (m) for the NAFO study area for each of four Shared Socio-economic Pathways (SSPs) and time periods.

SSP	2020-2039	2040-2059	2060-2079	2080-2099
1-2.6	17.27 ± 7.69	16.61 ± 6.88	16.49 ± 6.79	16.53 ± 6.90
2-4.5	16.90 ± 7.53	16.67 ± 7.21	16.26 ± 6.67	15.92 ± 6.29
3-7.0	16.93 ± 7.46	16.55 ± 7.30	15.84 ± 6.79	15.00 ± 5.91
5-8.5	16.75 ± 7.61	15.73 ± 6.24	15.17 ± 6.09	14.29 ± 5.35

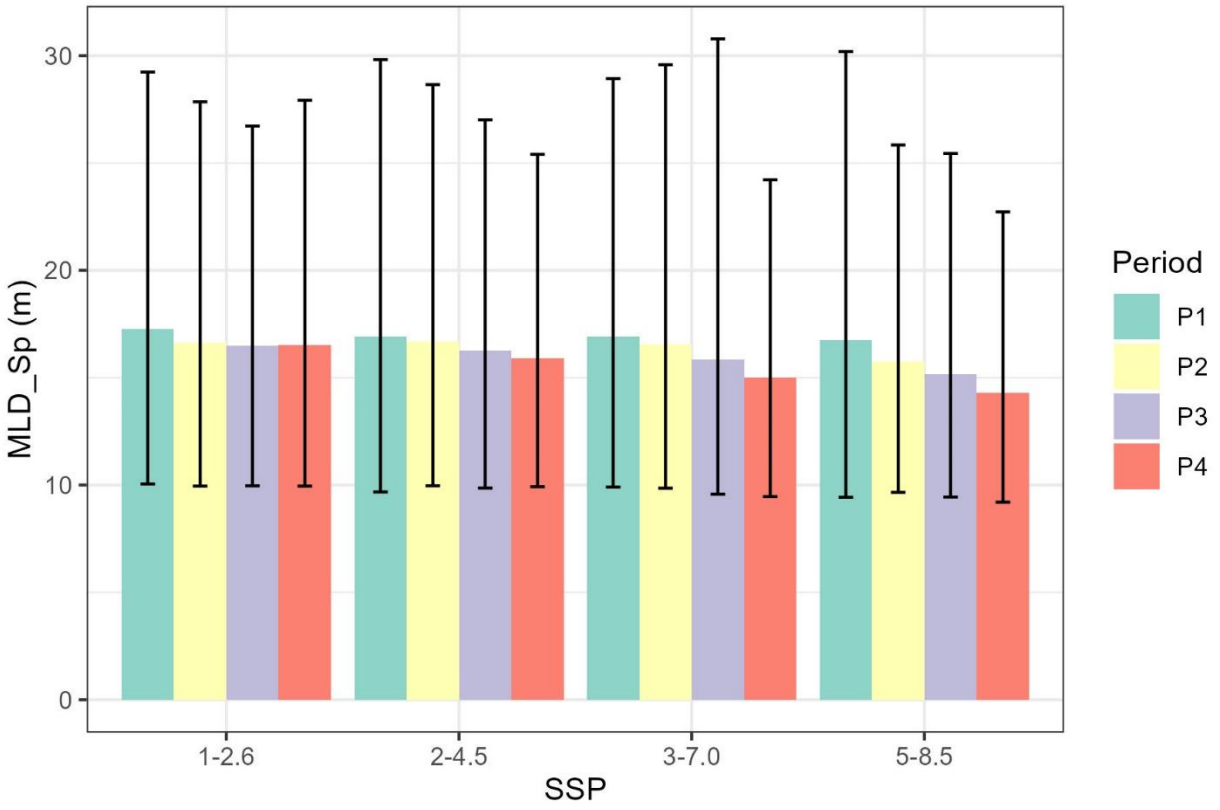

Figure 42. The mean Spring Mixed Layer Depth (MLD_{Sp}) (m) from the 22 ensembled CMIP6 models for the NAFO study area is shown for each of four Shared Socio-economic Pathways (SSPs) and time periods (P1: 2020-2039, P2: 2040-2059, P3: 2060-2079, P4: 2080-2099). Bars represent minimum, maximum values and range of the data products averaged over the spatial extent.

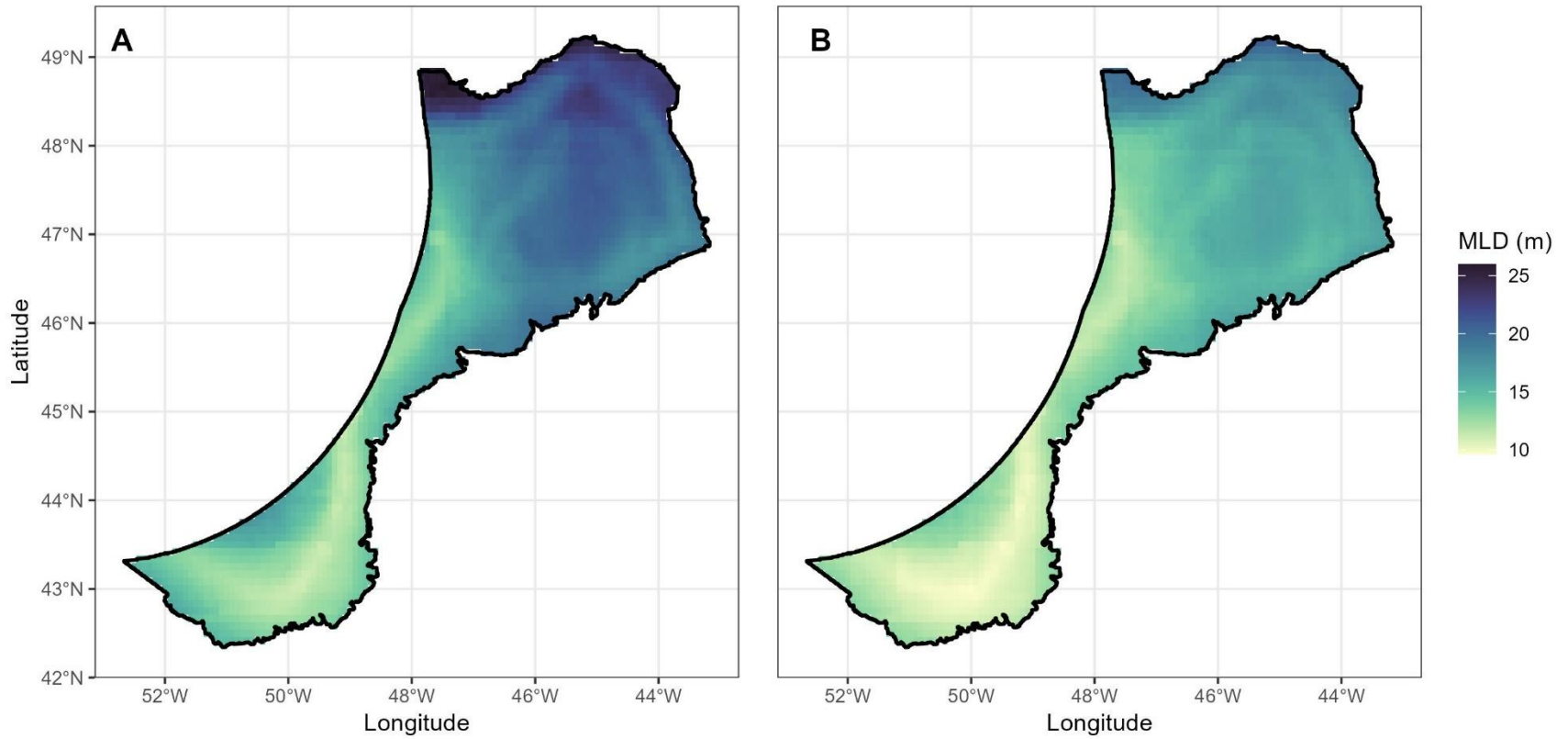

Figure 43. The spatial distribution of Mean Spring Mixed Layer Depth (MLD_{Sp}) from the 22 ensembled CMIP6 models for the NAFO study area. **A)** Time period 2020-2039 for Shared Socio-economic Pathway (SSP) 1-2.6. **B)** Time period 2080-2099 for Shared Socio-economic Pathway (SSP) 5-8.5.

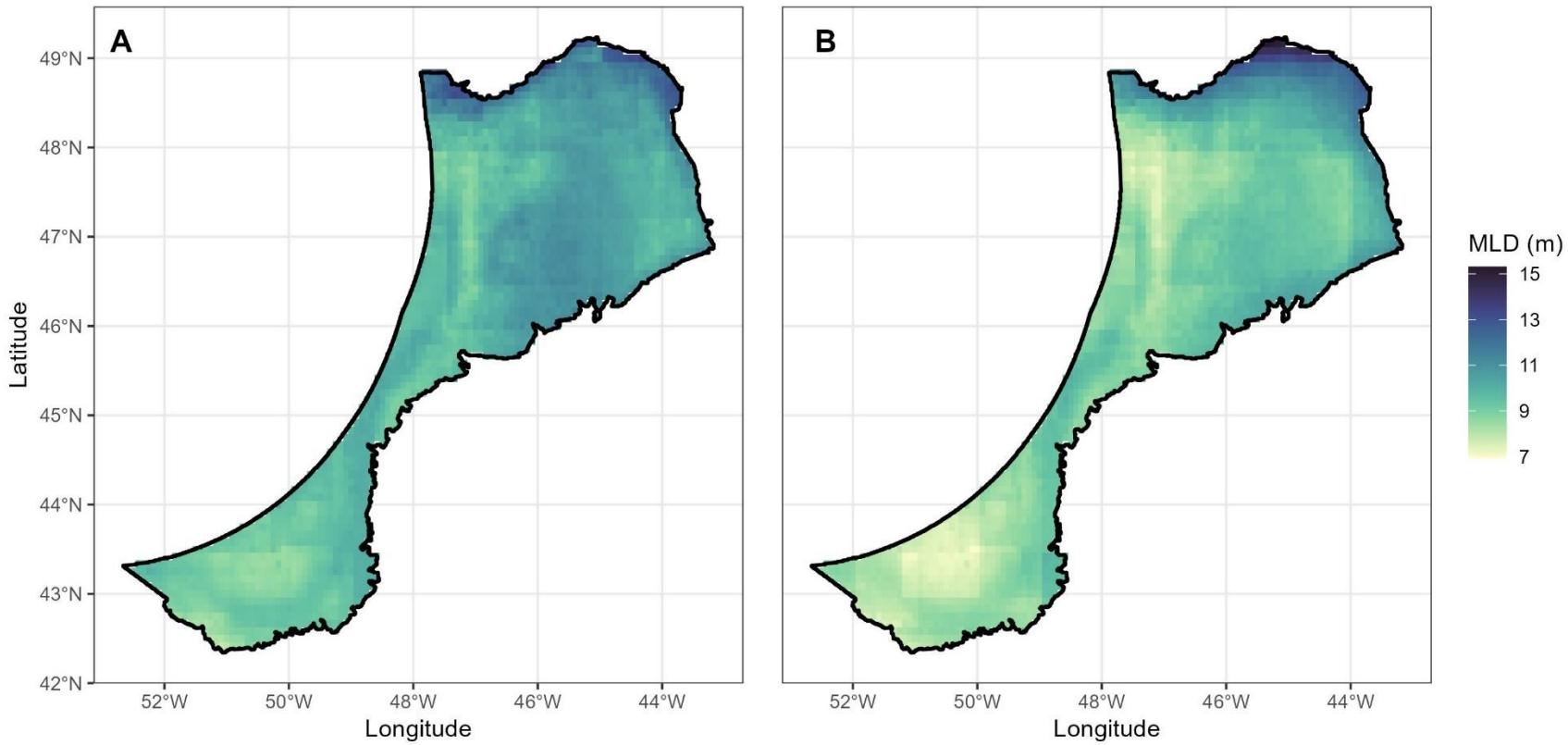

Figure 44. The spatial distribution of Minimum Mean Spring Mixed Layer Depth (MLD_{Sp}) from the 22 ensembled CMIP6 models for the NAFO study area. **Left panel.** Averaged for the time period 2020-2039 for Shared Socio-economic Pathway (SSP) 1-2.6. **Right panel.** Averaged for the time period 2080-2099 for Shared Socio-economic Pathway (SSP) 5-8.5.

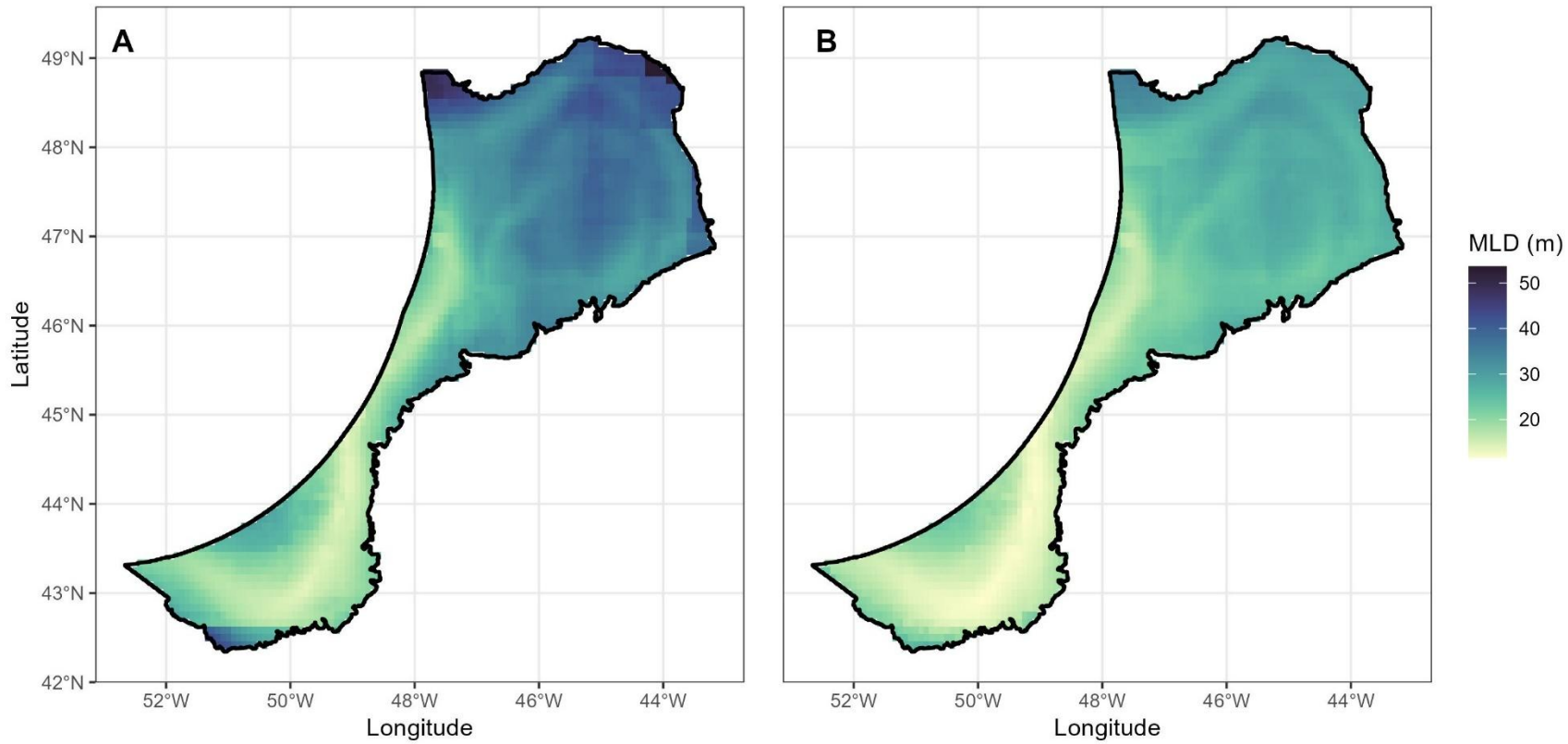

Figure 45. The spatial distribution of Maximum Mean Spring Mixed Layer Depth (MLD_{Sp}) from the 22 ensembled CMIP6 models for the NAFO study area. **Left panel.** Averaged for the time period 2020-2039 for Shared Socio-economic Pathway (SSP) 1-2.6. **Right panel.** Averaged for the time period 2080-2099 for Shared Socio-economic Pathway (SSP) 5-8.5.

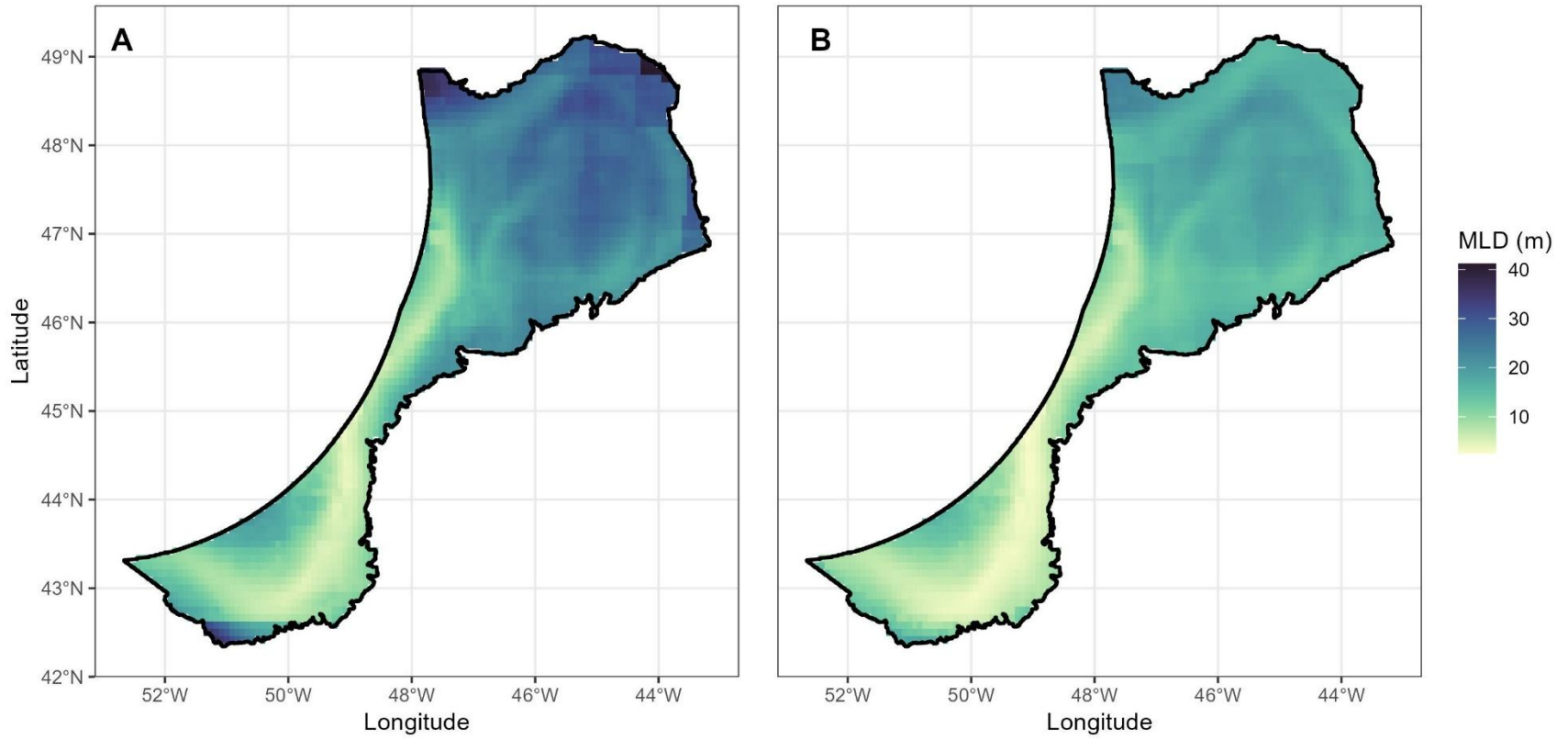

Figure 46. The spatial distribution of Range of Mean Spring Mixed Layer Depth (MLD_{Sp}) from the 22 ensembled CMIP6 models for the NAFO study area. **Left panel.** Averaged for the time period 2020-2039 for Shared Socio-economic Pathway (SSP) 1-2.6. **Right panel.** Averaged for the time period 2080-2099 for Shared Socio-economic Pathway (SSP) 5-8.5.

Bottom Temperature (BT)

Bottom Temperature (BT) showed increasing annual mean values over time (Figure 47) with slope increasing with increasing emissions (SSP). Mean BT ranged from 4.15 °C in P1/SSP5-8.5 to 5.97 °C in P4/SSP5-8.5 (Table 10), consistent with the projected warming of bottom temperatures by 2-3 °C by 2100 reported elsewhere (Boyce 2024). Mean bottom temperature increased within each time period with increasing SSP (Figure 48).

The spatial distribution of the variables is shown in Figures 49, 50, 51 and 52 for each variable for SSP1-2.6 and SSP5-8.5. The spatial variability is large in all variables and is larger under SSP5-8.5.

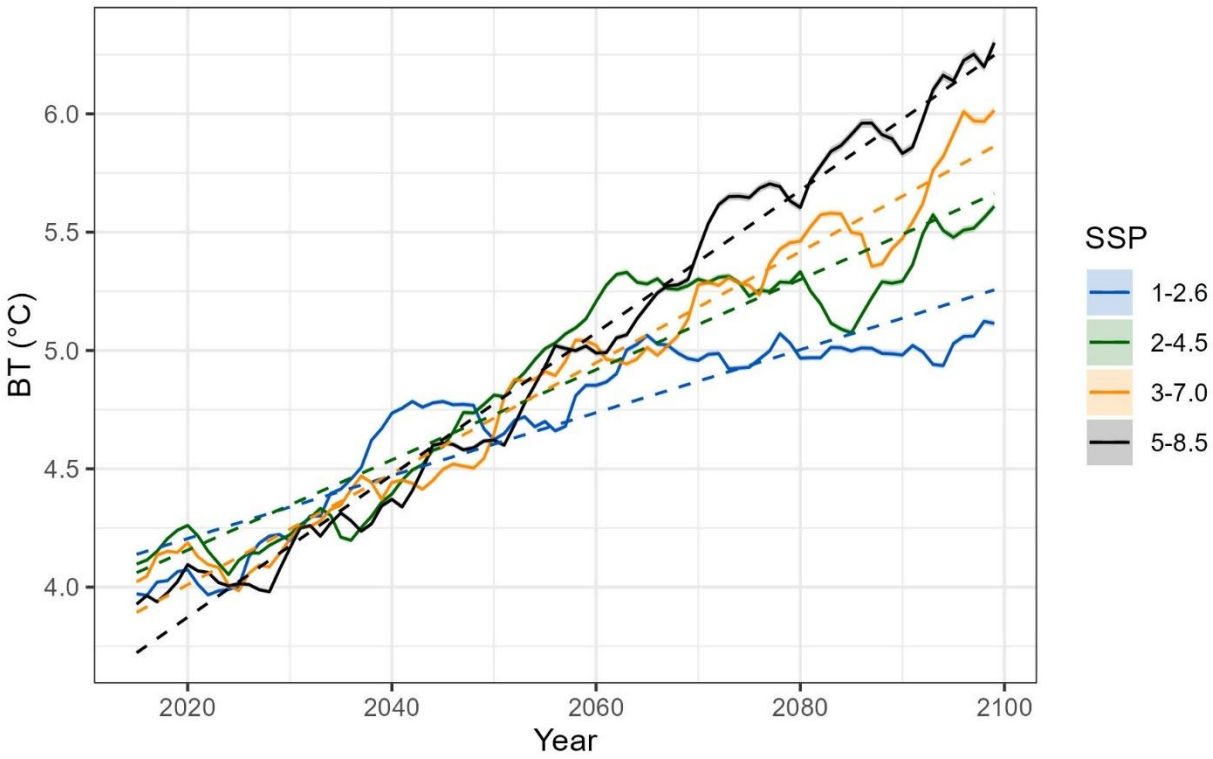

Figure 47. Annual mean Bottom Temperature (BT) in °C trends from the 22 ensembled CMIP6 models for the NAFO study area are shown for each of four Shared Socio-economic Pathways (SSPs) and each year from 2015 to 2100. Dashed lines indicate linear fit to the data. Shaded areas are the 95% confidence intervals for the ensembled means.

Table 10. The mean ± standard deviation from the 22 ensembled CMIP6 models of Bottom Temperature (BT) in °C for the NAFO study area for each of four Shared Socio-economic Pathways (SSPs) time periods.

SSP	2020-2039	2040-2059	2060-2079	2080-2099
1-2.6	4.24 ± 0.89	4.73 ± 1.05	4.97 ± 1.18	5.01 ± 1.20
2-4.5	4.21 ± 0.86	4.78 ± 1.09	5.28 ± 1.24	5.35 ± 1.42
3-7.0	4.21 ± 0.84	4.68 ± 1.06	5.16 ± 1.27	5.65 ± 1.55
5-8.5	4.15 ± 0.84	4.69 ± 1.12	5.39 ± 1.42	5.97 ± 1.82

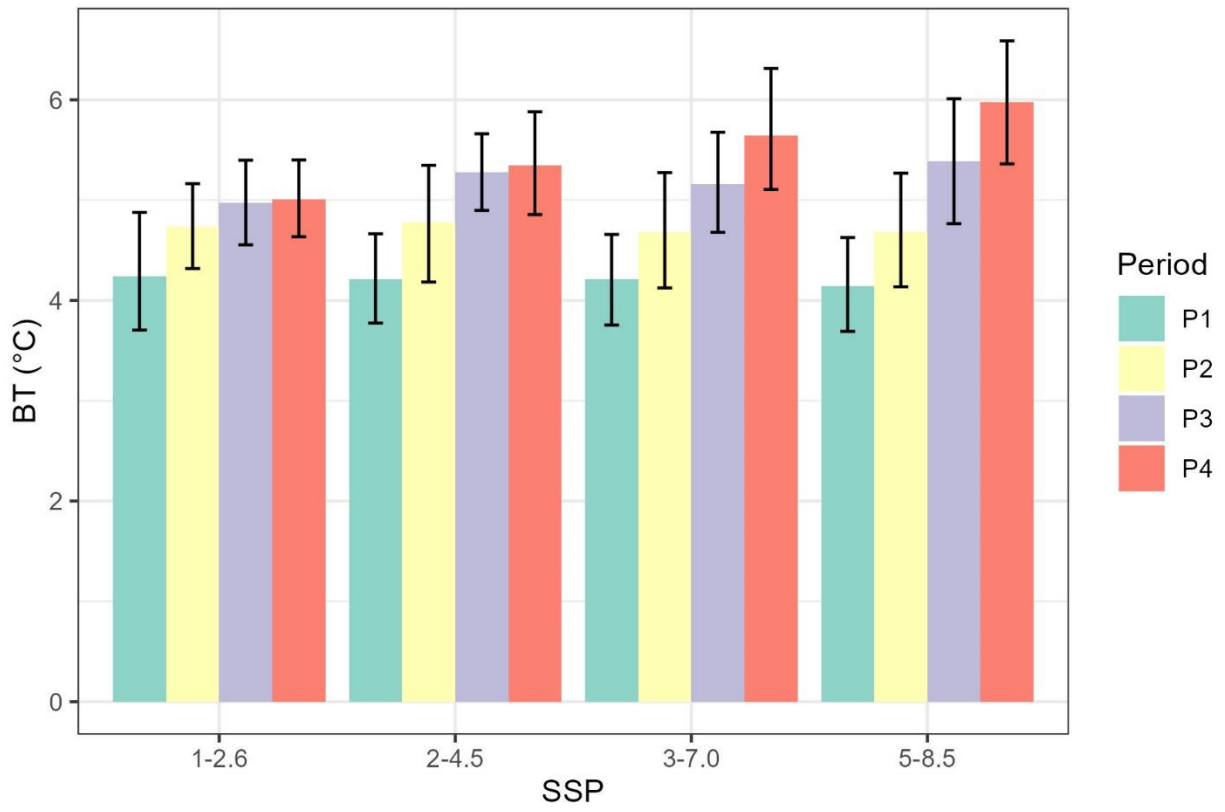

Figure 48. The mean Bottom Temperature (BT) in °C from the 22 ensembled CMIP6 models for the NAFO study area is shown for each of four Shared Socio-economic Pathways (SSPs) and time periods (P1: 2020-2039, P2: 2040-2059, P3: 2060-2079, P4: 2080-2099). Bars represent minimum, maximum values and range of the data products averaged over the spatial extent.

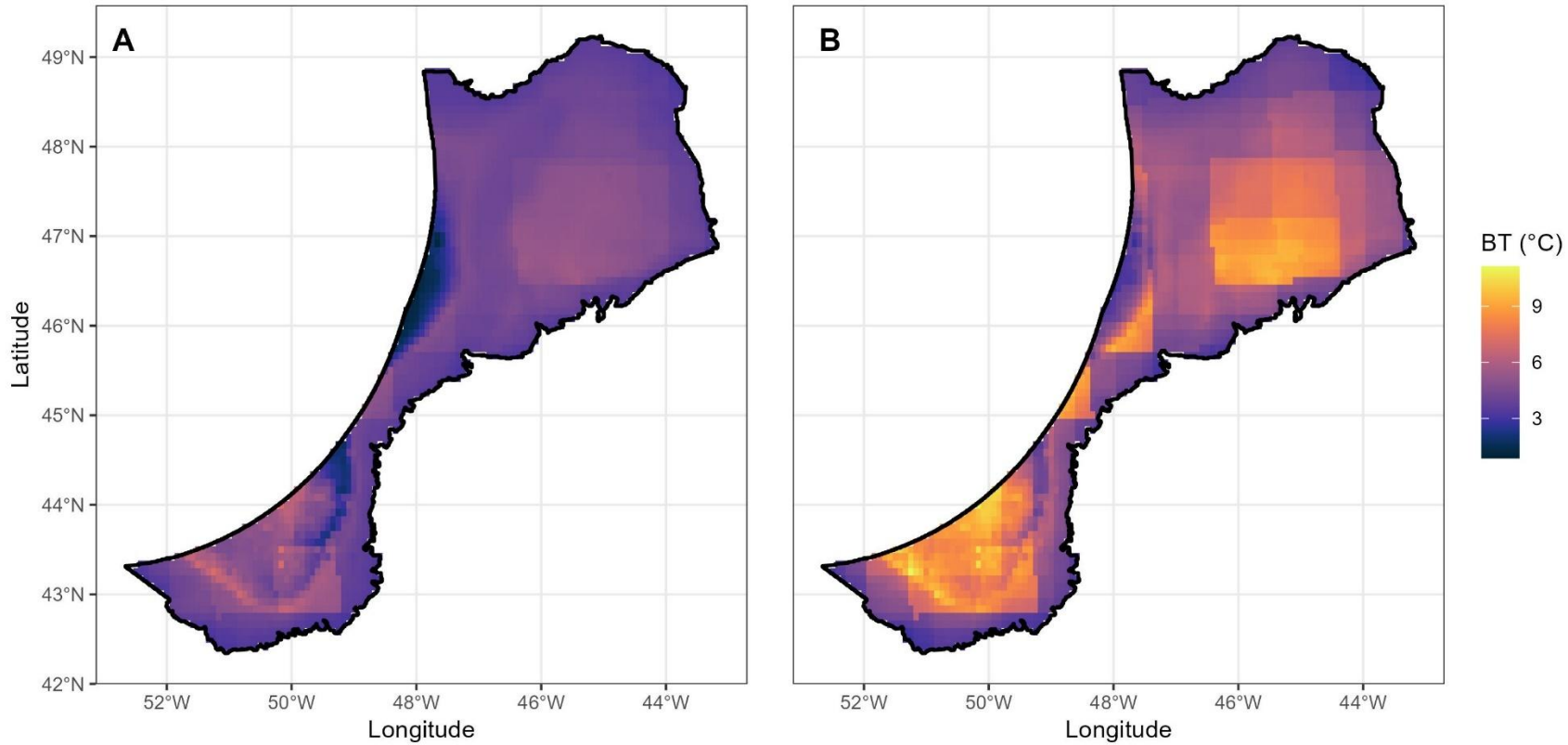

Figure 49. The spatial distribution of Mean Bottom Temperature (BT) from the 22 ensembled CMIP6 models for the NAFO study area. **A)** Time period 2020-2039 for Shared Socio-economic Pathway (SSP) 1-2.6. **B)** Time period 2080-2099 for Shared Socio-economic Pathway (SSP) 5-8.5.

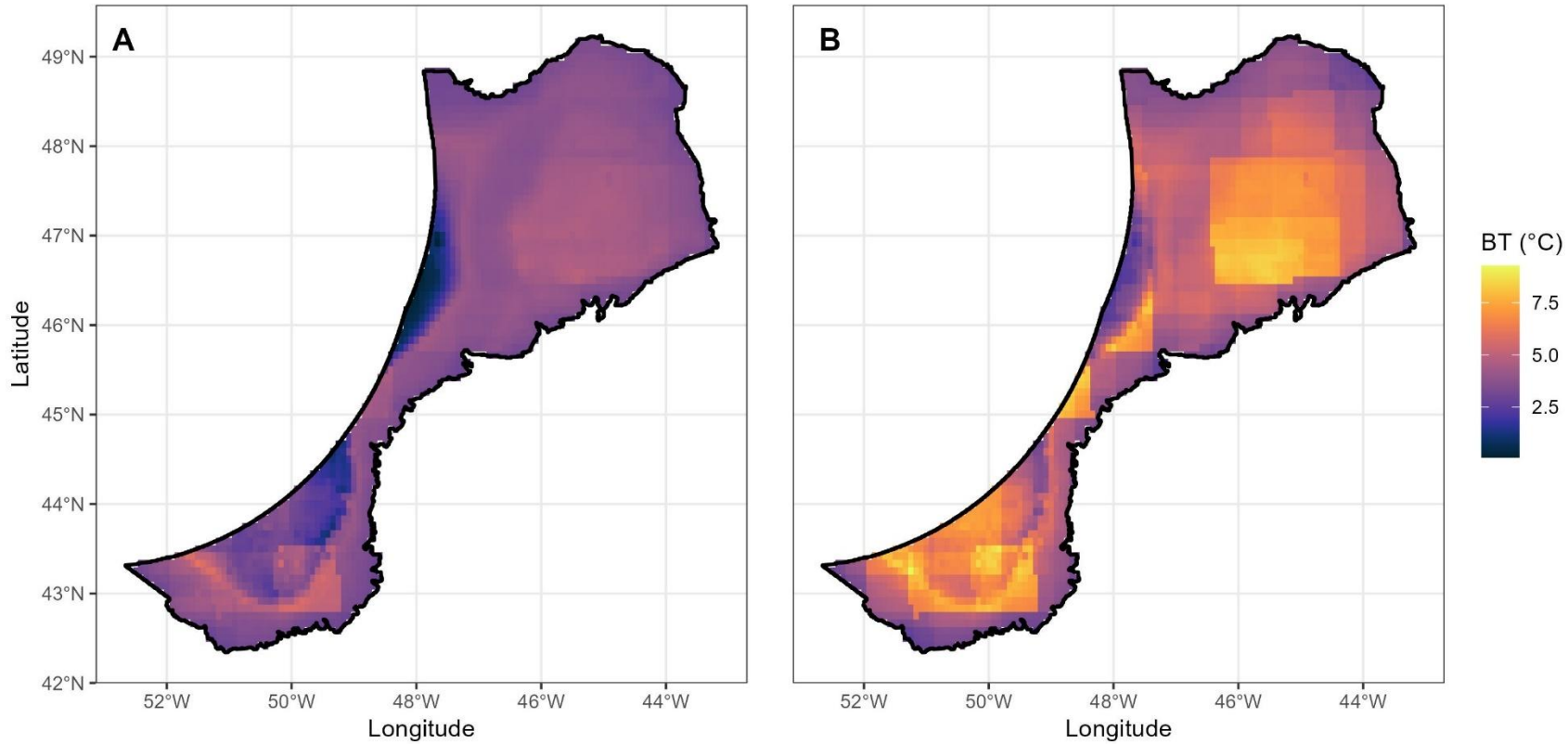

Figure 50. The spatial distribution of Minimum Mean Bottom Temperature (BT) from the 22 ensembled CMIP6 models for the NAFO study area. **Left panel.** Averaged for the time period 2020-2039 for Shared Socio-economic Pathway (SSP) 1-2.6. **Right panel.** Averaged for the time period 2080-2099 for Shared Socio-economic Pathway (SSP) 5-8.5.

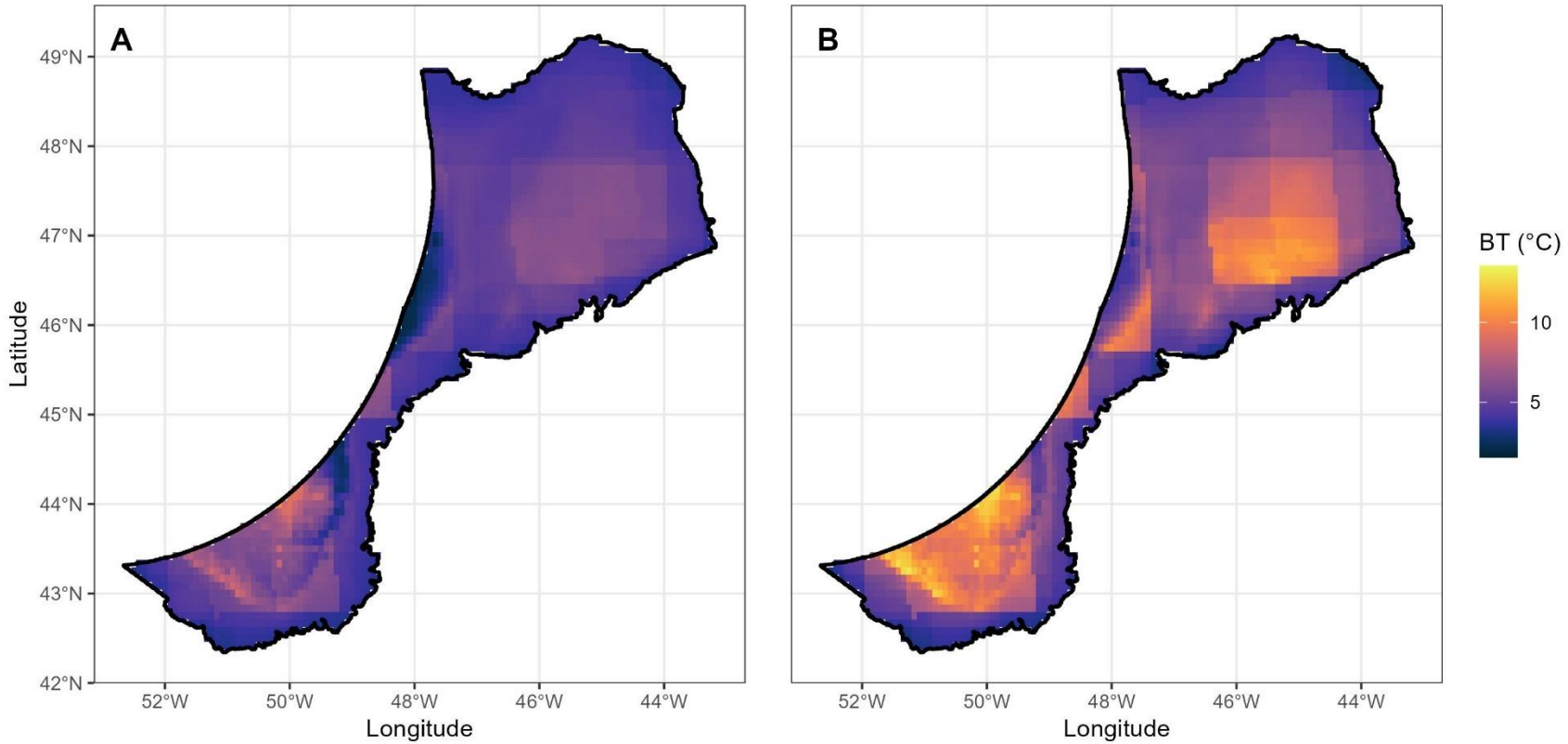

Figure 51. The spatial distribution of Maximum Mean Bottom Temperature (BT) from the 22 ensembled CMIP6 models for the NAFO study area. **Left panel.** Averaged for the time period 2020-2039 for Shared Socio-economic Pathway (SSP) 1-2.6. **Right panel.** Averaged for the time period 2080-2099 for Shared Socio-economic Pathway (SSP) 5-8.5.

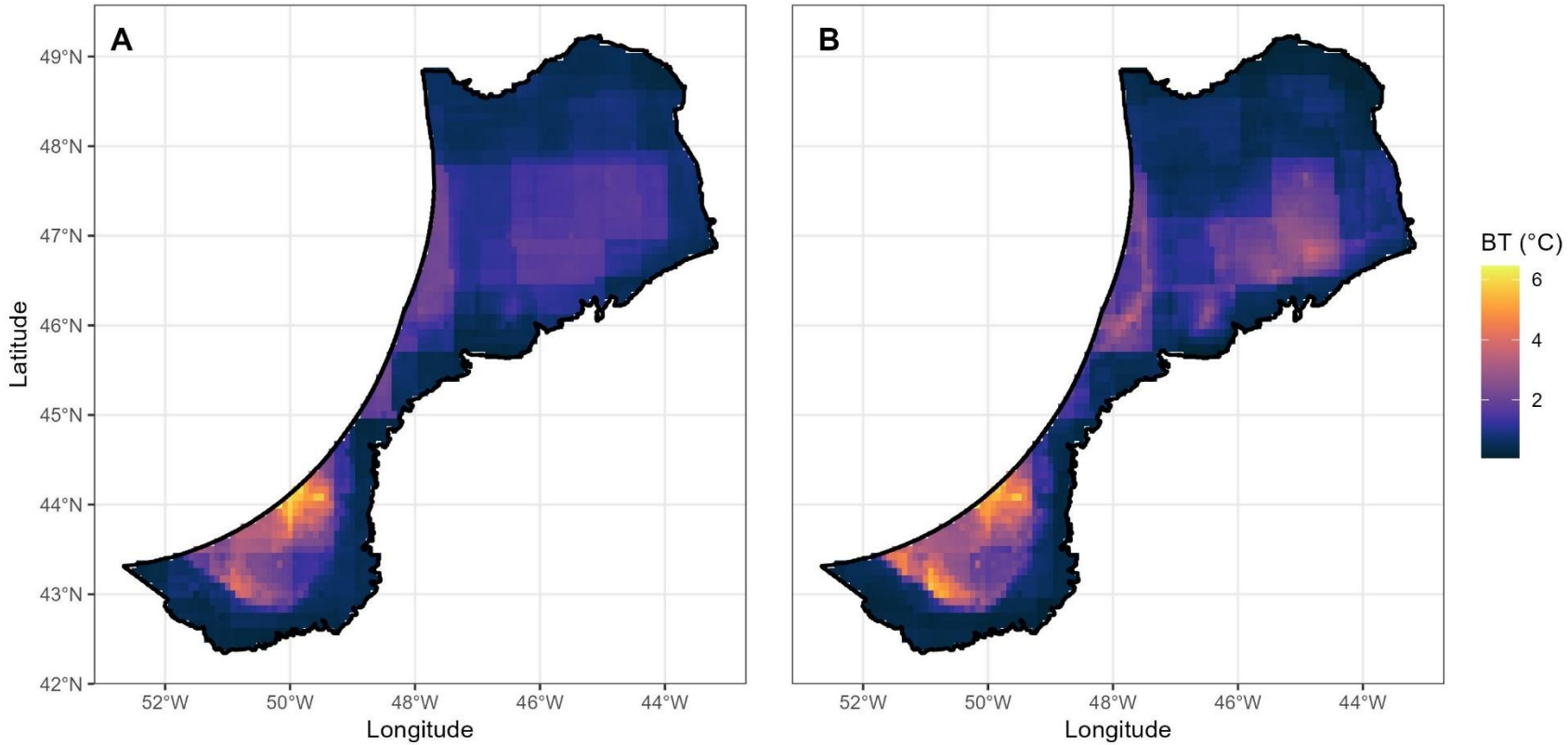

Figure 52. The spatial distribution of Range of Mean Bottom Temperature (BT) from the 22 ensembled CMIP6 models for the NAFO study area. **Left panel.** Averaged for the time period 2020-2039 for Shared Socio-economic Pathway (SSP) 1-2.6. **Right panel.** Averaged for the time period 2080-2099 for Shared Socio-economic Pathway (SSP) 5-8.5.

Bottom Salinity (BS)

Bottom Salinity (BS) showed high variability in the annual mean values over time (Figure 53) with very little change in mean values by SSP or Period (Table 11) but with slightly higher values appearing mid-century. A similar pattern was seen in the mean values in each time period (Figure 54).

The spatial distribution of the variables is shown in Figures 55, 56, 57 and 58 for each variable for SSP1-2.6 and SSP5-8.5. There is considerable spatial variation in BS for all variables with the Tail of Grand Bank being fresher with respect to the mean, minimum and maximum values (Figures 55, 56, 57). That area also saw the largest range in values (Figure 58).

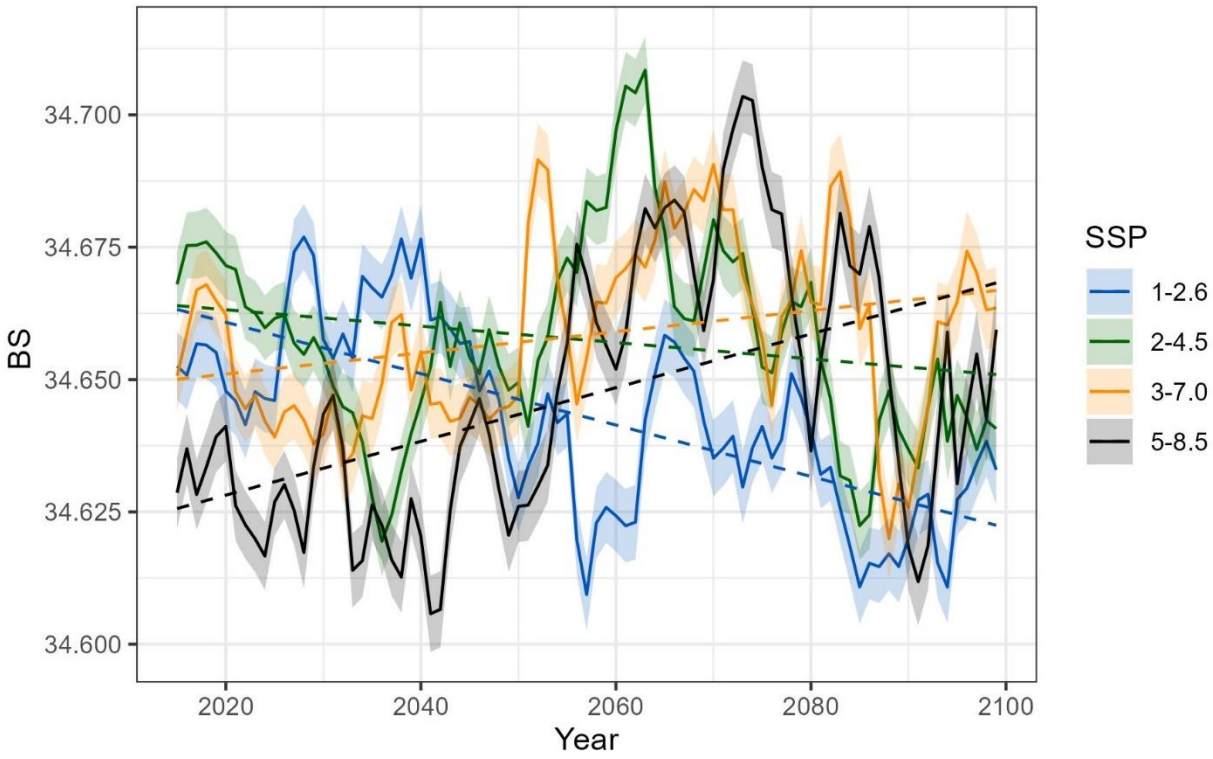

Figure 53. Annual mean Bottom Salinity (BS) trends from the 22 ensembled CMIP6 models for the NAFO study area are shown for each of four Shared Socio-economic Pathways (SSPs) and each year from 2015 to 2100. Dashed lines indicate linear fit to the data. Shaded areas are the 95% confidence intervals for the ensembled means.

Table 11. The mean ± standard deviation from the 22 ensembled CMIP6 models of Bottom Salinity (BS) for the NAFO study area for each of four Shared Socio-economic Pathways (SSPs) and time periods.

SSP	2020-2039	2040-2059	2060-2079	2080-2099
1-2.6	34.66 ± 0.57	34.64 ± 0.59	34.64 ± 0.62	34.62 ± 0.60
2-4.5	34.65 ± 0.58	34.66 ± 0.59	34.67 ± 0.60	34.64 ± 0.61
3-7.0	34.65 ± 0.59	34.66 ± 0.62	34.67 ± 0.61	34.66 ± 0.67
5-8.5	34.63 ± 0.60	34.64 ± 0.61	34.68 ± 0.63	34.65 ± 0.72

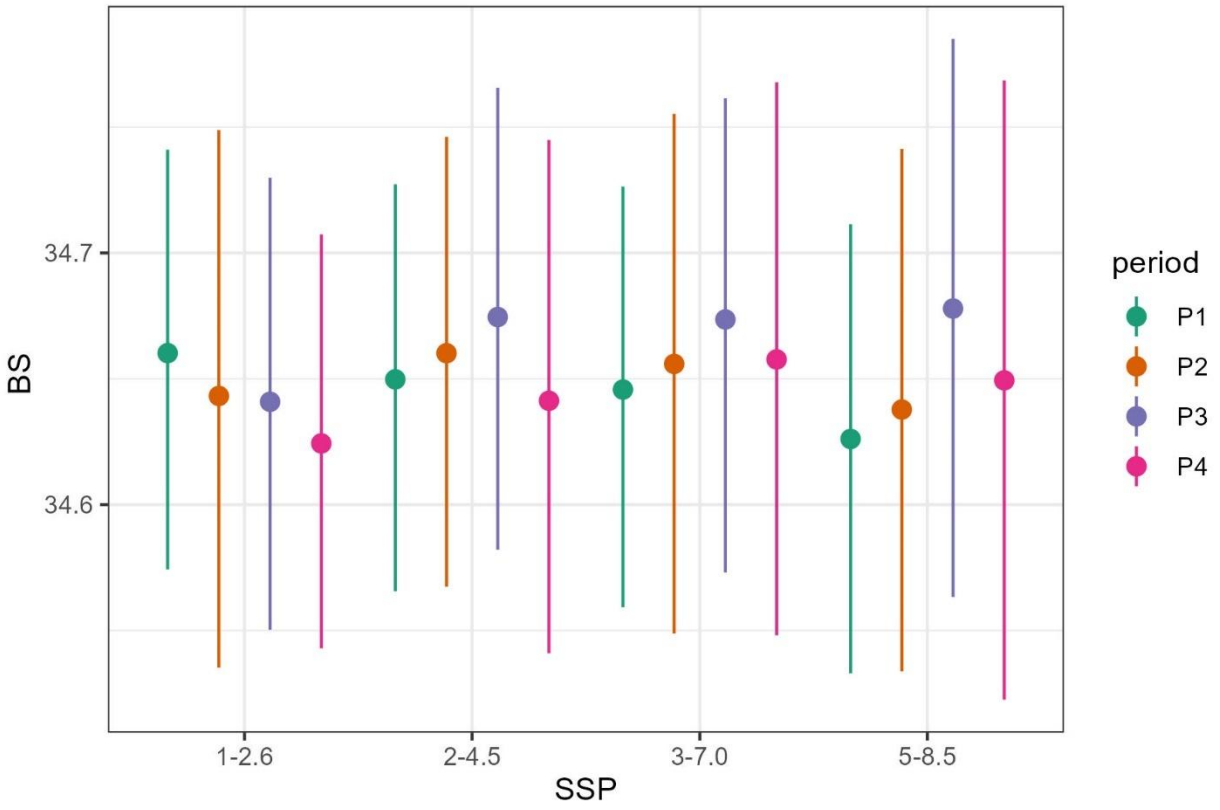

Figure 54. The mean Bottom Salinity (BS) from the 22 ensembled CMIP6 models for the NAFO study area is shown for each of four Shared Socio-economic Pathways (SSPs) and time periods (P1: 2020-2039, P2: 2040-2059, P3: 2060-2079, P4: 2080-2099). Bars represent minimum, maximum values and range of the data products averaged over the spatial extent.

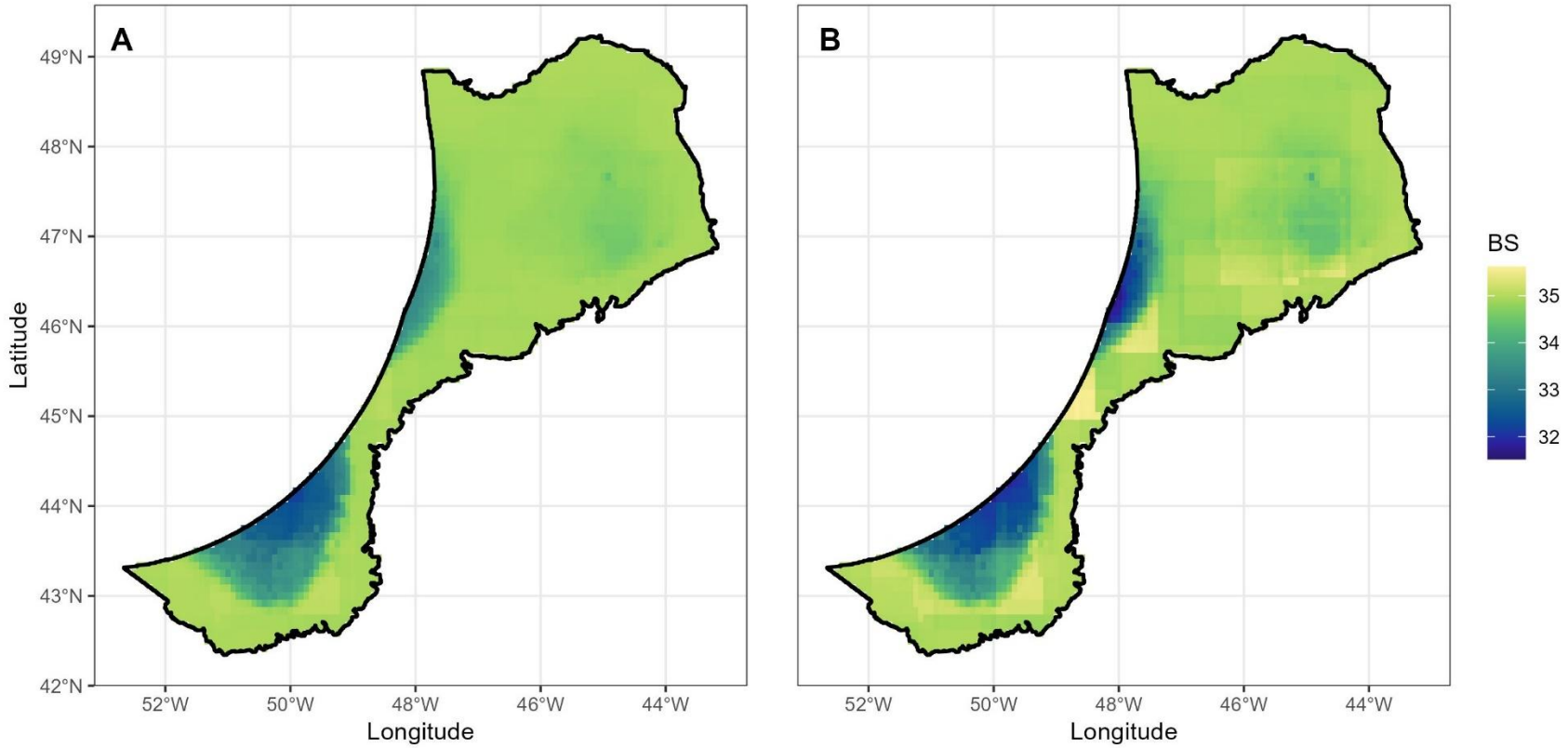

Figure 55. The spatial distribution of Mean Bottom Salinity (BS) from the 22 ensembled CMIP6 models for the NAFO study area. **A)** Time period 2020-2039 for Shared Socio-economic Pathway (SSP) 1-2.6. **B)** Time period 2080-2099 for Shared Socio-economic Pathway (SSP) 5-8.5.

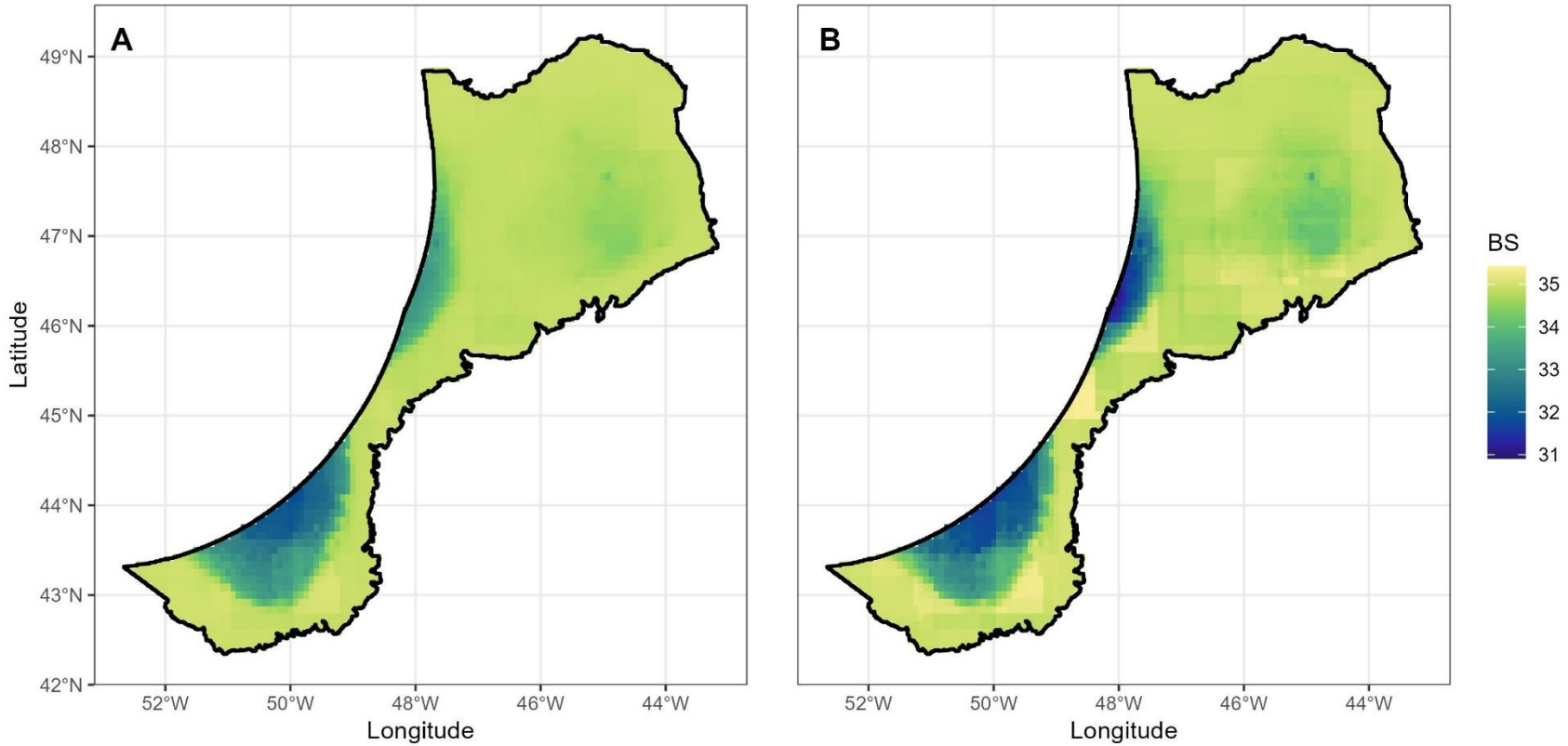

Figure 56. The spatial distribution of Minimum Mean Bottom Salinity (BS) from the 22 ensembled CMIP6 models for the NAFO study area. **Left panel.** Averaged for the time period 2020-2039 for Shared Socio-economic Pathway (SSP) 1-2.6. **Right panel.** Averaged for the time period 2080-2099 for Shared Socio-economic Pathway (SSP) 5-8.5.

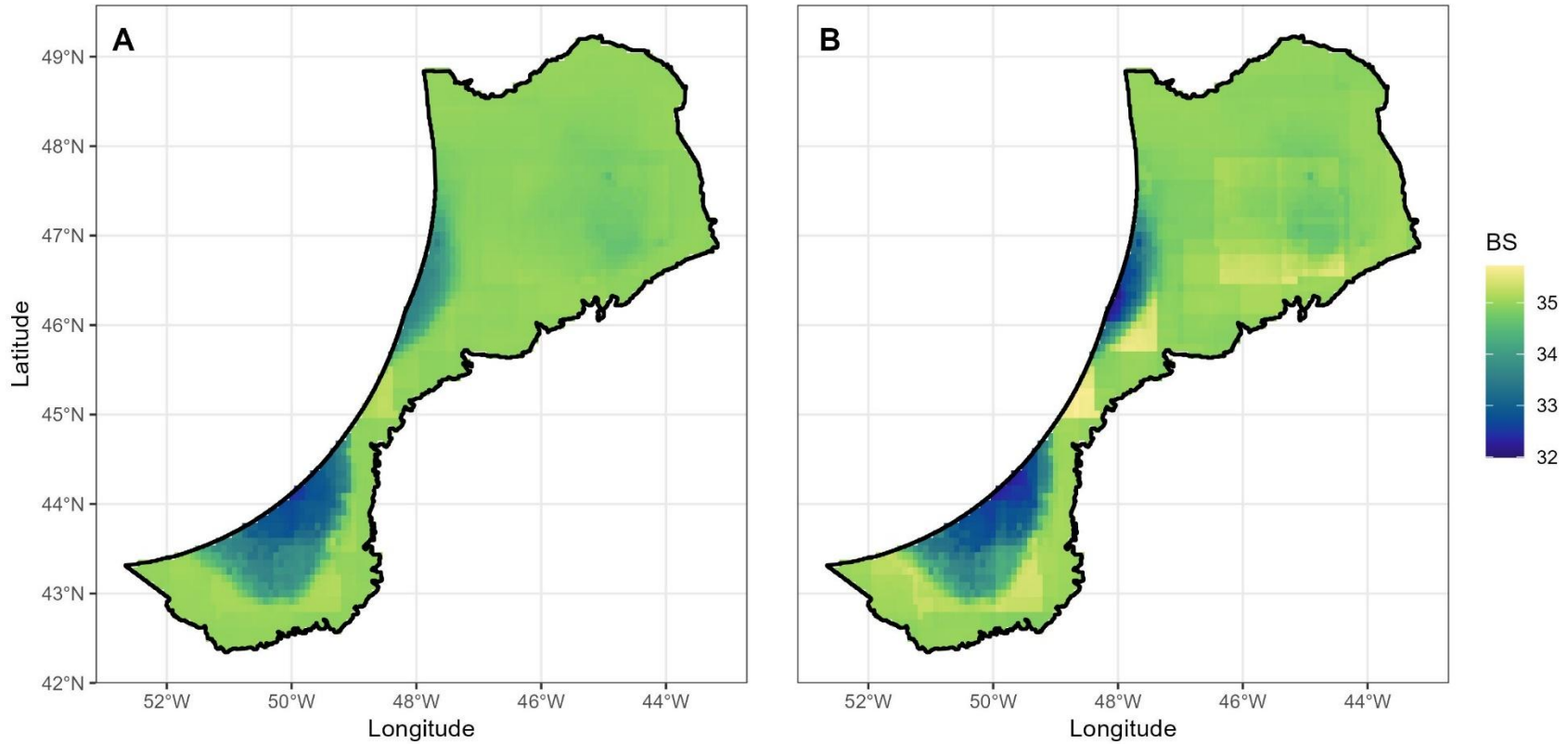

Figure 57. The spatial distribution of Maximum Mean Bottom Salinity (BS) from the 22 ensembled CMIP6 models for the NAFO study area. **Left panel.** Averaged for the time period 2020-2039 for Shared Socio-economic Pathway (SSP) 1-2.6. **Right panel.** Averaged for the time period 2080 2099 for Shared Socio-economic Pathway (SSP) 5-8.5.

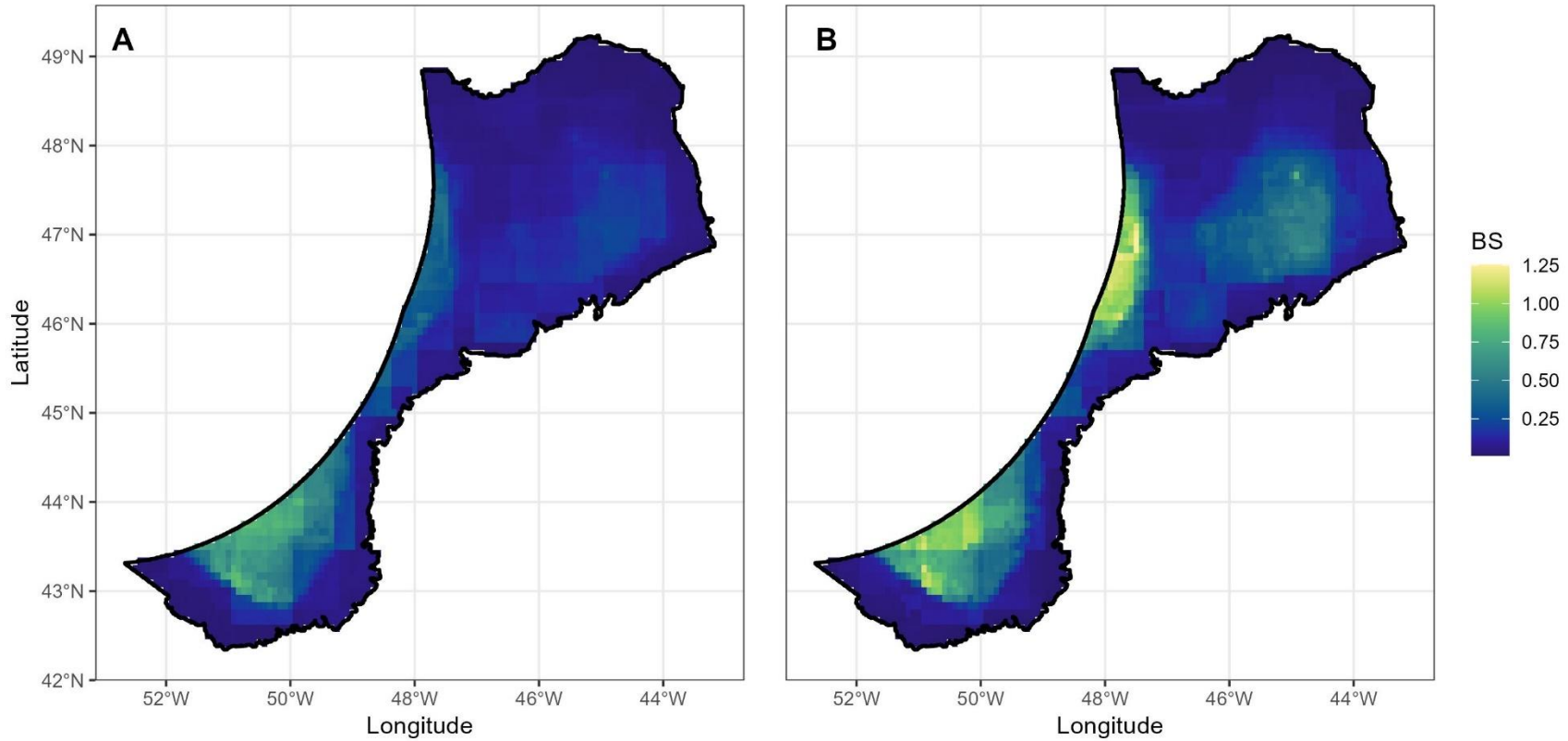

Figure 58. The spatial distribution of Range of Mean Bottom Salinity (BS) from the 22 ensembled CMIP6 models for the NAFO study area. **Left panel.** Averaged for the time period 2020-2039 for Shared Socio-economic Pathway (SSP) 1-2.6. **Right panel.** Averaged for the time period 2080-2099 for Shared Socio-economic Pathway (SSP) 5-8.5.

Bottom Current Speed (BCS)

Bottom Current Speed (BCS) showed decreases in the annual mean values over time (Figure 59) with SSP having less impact than in other variables (Figure 59). Mean values (Table 12, Figure 60) ranged from 0.05 to 0.07 m/s.

The spatial distribution of the variables is shown in Figures 61, 62, 63 and 64 for each variable for SSP1-2.6 and SSP5-8.5. They each show similar spatial distributions.

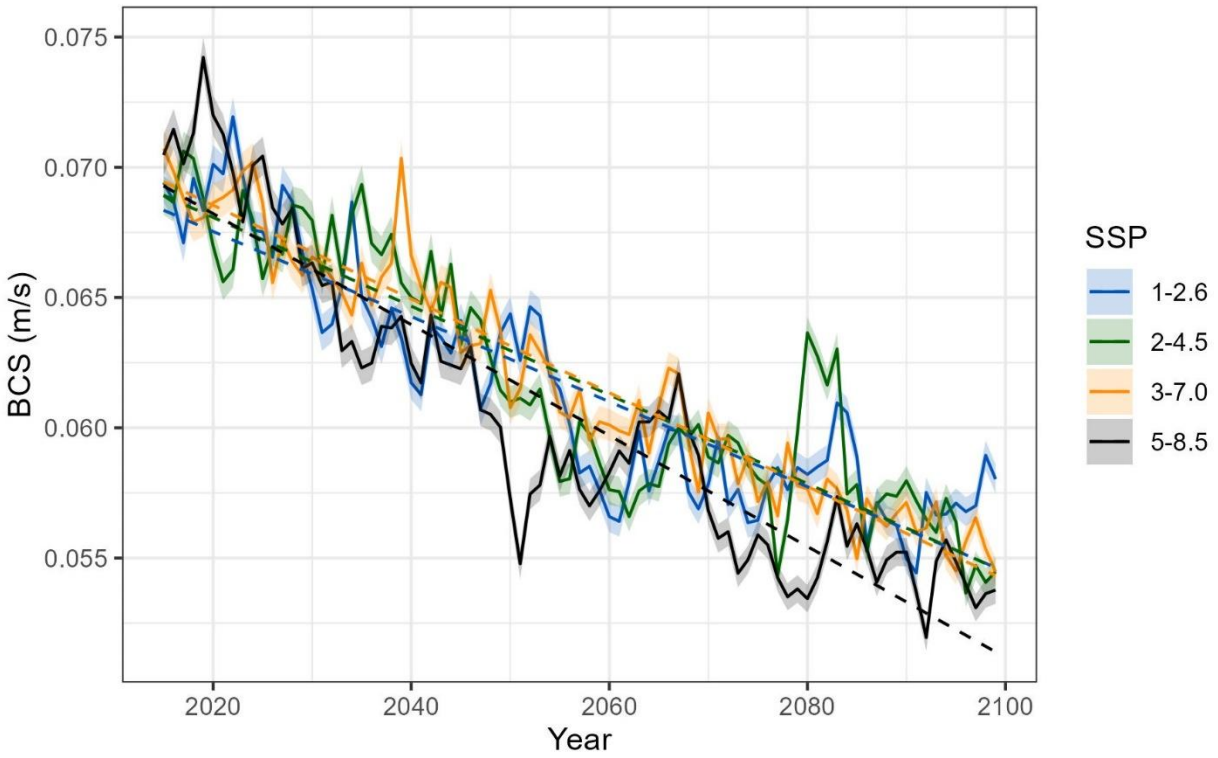

Figure 59. Annual mean Bottom Current Speed (BCS) in m/s trends from the 22 ensembled CMIP6 models for the NAFO study area are shown for each of four Shared Socio-economic Pathways (SSPs) and each year from 2015 to 2100. Dashed lines indicate linear fit to the data. Shaded areas are the 95% confidence intervals for the ensembled means.

Table 12. The mean ± standard deviation from the 22 ensembled CMIP6 models of Bottom Current Speed (BCS) in m/s for the NAFO study area for each of four Shared Socio-economic Pathways (SSPs) and time periods.

SSP	2020-2039	2040-2059	2060-2079	2080-2099
1-2.6	0.07 ± 0.06	0.06 ± 0.06	0.06 ± 0.05	0.06 ± 0.05
2-4.5	0.07 ± 0.06	0.06 ± 0.06	0.06 ± 0.05	0.06 ± 0.05
3-7.0	0.07 ± 0.06	0.06 ± 0.06	0.06 ± 0.05	0.06 ± 0.05
5-8.5	0.07 ± 0.06	0.06 ± 0.06	0.06 ± 0.05	0.05 ± 0.05

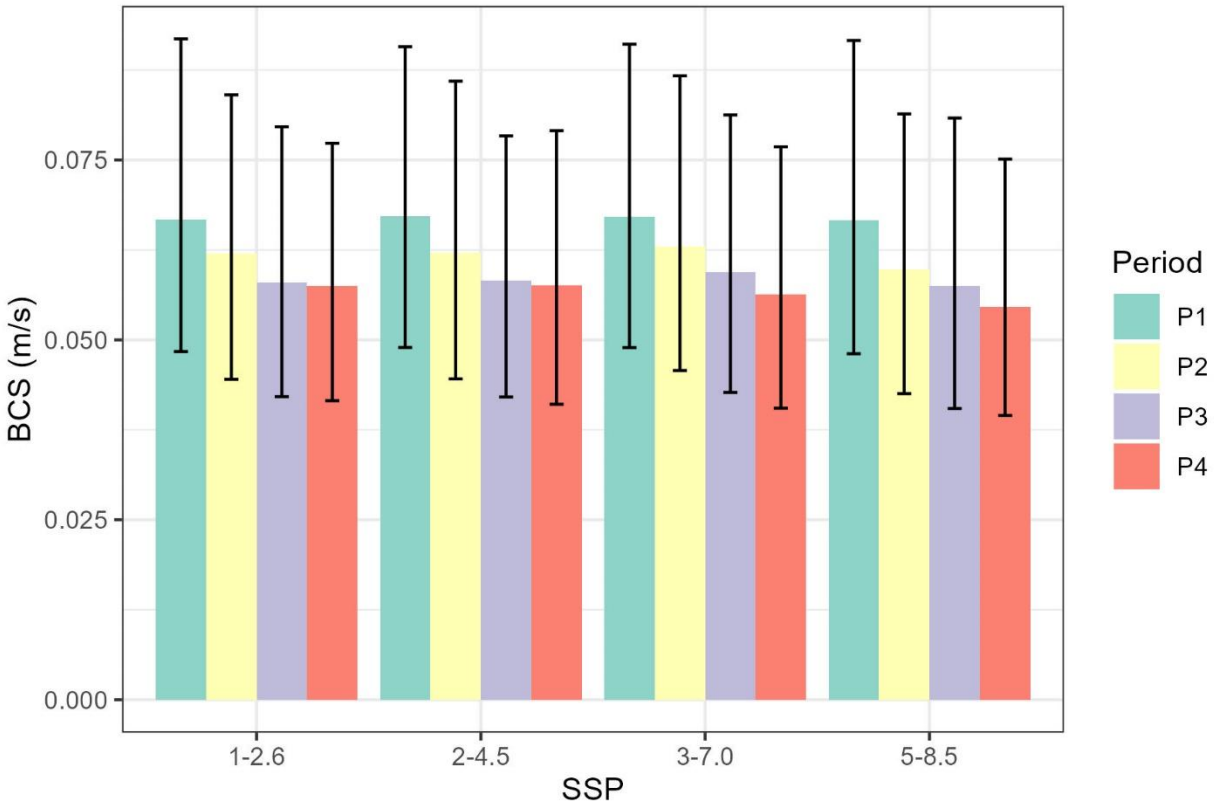

Figure 60. The mean Bottom Current Speed (BCS) in m/s from the 22 ensembled CMIP6 models for the NAFO study area is shown for each of four Shared Socio-economic Pathways (SSPs) and time periods (P1: 2020-2039, P2: 2040-2059, P3: 2060-2079, P4: 2080-2099). Bars represent minimum, maximum values and range of the data products averaged over the spatial extent.

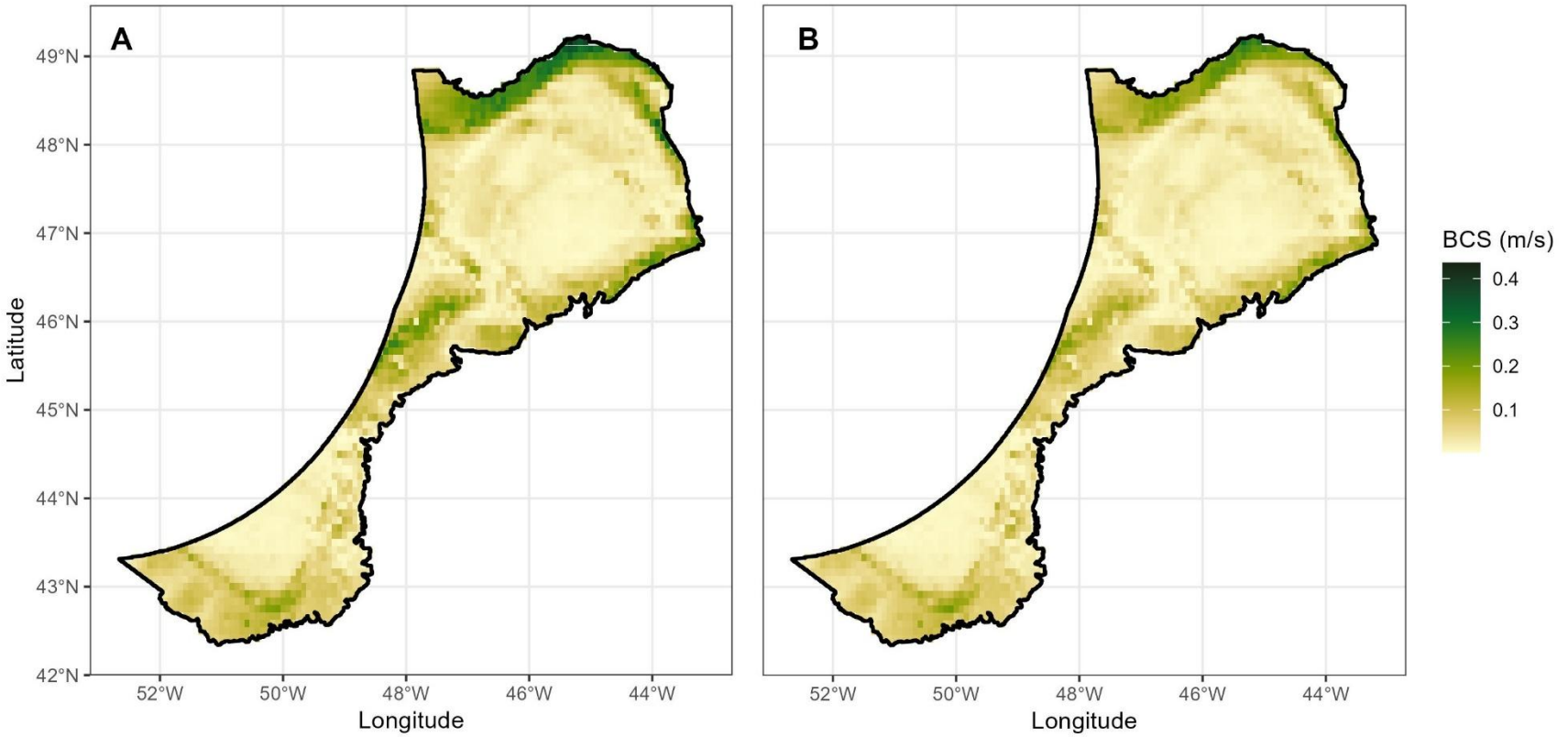

Figure 61. The spatial distribution of Mean Bottom Current Speed (BCS) from the 22 ensembled CMIP6 models for the NAFO study area. **A)** Time period 2020-2039 for Shared Socio-economic Pathway (SSP) 1-2.6. **B)** Time period 2080-2099 for Shared Socio-economic Pathway (SSP) 5-8.5.

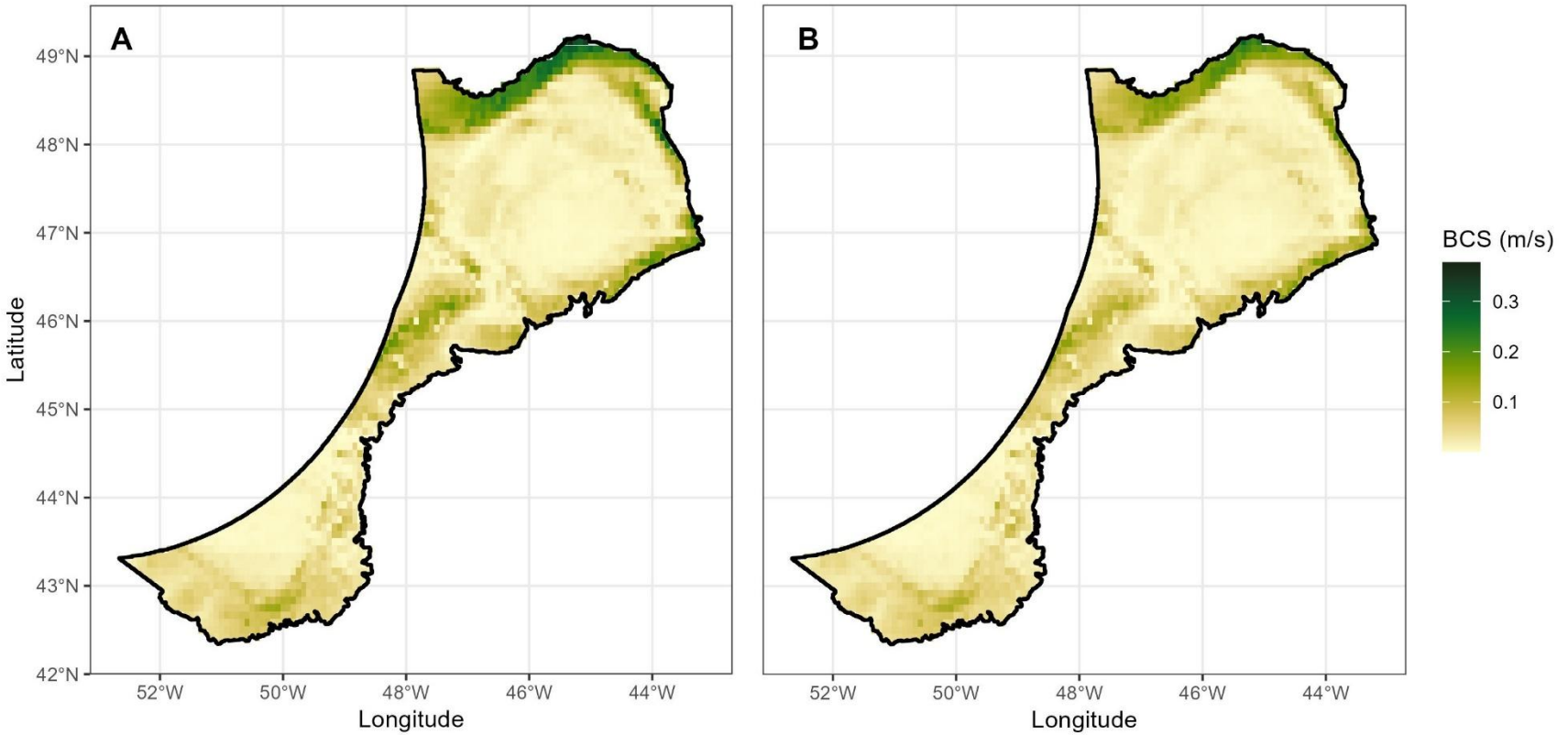

Figure 62. The spatial distribution of Minimum Mean Bottom Current Speed (BCS) from the 22 ensembled CMIP6 models for the NAFO study area. **Left panel.** Averaged for the time period 2020-2039 for Shared Socio-economic Pathway (SSP) 1-2.6. **Right panel.** Averaged for the time period 2080-2099 for Shared Socio-economic Pathway (SSP) 5-8.5.

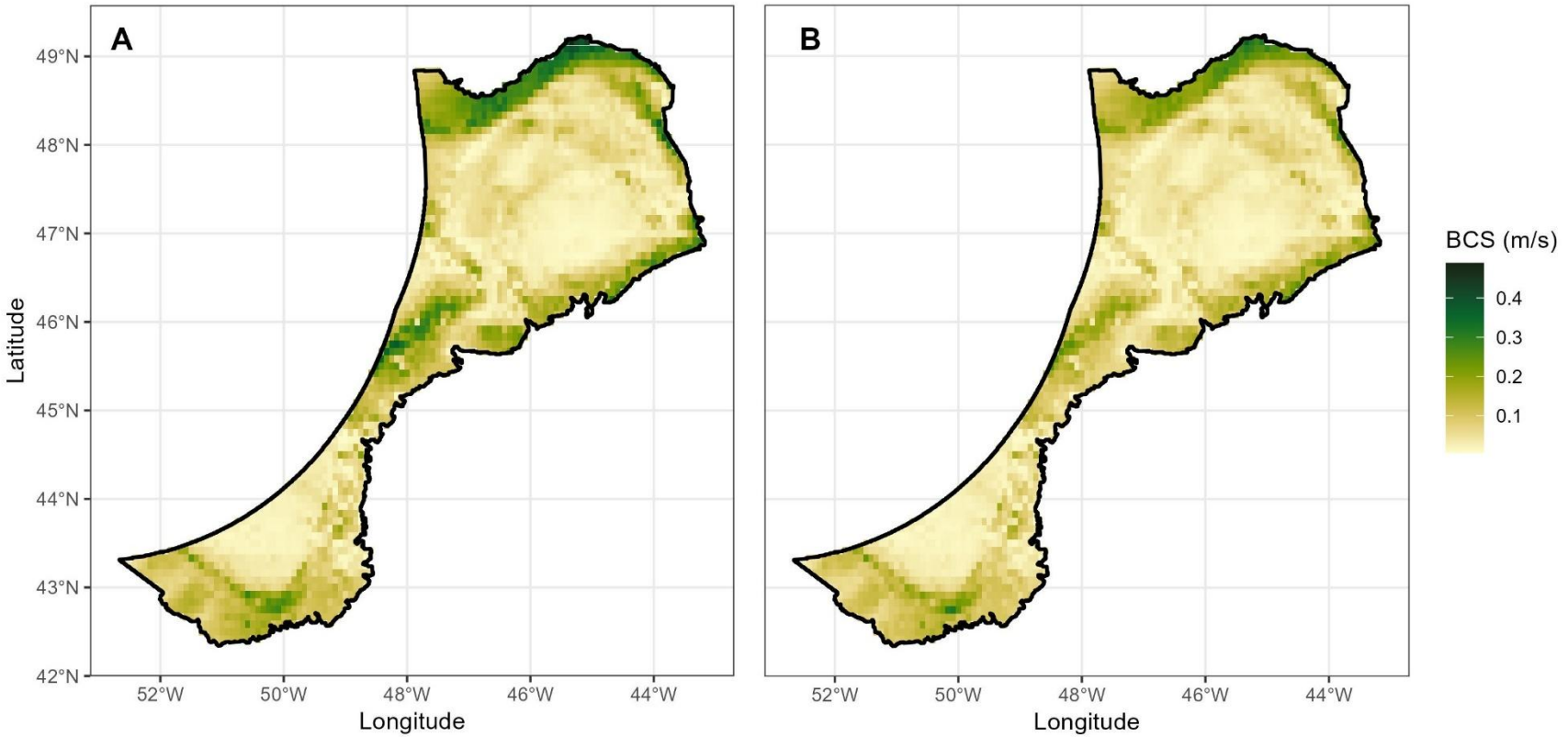

Figure 63. The spatial distribution of Maximum Mean Bottom Current Speed (BCS) from the 22 ensembled CMIP6 models for the NAFO study area. **Left panel.** Averaged for the time period 2020-2039 for Shared Socio-economic Pathway (SSP) 1-2.6. **Right panel.** Averaged for the time period 2080-2099 for Shared Socio-economic Pathway (SSP) 5-8.5.

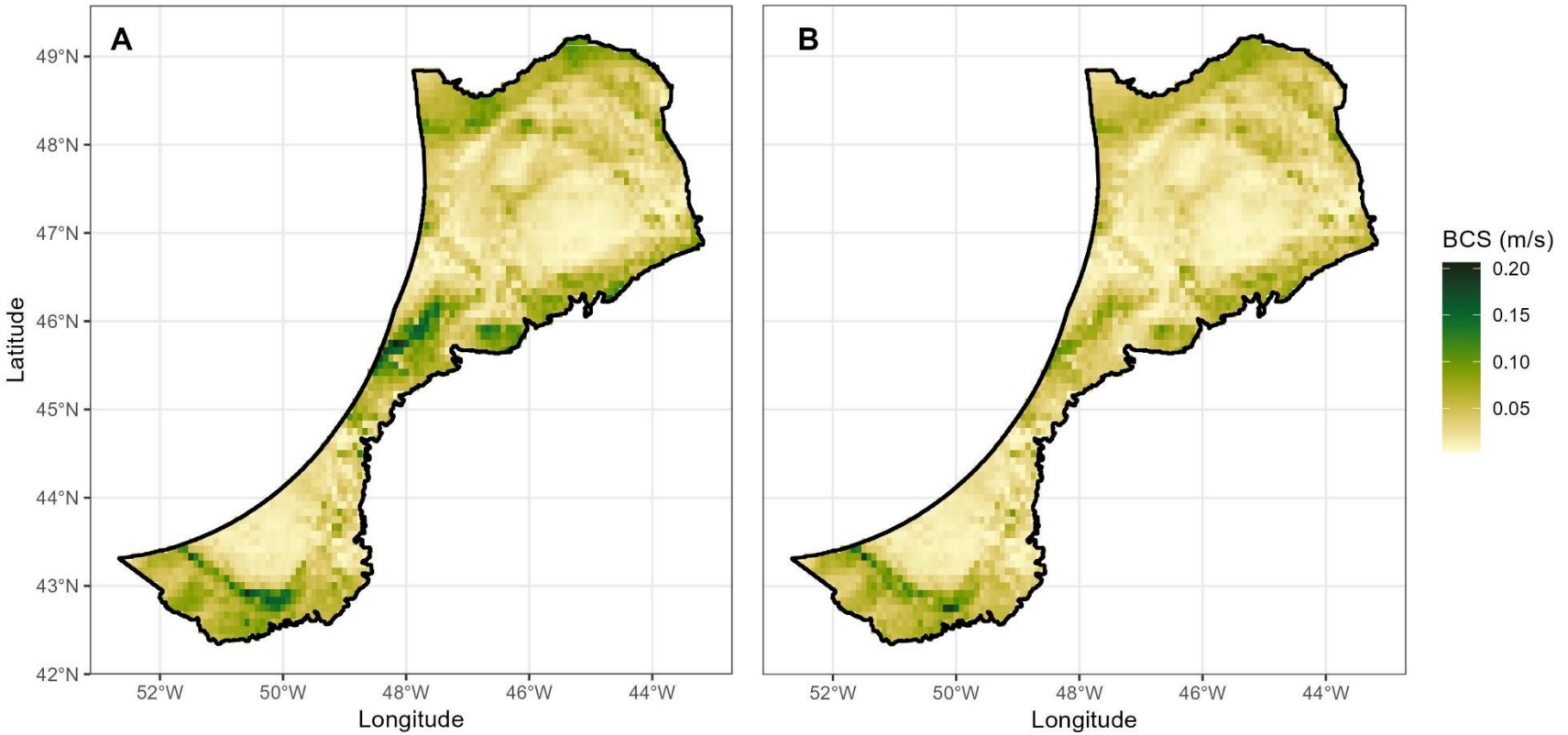

Figure 64. The spatial distribution of Range of Mean Bottom Current Speed (BCS) from the 22 ensembled CMIP6 models for the NAFO study area. **Left panel.** Averaged for the time period 2020-2039 for Shared Socio-economic Pathway (SSP) 1-2.6. **Right panel.** Averaged for the time period 2080-2099 for Shared Socio-economic Pathway (SSP) 5-8.5.

Bottom Stress (BStr)

Bottom Stress (BStr) showed decreases in the annual mean values over time (Figure 65) with SSP having less impact than time. Mean values (Table 13, Figure 66) ranged from 0.02 to 0.03 Pa. Decreasing trends were seen in the mean, minimum and maximum values with increasing time period (Figure 67).

The spatial distribution of the variables is shown in Figures 67, 68, 69 and 70 for each variable for SSP1-2.6 and SSP5-8.5. They each show similar spatial distributions.

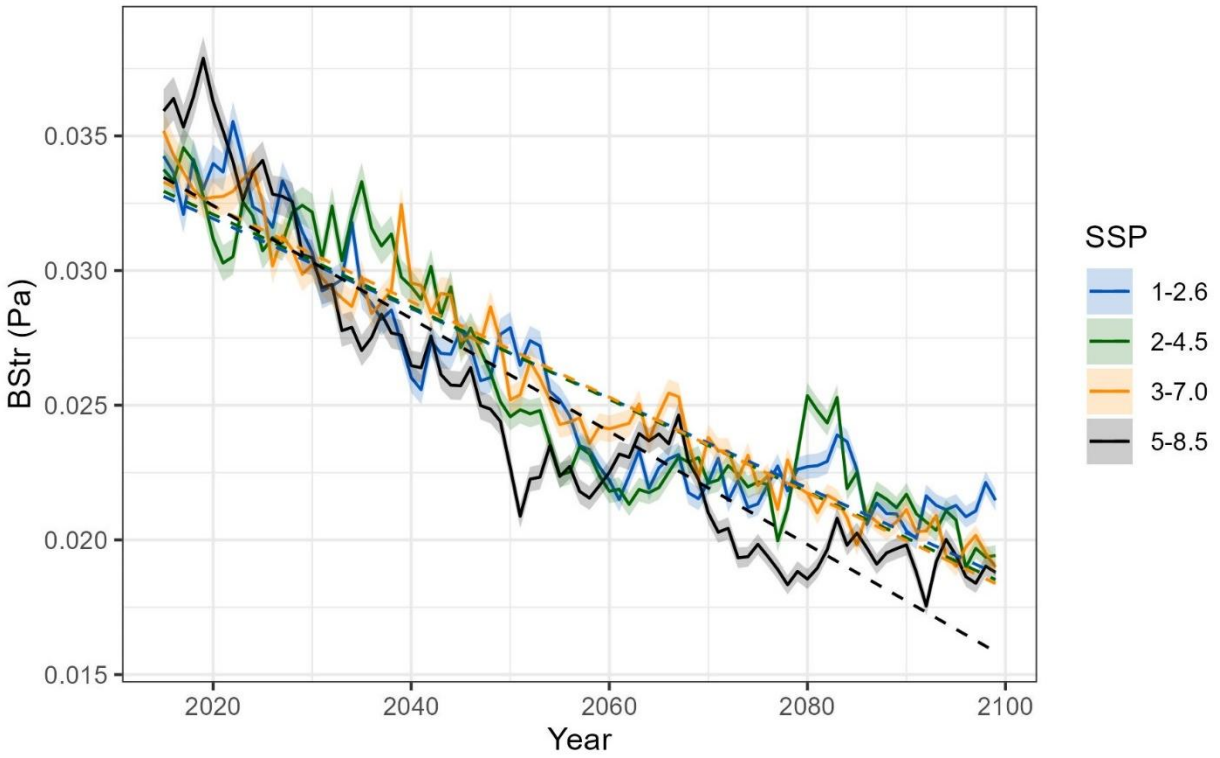

Figure 65. Annual mean Bottom Stress (BStr) in Pascals (Pa) trends for the NAFO study area are shown for each of four Shared Socio-economic Pathways (SSPs) and each year from 2015 to 2100. Dashed lines indicate linear fit to the data. Shaded areas are the 95% confidence intervals for the ensembled means.

Table 13. The mean ± standard deviation of Bottom Stress (BStr) in Pascals (Pa) for the NAFO study area for each of four Shared Socio-economic Pathways (SSPs) and time periods.

SSP	2020-2039	2040-2059	2060-2079	2080-2099
1-2.6	0.03 ± 0.06	0.03 ± 0.05	0.02 ± 0.04	0.02 ± 0.04
2-4.5	0.03 ± 0.06	0.03 ± 0.05	0.02 ± 0.04	0.02 ± 0.04
3-7.0	0.03 ± 0.06	0.03 ± 0.05	0.02 ± 0.04	0.02 ± 0.04
5-8.5	0.03 ± 0.06	0.02 ± 0.05	0.02 ± 0.04	0.02 ± 0.03

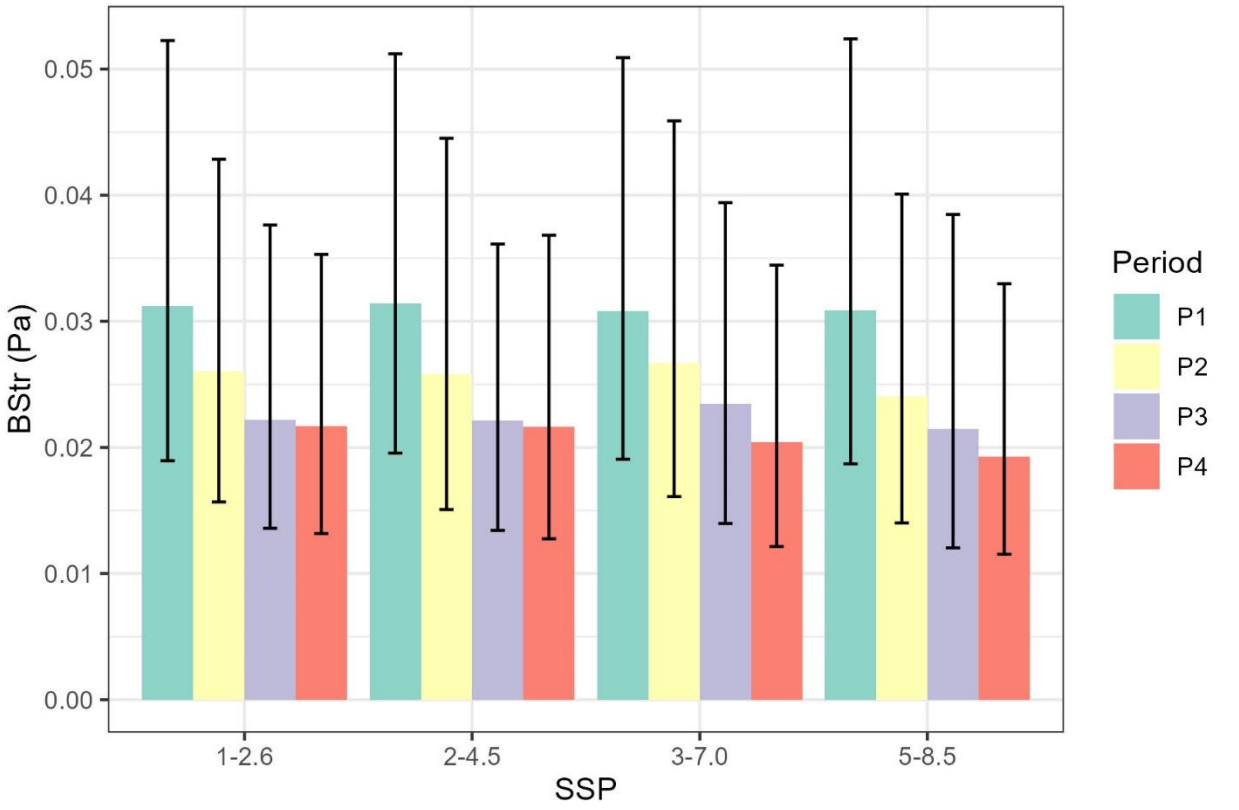

Figure 66. The mean Bottom Stress (BStr) for the NAFO study area is shown for each of four Shared Socio-economic Pathways (SSPs) and time periods (P1: 2020-2039, P2: 2040-2059, P3: 2060-2079, P4: 2080-2099). Bars represent minimum, maximum values and range of the data products averaged over the spatial extent.

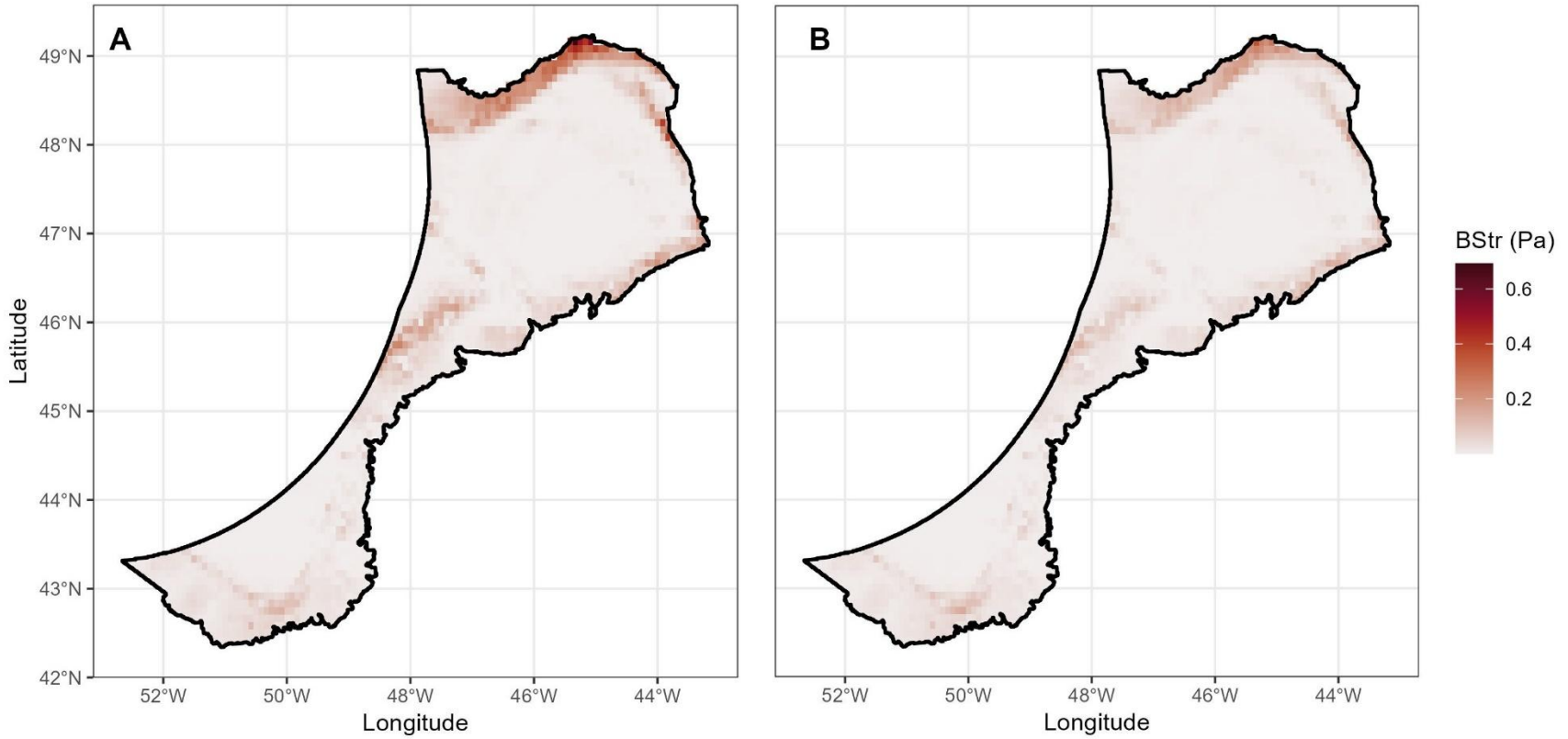

Figure 67. The spatial distribution of Mean Bottom Stress (BStr) for the NAFO study area. **A)** Time period 2020-2039 for Shared Socio-economic Pathway (SSP) 1-2.6. **B)** Time period 2080-2099 for Shared Socio-economic Pathway (SSP) 5-8.5. Pa = Pascal.

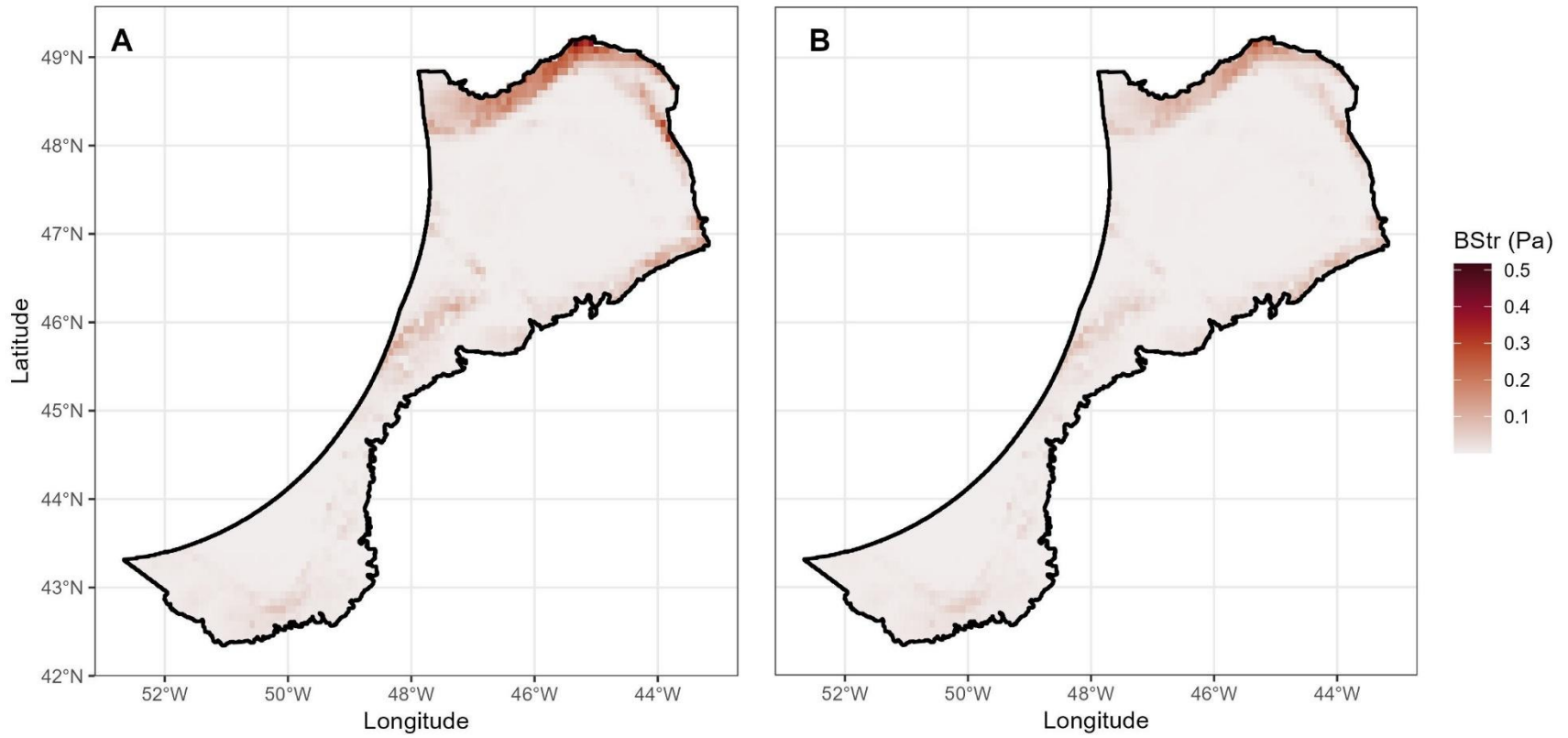

Figure 68. The spatial distribution of Minimum Mean Bottom Stress (BStr) for the NAFO study area. **Left panel.** Averaged for the time period 2020-2039 for Shared Socio-economic Pathway (SSP) 1-2.6. **Right panel.** Averaged for the time period 2080-2099 for Shared Socio-economic Pathway (SSP) 5-8.5. Pa = Pascal.

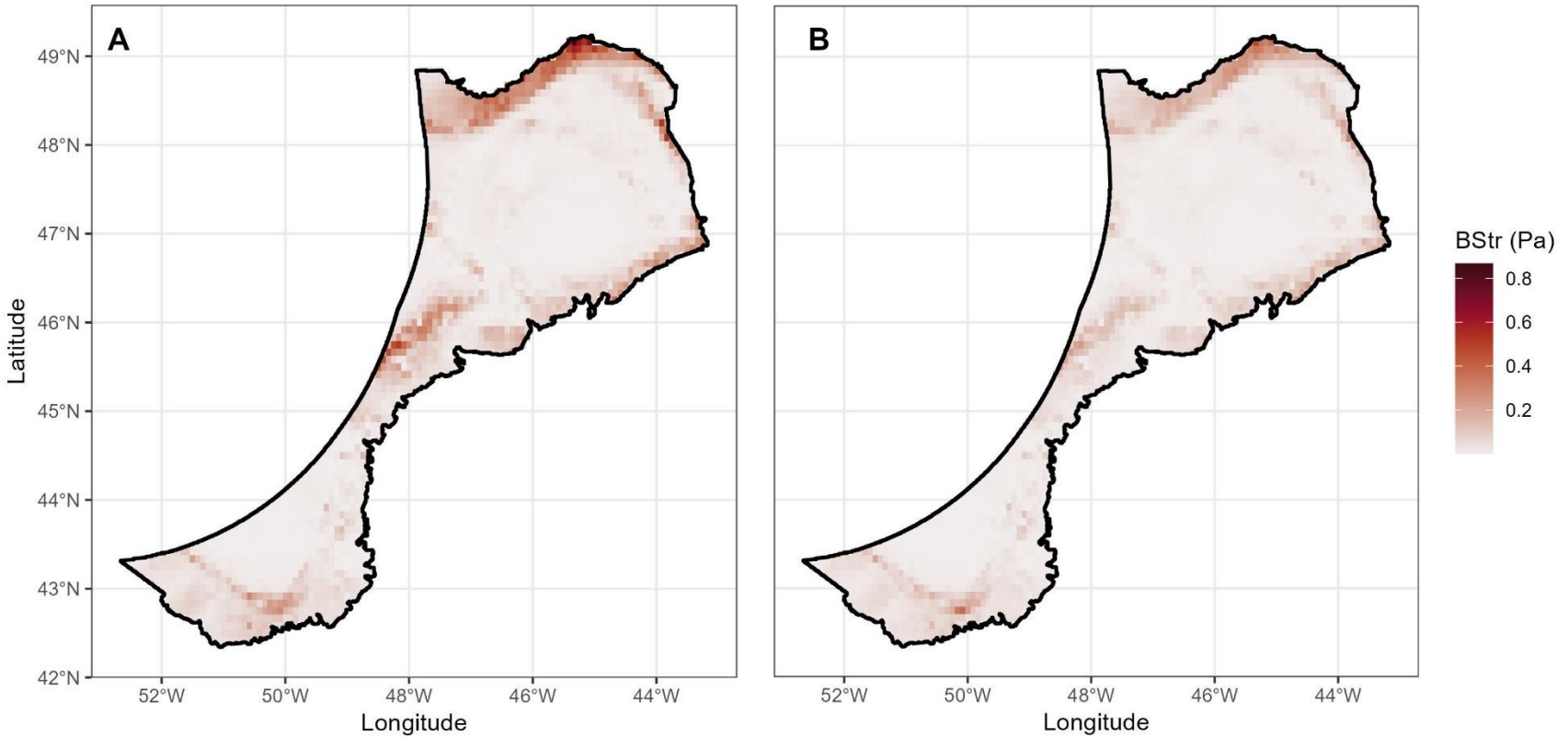

Figure 69. The spatial distribution of Maximum Mean Bottom Stress (BStr) for the NAFO study area. **Left panel.** Averaged for the time period 2020-2039 for Shared Socio-economic Pathway (SSP) 1-2.6. **Right panel.** Averaged for the time period 2080-2099 for Shared Socio-economic Pathway (SSP) 5-8.5. Pa = Pascal.

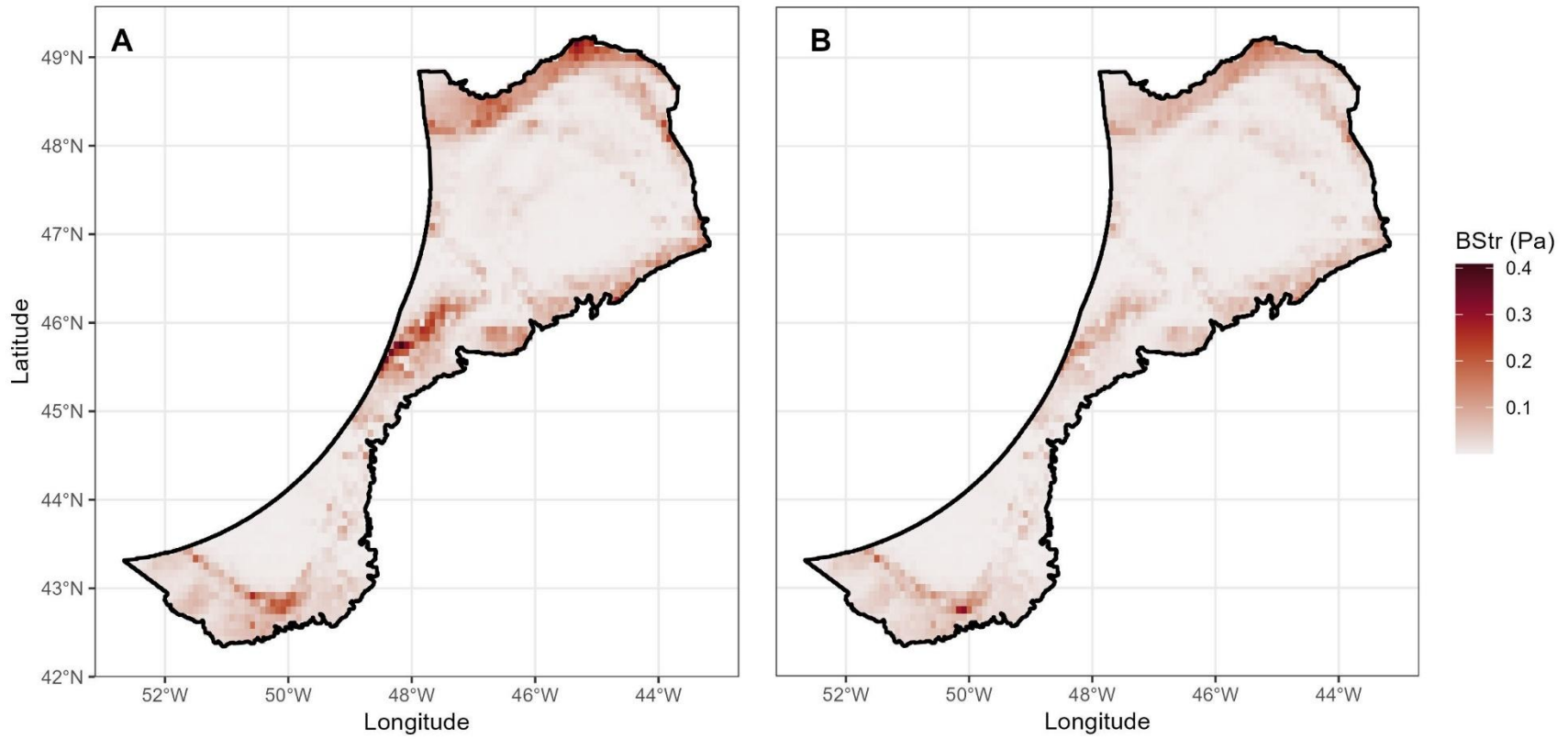

Figure 70. The spatial distribution of Range of Mean Bottom Stress (BStr) for the NAFO study area. **Left panel.** Averaged for the time period 2020-2039 for Shared Socio-economic Pathway (SSP) 1-2.6. **Right panel.** Averaged for the time period 2080-2099 for Shared Socio-economic Pathway (SSP) 5-8.5. Pa = Pascal.

Comparison with BNAM Data Products

There was a significant correlation between all of the BNAM- and CMIP6-derived variables (Figure 71), with the highest correlations (> 0.8) in the MLD (Max), MLD_W (Max), MLD_F (Max), SSS (Mean, Max), SST (Mean, Max, Min) and BS (Mean, Max, Min). The lowest correlations were with the BT (Min) and BT (Mean) variables. The spatial distribution of the differences between the BNAM and CMIP6 products showed the greatest similarity for the BStr variables (Mean, Min, Max) and Maximum Annual, Fall and Winter MLD. CMIP6 products generally were warmer than BNAM products in SST and less saline (SSS). Details for these comparisons by variable are provided below. Collectively the results suggest that the BNAM products are similar to the CMIP6 products and that SDMs for Period 1 and SSP2-4.5 should produce similar maps of occurrence.

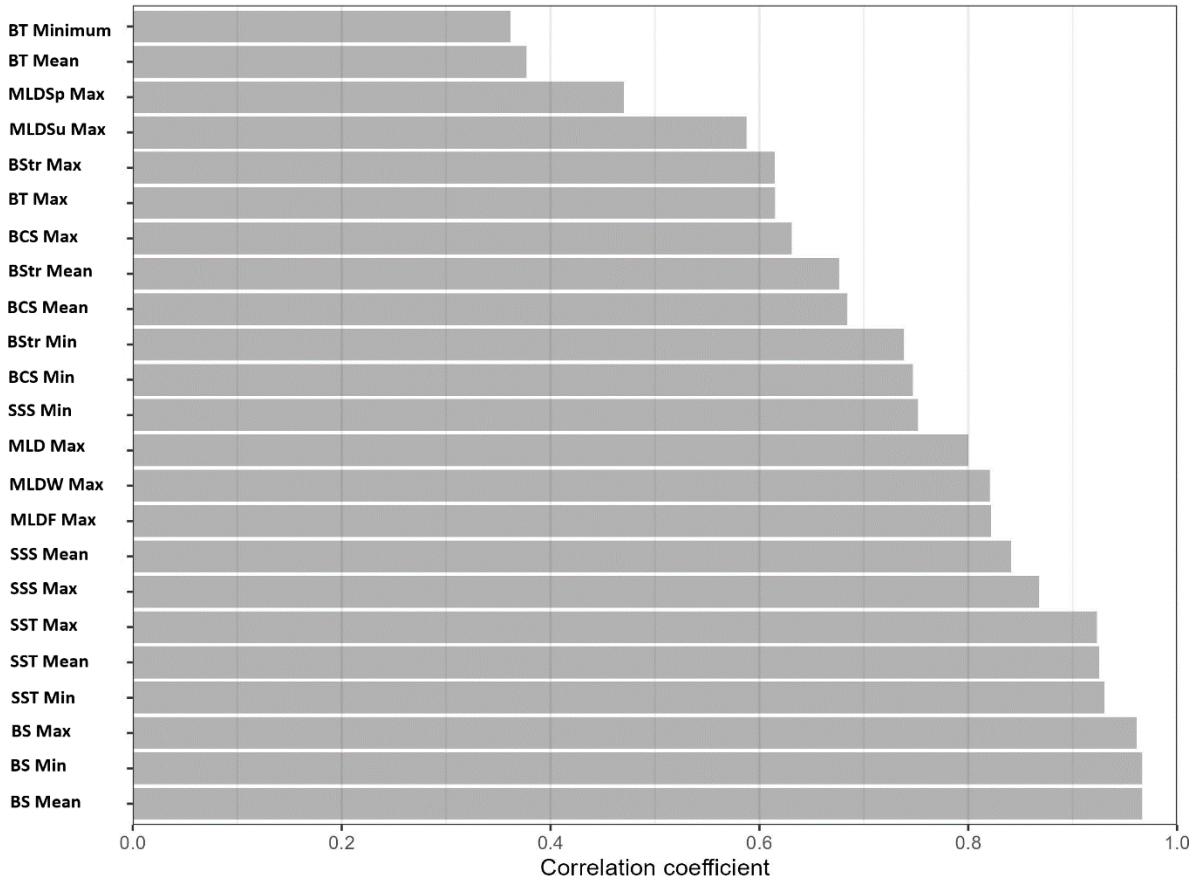

Figure 71. Pearson correlation (r) between BNAM and CMIP6 data. All correlations are statistically significant. Variable names are given in full in Table 2.

Sea Surface Temperature (SST)

The differences between the BNAM and CMIP6 products for the SST variables showed an even distribution of difference across the spatial domain in all three variables (Mean, Min, Max) (Figure 72). CMIP6 products generally were warmer than BNAM products, which may be reflective of the longer time period for the CMIP6 projects (1990-2023 vs 2020-2039 respectively).

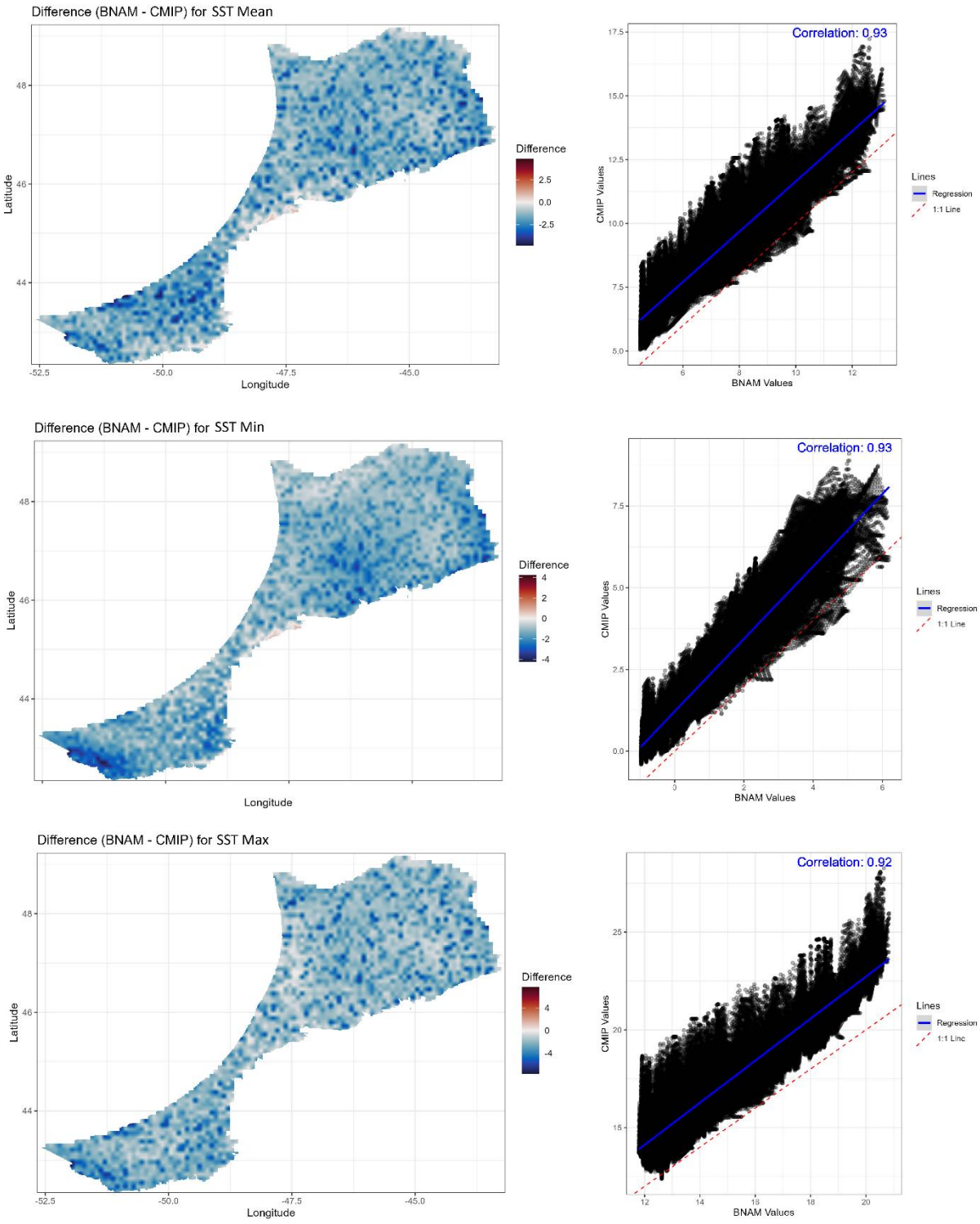

Figure 72. Spatial differences (left column) and correlation (right column) between the BNAM and CMIP6 Sea Surface Temperature (SST) variables (top to bottom: Mean, Min, Max).

Sea Surface Salinity (SSS)

The differences between the BNAM and CMIP6 products for the SSS variables showed an even distribution of difference across the spatial domain in all three variables (Mean, Min, Max) (Figure 73). CMIP6 products generally were fresher (lower S) than BNAM products, which may be reflective of the longer time period for the CMIP6 projects (1990-2023 vs 2020-2039 respectively) given the negative slope of the trend lines (Figure 11).

Mixed Layer Depth (MLD)

Maximum Mixed Layer Depth showed similar annual, fall, and winter seasonal patterns (Figures 74, 75) with CMIP6 products predicting greater maximum MLD on the north and eastern slopes of Flemish Cap and in Flemish Pass than BNAM, and shallower maximum MLD on the Tail of Grand Bank and on Flemish Cap. The largest differences occurred along the northern extent of the study area. Maximum Annual MLD, Fall (Figure 74) and Winter (Figure 75) were very similar between the model products. In Summer, CMIP6 products showed greater maximum MLD than BNAM products in most parts of the spatial extent except for on Flemish Cap where smaller maximum MLD occured. The correlation between these model products is low at 0.59, albeit statistically significant (Figure 74). In Spring, CMIP6 products showed greater maximum MLD than BNAM products in most parts of the spatial extent except for on the slopes of the Tail of Grand Bank where shallower maximum MLD occurs. The correlation between these model products is lower at 0.47 (Figure 75).

Bottom Temperature (BT)

The differences between the BNAM and CMIP6 products for the BT variables showed good congruence for the slope waters and Flemish Pass in all three variables (Mean, Min, Max) (Figure 76). CMIP6 products were warmer than BNAM products on the banks, which may be reflective of the longer time period for the CMIP6 projects (1990-2023 vs 2020-2039 respectively) and increasing trend lines (Figure 47). Maximum BT was colder in the CMIP6 product for small areas on the Tail of Grand Bank.

Bottom Current Speed (BCS)

The spatial distribution of the differences between the BNAM and CMIP6 products for the BCS variables (Mean, Min, Max) showed similar spatial patterns (Figure 77) with areas of lower and higher projections. In general the mid-slope areas showed slower currents in the CMIP6 products but this is not consistent.

Bottom Stress (BStr)

The spatial distribution of the differences between the BNAM and CMIP6 products for the BStr variables (Mean, Min, Max) were one of the most similar among the variable comparisons (Figure 78), comparing with Maximum Annual, Fall and Winter MLD (Figures 74, 75). Where differences occurred, Bottom stress from the CMIP6 products was higher than BNAM products along some of the deeper slope areas and smaller on the banks and the eastern slope of Grand Bank (Figure 78).

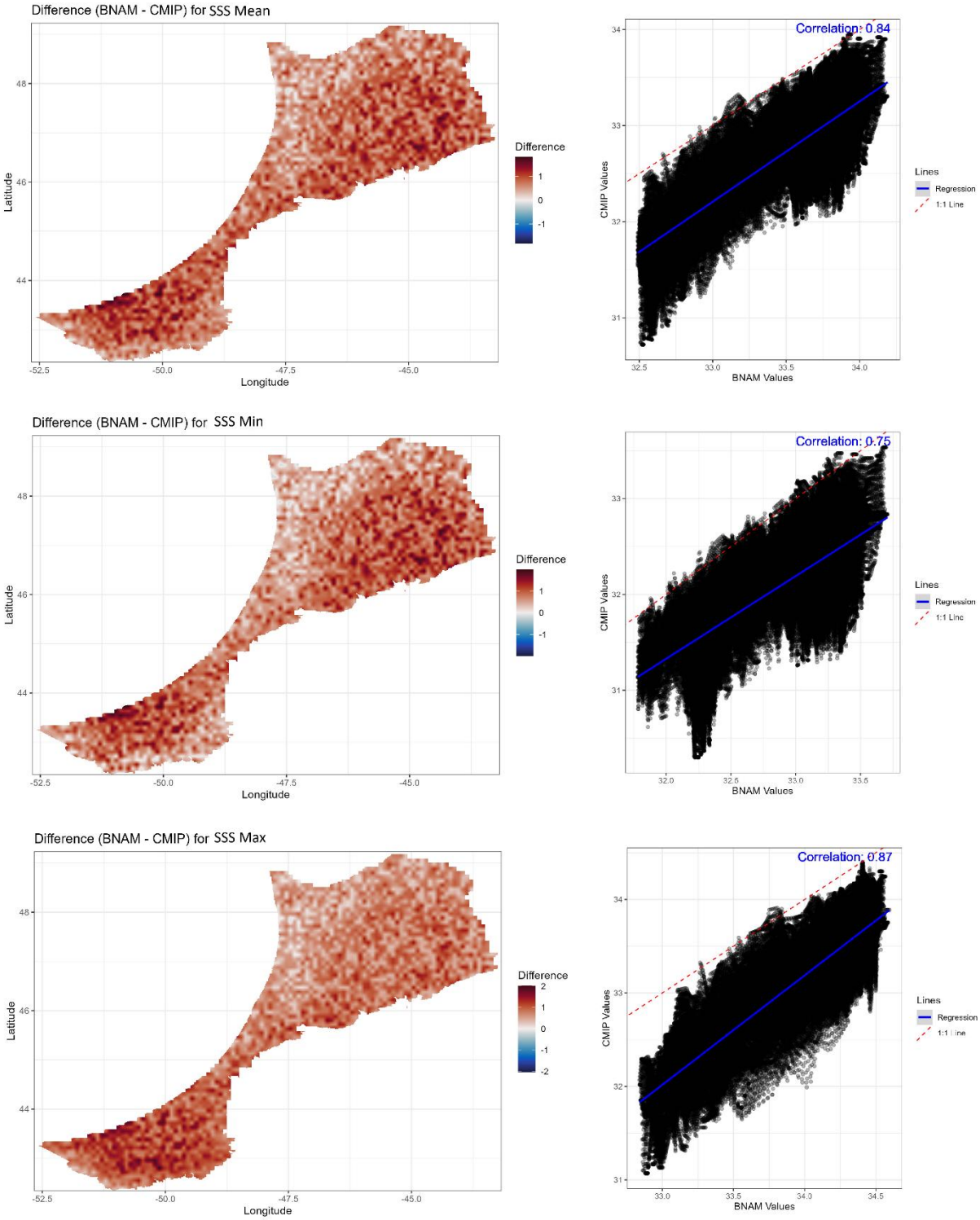

Figure 73. Spatial differences (left column) and correlation (right column) between the BNAM and CMIP6 Sea Surface Salinity (SSS) variables (top to bottom: Mean, Min, Max).

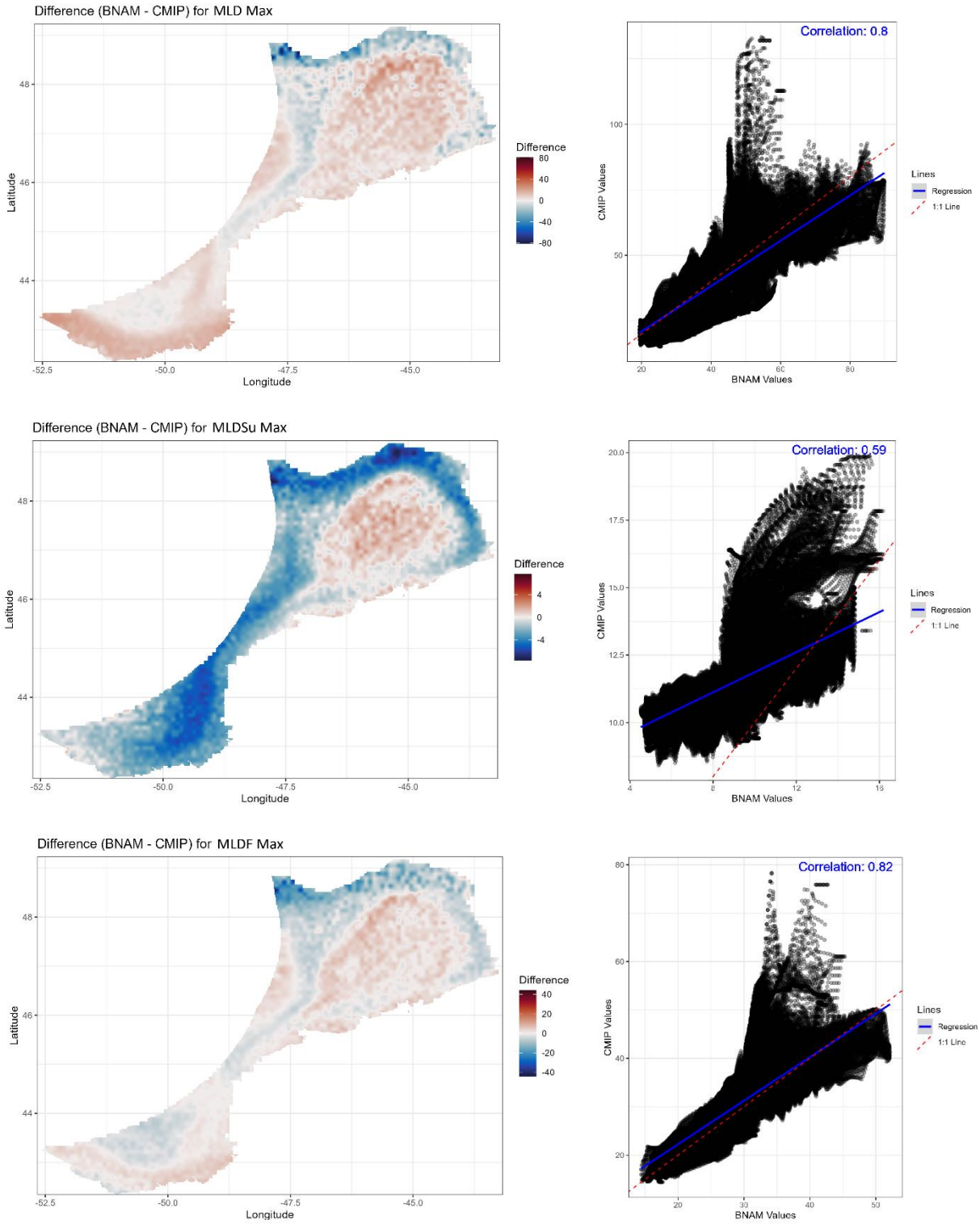

Figure 74. Spatial differences (left column) and correlation (right column) between the BNAM and CMIP6 Mixed Layer Depth (MLD) Maximum (Max) variables (top to bottom: Annual, Summer, Fall).

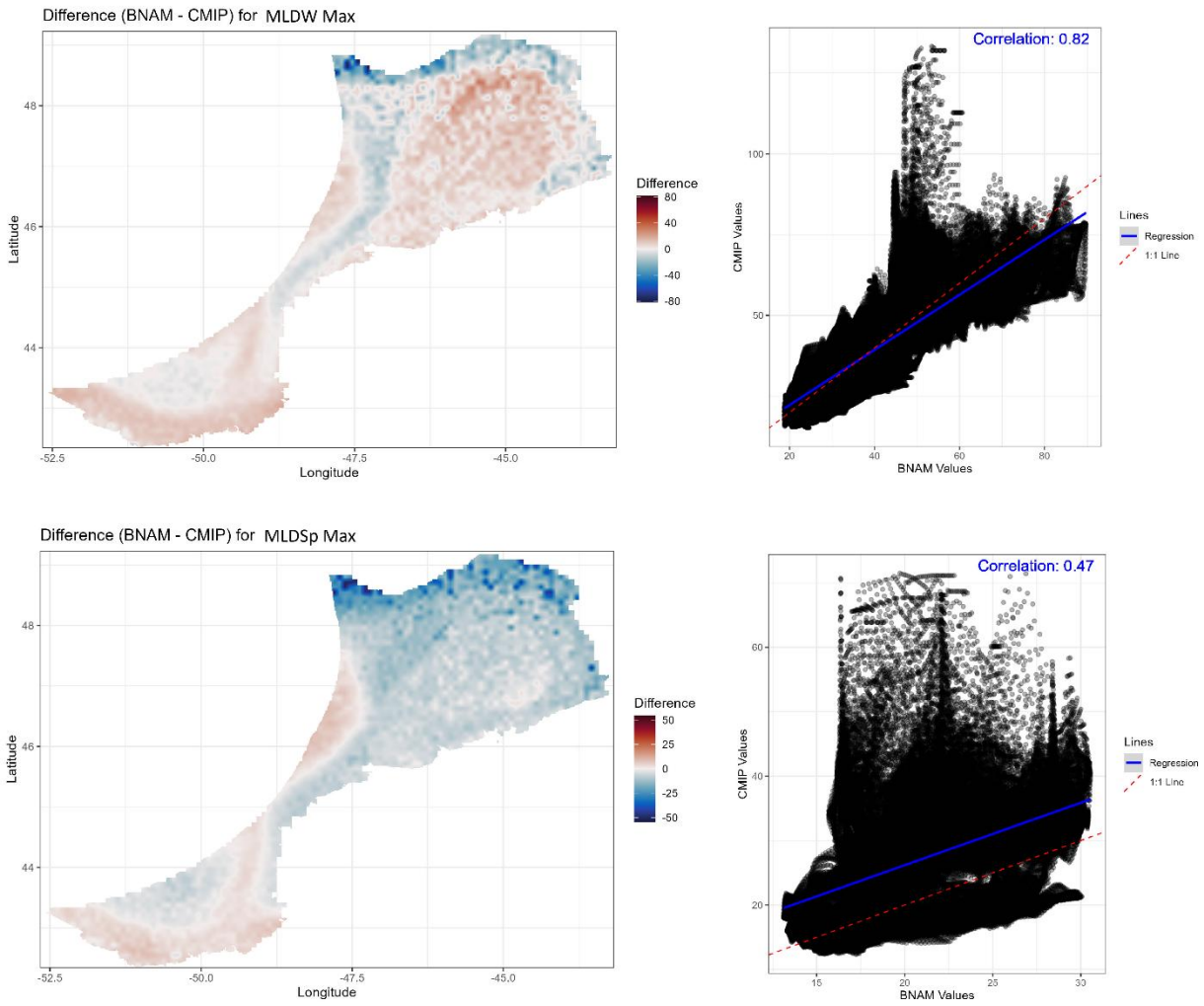

Figure 75. Spatial differences (left column) and correlation (right column) between the BNAM and CMIP6 Mixed Layer Depth (MLD) Maximum (Max) variables (top to bottom: Winter, Spring).

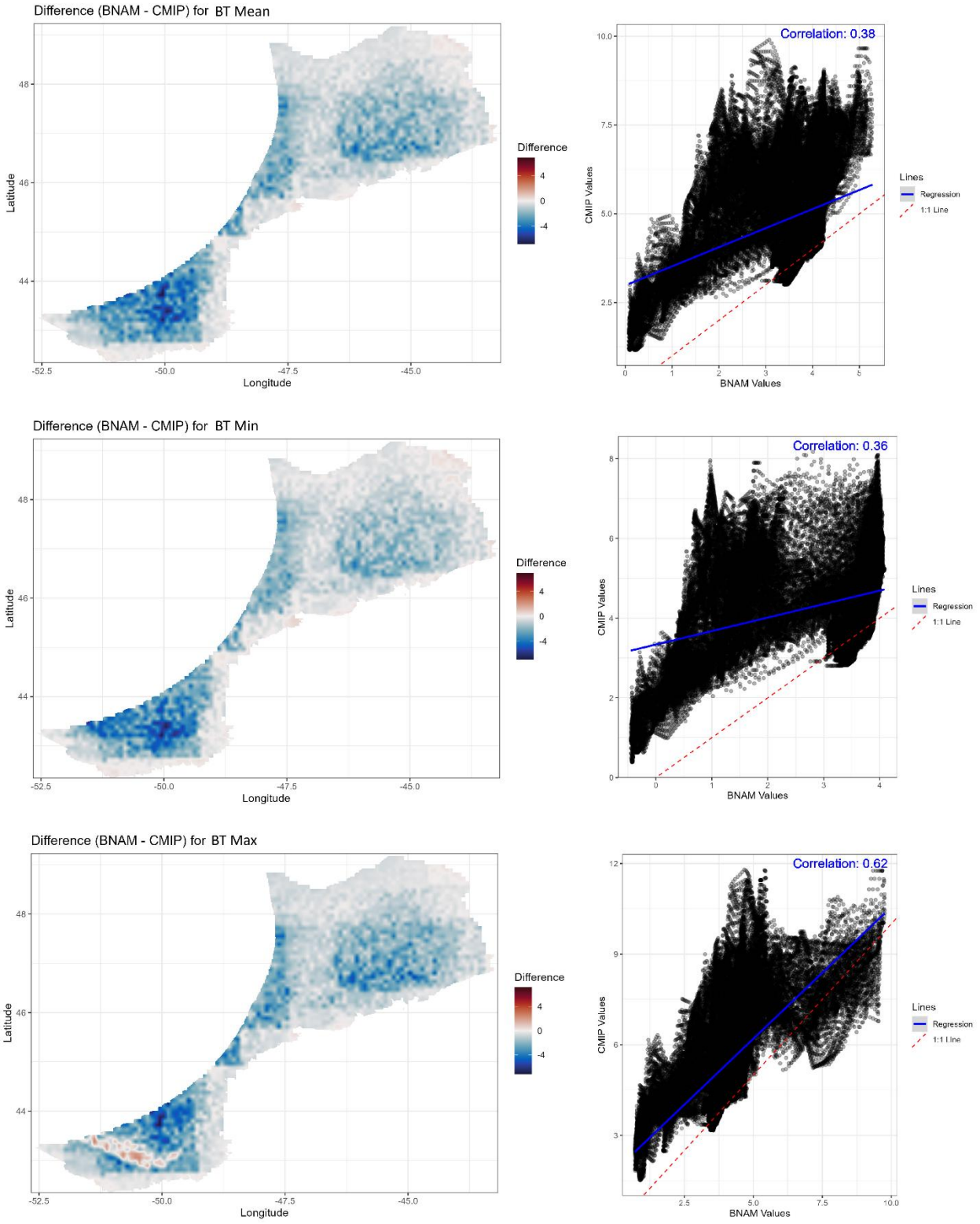

Figure 76. Spatial differences (left column) and correlation (right column) between the BNAM and CMIP6 Bottom Temperature (BT) variables (top to bottom: Mean, Min, Max).

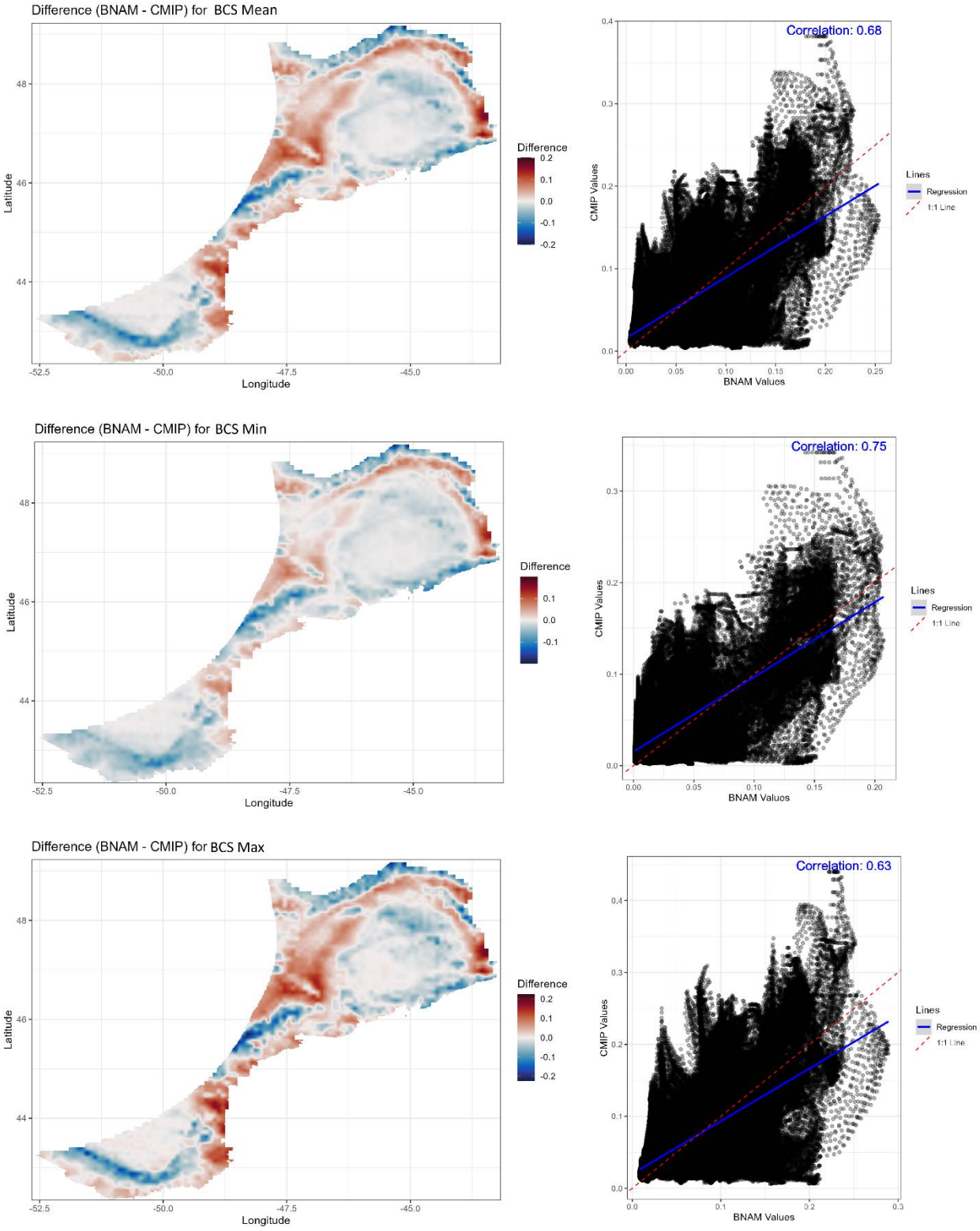

Figure 77. Spatial differences (left column) and correlation (right column) between the BNAM and CMIP6 Bottom Current Speed (BCS) variables (top to bottom: Mean, Min, Max).

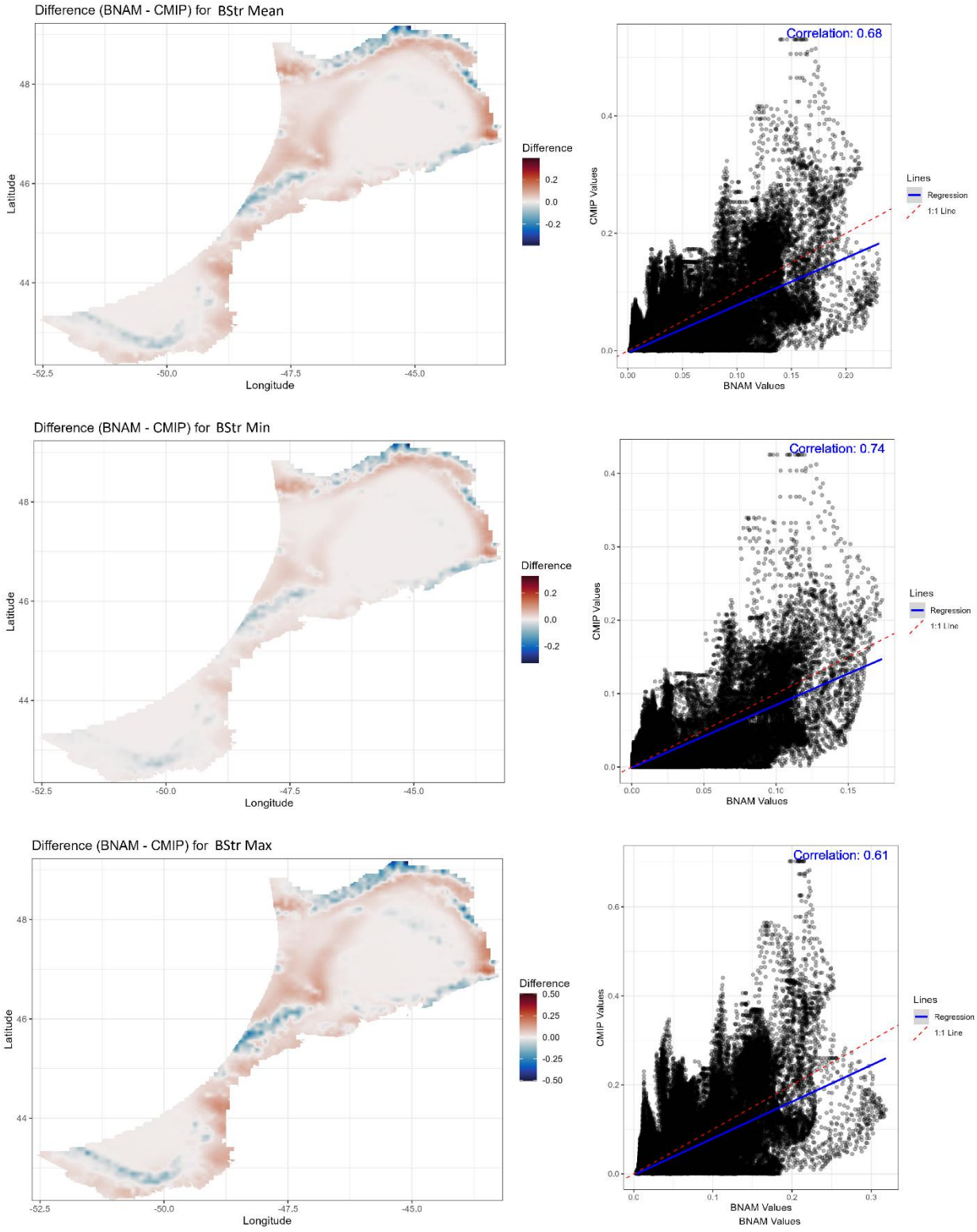

Figure 78. Spatial differences (left column) and correlation (right column) between the BNAM and CMIP6 Bottom Stress (BStr) variables (top to bottom: Mean, Min, Max).

Data Availability

The mapped data layers for use in species distribution modelling will be made available on the NAFO WG-ESA Sharepoint site. Those layers have been calculated to produce bi-decadal means for each of the variables for each of four time periods. We only show maps of Mean (Variable)/SSP1-2.6/Period 1 and Mean (Variable)/SSP5-8.5/Period 4 in this report. Researchers interested in obtaining the raw data prior to averaging (monthly means/grid cell/SSP) for the full spatial domain of the bounding box for each year from 2015 to 2100 should contact Dr. Zeliang Wang, Bedford Institute of Oceanography (Zeliang.Wang@dfo-mpo.gc.ca).

Discussion

There are many advantages in using results from the CMIP6 ESMs, as these models include improved representations of physical, chemical, and biological processes at the global scale (IPCC, 2021a). The data layers produced here are intended for use in species distribution models to identify vulnerable marine ecosystem (VME) indicator species and habitats that may be impacted by climate change in future, and to evaluate the stability of the environment around the current area closures to protect VMEs.

As with any modelling effort there are multiple sources of uncertainty in the data layers produced, among others, model resolutions, unresolved physical processes, and parametrizations. Under CMIP6 the established protocols and guidelines for climate model simulations and data were standardized, which enabled consistent, comparable, and robust analysis of global climate model outputs (Eyring et al., 2016). However, there are inherent biases in the use of ensembled products, such as model similarity that violates assumptions of independence and can lead to projections biased toward the largest set of similar models, and the underestimation of inter-model variability (Pathak et al., 2023). Ideally, in order to understand future climate impacts in the context of ESM uncertainty, the outputs of multiple ESMs under multiple scenarios would serve as inputs to impact models (Snyder et al., 2024). However that is computationally demanding and CMIP6 addresses uncertainty by using multiple climate models and multiple future emission scenarios (SSPs) to capture the full range of model uncertainty and scenario uncertainty. This 'multi-model ensemble framework' allows for the isolation and quantification of uncertainty from various sources. Thus, different aspects of climate variability are partitioned between and among SSPs/Time Periods and the ensemble approach offers a more comprehensive and generally more reliable projection by combining the diverse strengths of multiple models.

The U.S. Geological Survey guidance for scientists and technical users of CMIP products recommends the consideration of an ensemble of model projections for resource-management applications, since no single model performs best in every region or for every variable of interest (Boyles et al., 2024). Multiple-emissions scenarios and multiple ESMs for each scenario are recommended to capture a range of possible future conditions. This is the approach followed herein.

Acknowledgments

We thank Brendan DeTracey (Bedford Institute of Oceanography, Department of Fisheries and Oceans, Dartmouth, Nova Scotia, Canada) for his work in assembling the CMIP6 models for this study. This project was funded through Fisheries and Oceans, Canada's Competitive Science Research Fund Project "Distribution modeling of Vulnerable Marine Ecosystems (VME) in the Northwest Atlantic Fisheries Organization".

References

Andres, H.J., Soontiens, N., Penney, J. and Cyr, F. 2024. Seasonal variations of the cold intermediate layer on the Newfoundland and Labrador Shelf. Progress in Oceanography 229: 103379. https://doi.org/10.1016/j.pocean.2024.103379

Beazley, L., Kenchington, E., Murillo, F.J., Brickman, D., Wang, Z., Davies, A.J., Roberts, E.M., and Rapp, H.T. 2020. Climate change winner in the deep sea: Predicting the impacts of climate change on the distribution of the glass

sponge *Vazella pourtalesii*. Marine Ecology Progress Series 657: 1-23. http://www.int-res.com/articles/feature/m657p001.pdf

Boyce, D. 2024. Addressing the impacts of climate variability and change on NAFO Fisheries. NAFO Scientific Council Research Document, SCR Doc. 24/009: 1-86. https://www.nafo.int/Portals/0/PDFs/sc/2024/scr24-009.pdf

Boyles, R., Nikiel, C.A., Miller, B.W., Littell, J., Terando, A.J., Rangwala, I., Alder, J.R., Rosendahl, D.H., and Wootten, A.M. 2024, Approaches for using CMIP projections in climate model ensembles to address the 'hot model' problem. U.S. Geological Survey Open-File Report 2024–1008, 14 pp. https://doi.org/10.3133/ofr20241008

Busch, K., Murillo, F.J., Lirette, C., Wang, Z., and Kenchington, E. 2024. Putative past, present, and future spatial distributions of deep-sea coral and sponge microbiomes revealed by predictive models. ISME Communications 4: ycae142. https://doi.org/10.1093/ismeco/ycae142

Danielson, R. E., Zhang, M., Chassé, J., and Perrie, W. 2025. A seasonal to decadal calibration of 1990-2100 eastern Canadian freshwater discharge simulations by observations, data models, and neural networks, arXiv:2506.05261 [stat.AP] (to appear in 2026, Atmosphere-Ocean 64: 1-16, doi:10.1080/07055900.2025.2521502).

Drenkard, E.J., Stock, C., Ross, A.C., Dixon, K.W., Adcroft, A., Alexander, M., Balaji, V., Bograd, S.J., Butenschön, M., Cheng, W., and Curchitser, E. 2021. Next-generation regional ocean projections for living marine resource management in a changing climate. ICES Journal of Marine Science 78: 1969-1987.

Eyring, V., Bony, S., Meehl, G. A., Senior, C. A., Stevens, B., Stouffer, R. J., Taylor, K. E. 2016. Overview of the Coupled Model Intercomparison Project Phase 6 (CMIP6) experimental design and organization. Geoscientific Model Development 9: 1937-1958.

Greenan, B.J.W., James, T.S., Loder, J.W., Pepin, P., Azetsu-Scott, K., Ianson, D., Hamme, R.C., Gilbert, D., Tremblay, J-E., Wang, X.L. and Perrie, W. 2018. Changes in oceans surrounding Canada; Chapter 7 in (eds.) Bush and Lemmen, Canada's Changing Climate Report; Government of Canada, Ottawa, Ontario, p. 343–423. https://natural-resources.canada.ca/sites/www.nrcan.gc.ca/files/energy/Climate-change/pdf/CCCR-Chapter7-ChangesInOceansSurroundingCanada.pdf

Hijmans, R. 2025. _terra: Spatial Data Analysis. R package version 1.8-54. https://CRAN.R-project.org/package=terra

Innes, M., Saba, E., Fischer, K., Gandhi, D., Rudilosso, M. C., Joy, N. M., Karmali, T., Pal, A., and Shah, V. B. 2018. Fashionable modelling with Flux, arXiv:1811.01457 [cs.PL].

IPCC. 2021a. Summary for Policymakers. In: Climate Change 2021: The Physical Science Basis. Contribution of Working Group I to the Sixth Assessment Report of the Intergovernmental Panel on Climate Change [Masson-Delmotte, V., P. Zhai, A. Pirani, S. L. Connors, C. Péan, S. Berger, N. Caud, Y. Chen, L. Goldfarb, M. I. Gomis, M. Huang, K. Leitzell, E. Lonnoy, J.B.R. Matthews, T. K. Maycock, T. Waterfield, O. Yelekçi, R. Yu & B. Zhou (eds.)]. Cambridge University Press.

IPCC. 2021b. Annex II: Models [Gutiérrez, J M., A.-M. Tréguier (eds.)]. In Climate Change 2021: The Physical Science Basis. Contribution of Working Group I to the Sixth Assessment Report of the Intergovernmental Panel on Climate Change [Masson-Delmotte, V., P. Zhai, A. Pirani, S.L. Connors, C. Péan, S. Berger, N. Caud, Y. Chen, L. Goldfarb, M.I. Gomis, M. Huang, K. Leitzell, E. Lonnoy, J.B.R. Matthews, T.K. Maycock, T. Waterfield, O. Yelekçi, R. Yu, and B. Zhou (eds.)]. Cambridge University Press, Cambridge, United Kingdom and New York, NY, USA, pp. 2087–2138. doi:10.1017/9781009157896.016.

Lange, S. 2019. Trend-preserving bias adjustment and statistical downscaling with ISIMIP3BASD (v1. 0). Geoscientific Model Development 12: 3055-3070. https://doi.org/10.5194/gmd-12-3055-2019

Lellouche, J.-M., Greiner, E., Bourdallé-Badie, R., Garric, G., Melet, A., Drévillon, M., Bricaud, C., Hamon, M., Le Galloudec, O., Regnier, C., Candela, T., Testut C.-E., Gasparin, F., Ruggiero, G., Benkiran, M., Drillet, Y., and Le Traon, P.-Y. 2021. The Copernicus global 1/12 oceanic and sea ice GLORYS12 reanalysis. Frontiers in Earth Science 9: 1–27.

Loder, J. W., Baaren, A., and Yashayaev, I. 2015. Climate comparisons and change projections for the northwest Atlantic from Six CMIP5 models. Atmosphere-Ocean 53: 529–555. https://doi.org/10.1080/07055900.2015.1087836

Maraun, D., 2016. Bias correcting climate change simulations-a critical review. Current Climate Change Reports 2: 211-220. https://doi.org/10.1007/s40641-016-0050-x.

McKee, E., Danielson, R., DeTracey, B., Kenchington, E., Skinner, M., Greenan, B., and Wang, Z. 2025. High-resolution AI mapping of climate projections for Marine Protected Areas in the Maritimes. MS prepared for publication in Canadian Technical Report of Hydrography and Ocean Sciences 406: v + 29 p.

McKee, E., Wang, Z., and DeTracey, B. 2023. Evaluation of Bottom Temperature from GLORYS12 and EN4 for North American Continental Shelf Waters: From the North Atlantic, to the Arctic, to the North Pacific Oceans. Canadian Technical Report of Hydrography and Ocean Sciences 355: vii + 34 p.

Mercator Océan International. 2022. Global Ocean Physics Reanalysis, Dataset. https://doi.org/10.48670/moi-00021.

Murillo, F.J., Abalo Morla, S., Downie, A.-L., Lirette, C., Paulin, N., Wang, Z., Devred, E., Clay, S., Sacau, M., Nozères, C., Koen-Alonso, M., Gullage, L., Hayes, V., Caetano, M., Gonçalves, P., and Kenchington, E. 2025. Vulnerable Marine Ecosystems in the NAFO Regulatory Area: Updated Species Distribution Models of Selected Vulnerable Marine Ecosystem Indicators (Large and Small Gorgonian Corals, Erect Bryozoans and Sea Squirts). NAFO Scientific Council Research Document, SCR Doc. 25/035: 1-62.

Murillo, F.J., Downie, A.-L., Abalo Morla, S., Lirette, C., Paulin, N., Wang, Z., Devred, E., Clay, S., Sacau, M., Nozères, C., Koen-Alonso, M., Gullage, L., and Kenchington, E. 2024. Vulnerable Marine Ecosystems in the NAFO Regulatory Area: Updated Species Distribution Models of Selected Vulnerable Marine Ecosystem Indicators (Large-Sized Sponges, Sea Pens and Black Corals). NAFO Scientific Council Research Document, SCR Doc. 24/063: 1-105. https://www.nafo.int/Portals/0/PDFs/sc/2024/scr24-063.pdf

O'Neill, B. C., Tebaldi, C., van Vuuren, D. P., Eyring, V., Friedlingstein, P., Hurtt, G., Knutti, R., Kriegler, E., Lamarque, J.-F., Lowe, J., Meehl, G. A., Moss, R., Riahi, K., and Sanderson, B. M. 2016. The Scenario Model Intercomparison Project (ScenarioMIP) for CMIP6. Geoscientific Model Development 9: 3461–3482. https://doi.org/10.5194/gmd-9-3461-2016

Pathak, R., Dasari, H.P., Ashok, K. , and Hoteit, I. 2023. Effects of multi-observations uncertainty and models similarity on climate change projections. Npj Climate and Atmospheric Science 6: 144. https://doi.org/10.1038/s41612-023-00473-5

Pebesma, E. 2018. Simple Features for R: Standardized Support for Spatial Vector Data. The R Journal 10 (1): 439-446. https://doi.org/10.32614/RJ-2018-009

R Core Team. 2025. R: A Language and Environment for Statistical Computing. R Foundation for Statistical Computing, Vienna, Austria. https://www.R-project.org/

Riahi, K., Van Vuuren, D.P., Kriegler, E., Edmonds, J., O'Neill, B.C., Fujimori, S., et al. 2017. The Shared Socio-economic Pathways and their energy, land use, and greenhouse gas emissions implications: An overview. Global Environmental Change 42: 153-168.

Schmidt, G. A., Bader, D., Donner, L. J., Elsaesser, G. S., Golaz, J.-C., Hannay, C., Molod, A., Neale, R. B., and Saha, S. 2017. Practice and philosophy of climate model tuning across six US modelling centers. Geosci. Model Dev. 10: 3207–3223, https://doi.org/10.5194/gmd-10-3207-2017

Schulzweida, Uwe. 2023. CDO User Guide (2.3.0). Zenodo. https://doi.org/10.5281/zenodo.10020800

Snyder, A., Prime, N., Tebaldi, C., and Dorheim, K. 2024. Uncertainty-informed selection of CMIP6 Earth system model subsets for use in multisectoral and impact models. Earth Syst. Dynam. 15: 1301–1318. https://doi.org/10.5194/esd-15-1301-2024

Tittensor, D.P., Eddy, T.D., Lotze, H.K., Galbraith, E.D., Cheung, W., Barange, M., Blanchard, J.L., Bopp, L., Bryndum-Buchholz, A., Büchner, M. and Bulman, C. 2018. A protocol for the intercomparison of marine fishery and ecosystem models: Fish-MIP v1. 0. Geoscientific Model Development 11: 1421-1442. https://doi.org/10.5194/gmd-11-1421-2018

Wang, S., Murillo, F.J., and Kenchington, E. 2022. Climate-change refugia for the bubblegum coral Paragorgia arborea in the northwest Atlantic. Frontiers in Marine Science 9: 863693 https://doi/10.3389/fmars.2022.863693

Wang, Z., Brickman, D., Greenan, B., Christian, J., DeTracey, B., and Gilbert, D. 2023. Assessment of ocean temperature trends for the Scotian Shelf and Gulf of Maine using 22 CMIP6 Earth System Models. Atmosphere-Ocean 62(1): 24–34. https://doi.org/10.1080/07055900.2023.2264832

Wang, Z., Lu, Y., Greenan, B., Brickman, D., and DeTracey, B. 2018. An eddy-resolving North Atlantic model (BNAM) to support ocean monitoring. Canadian Technical Report of Hydrography and Ocean Sciences 327: vii + 18 pp.

Wang, Z., and Greenan, B.J.W. 2013. Ocean circulation in the Northwest Atlantic: an evaluation of the GLORYS reanalysis. Canadian Technical Report of Hydrography and Ocean Sciences 294: vi + 31pp.